NTNU

Norwegian University of
Science and Technology

Multiphase flow simulation of rich gas pipelines with traces of liquid glycol

Flerfasesimulering av rikgassrørledninger
med små mengder glykol væske

Jørgen Børsum Haugen

Petter Holm Reiso

Master of Science in Mechanical Engineering
Submission date: June 2016
Supervisor: Even Solbraa, EPT

Norwegian University of Science and Technology
Department of Energy and Process Engineering

NTNU
Norwegian University
of Science and Technology

Department of Energy
and Process Engineering

EPT-M-2016-53/101

MASTER THESIS

for

Student
Jørgen Børsum Haugen and Petter Reiso

Spring 2016

Multiphase flow simulation of rich gas pipelines with traces of liquid glycol

Flerfasesimulering av rikgassrørledninger med små mengder glykol væske

Background and objective

Long distance multiphase transport of gas, oil, water and chemicals is a key technology in the development of future oil and gas fields. The most used industrial simulation tool used for multiphase flow design today is OLGA, commercialized by the SPT Group.

Methanol or glycol is typical injected in the well stream to prevent hydrate formation in pipelines. Both methanol and glycol has limited solubility in gas and oil – but anyhow this solubility sometimes can be important and has to be accounted for. An example can be a situation where the water cut is low – and where the relative amount of water and hydrate inhibitor dissolved in oil and gas is significant.

A multiphase flow simulator involves advances fluid mechanical and numerical models. The thermodynamic and physical properties used in the simulation are typically generated by a property table generation tool such as PVTsim by Calsep. These property packages are typically fitted to experimental reservoir fluid PVT data. PVTsim uses classical equations of state such as SRK or PR. The mixing rules utilized are simple classical mixing rules for hydrocarbons and eventually more advanced mixing rules for water and glycol. A property package needs to calculate the number of phases (oil, gas and water), thermodynamic properties of the phases, and physical properties such as viscosity, interfacial tension, etc.

In recent years, more fundamental and accurate thermodynamic models have been developed for calculation of phase behaviour of gas, oil, water and chemicals. One of the most promising models is the CPA-EoS (Cubic Plus Association Equation of State). The CPA-EoS is available in the NeqSim simulation tool developed at the department.

It is the purpose of this work to develop and evaluate NeqSim as a property generator for multiphase simulation as well as measuring interfacial tension of glycol (TEG) at high pressures. The experiments will be done at Statoil RDI laboratories at Rotvoll, Trondheim.

A number of techniques have been presented in literature for experimental measurement of surface tension between a gas and liquid. The pendant drop method is a popular method used for such measurements. In this work a high pressure pendant drop experimental equipment will be

used to measure surface tension in gas and oil/glycol systems. Finally theoretical models will be evaluated for their accuracy of predicting surface tension.

The following tasks are to be considered:

1. Review of experimental data of interfacial tension and viscosity of TEG/water solutions.
2. Experimental measurement of interfacial tension of high pressure TEG and natural gas
3. Status and further development of NeqSim as a property generation tool for multiphase flow simulators
4. Simulation of a rich gas pipeline (Åsgard transport) with a free liquid glycol phase. Comparison of the effect of various property generation models and tools

-- " --

Within 14 days of receiving the written text on the master thesis, the candidate shall submit a research plan for his project to the department.

When the thesis is evaluated, emphasis is put on processing of the results, and that they are presented in tabular and/or graphic form in a clear manner, and that they are analyzed carefully.

The thesis should be formulated as a research report with summary both in English and Norwegian, conclusion, literature references, table of contents etc. During the preparation of the text, the candidate should make an effort to produce a well-structured and easily readable report. In order to ease the evaluation of the thesis, it is important that the cross-references are correct. In the making of the report, strong emphasis should be placed on both a thorough discussion of the results and an orderly presentation.

The candidate is requested to initiate and keep close contact with his/her academic supervisor(s) throughout the working period. The candidate must follow the rules and regulations of NTNU as well as passive directions given by the Department of Energy and Process Engineering.

Risk assessment of the candidate's work shall be carried out according to the department's procedures. The risk assessment must be documented and included as part of the final report. Events related to the candidate's work adversely affecting the health, safety or security, must be documented and included as part of the final report. If the documentation on risk assessment represents a large number of pages, the full version is to be submitted electronically to the supervisor and an excerpt is included in the report.

Pursuant to "Regulations concerning the supplementary provisions to the technology study program/Master of Science" at NTNU §20, the Department reserves the permission to utilize all the results and data for teaching and research purposes as well as in future publications.

The final report is to be submitted digitally in DAIM. An executive summary of the thesis including title, student's name, supervisor's name, year, department name, and NTNU's logo and name, shall be submitted to the department as a separate pdf file. Based on an agreement with the supervisor, the final report and other material and documents may be given to the supervisor in digital format.

☐ Work to be done in lab (Water power lab, Fluids engineering lab, Thermal engineering lab)
☐ Field work

Department of Energy and Process Engineering, 13. January 2016

Olav Bolland
Department Head

Even Solbraa
Academic Supervisor

Research Advisor:

Preface

This Master's thesis was written at the Department of Energy and Process Engineering at the Norwegian University of Science and Technology in Trondheim in the spring of 2016. The experimental work was conducted at Statoil Research and Development center at Rotvoll, Trondheim. Statoil provided field data from the Åsgard transport pipeline which have been used in the OLGA simulations. The report is a continuation of a project thesis written in the fall of 2015. This assignment represents the workload of 30 ECTS.

Trondheim, 2016-06-13

Petter Holm Reiso

Jørgen Børsum Haugen

Acknowledgement

We would like to thank our supervisor, professor II Even Solbraa, for his guidance and help throughout the assignment. We encountered several complex issues where he was essential in finding the solutions.

We would like to thank Ole Johan Berg at Statoil for guidance and support with the experimental work. We would also like to thank Knud Lunde who provided field data and OLGA files for the Åsgard transport pipeline. Finally, we would like to thank Marie Vikre Danielsen at Statoil for measuring the liquid mixtures utilized for the experimental work.

P.H.R

J.B.H

Abstract

Long distance transport of multiphase flow is an important technology in the development of oil and gas fields. Predicting phase behaviour in long pipelines is a demanding and complicated process. To realistically simulate these situations, the industry is reliant on software that can calculate accurate fluid properties. The most used simulation tool today, is a computer program named OLGA (OiL and GAs simulator). OLGA requires input in the form of a fluid property table to conduct these simulations. These property tables are generated by tools like PVTsim (Pressure, Volume and Temperature simulator) and NeqSim (Non-Equilibrium Simulator). The purpose of this Master's thesis was to further develop and improve NeqSim as a fluid property table generator. This task was specifically aimed towards liquid viscosity and interfacial tensions of aqueous TEG (TriEthylene Glycol). These properties are regarded among the most influential parameters for fluid behaviour.

Experimental work was conducted to measure the interfacial tensions of high pressure aqueous TEG and methane. There is low availability of such data in the literature. The measurement method utilized was the pendant drop method. The interfacial tensions were measured with an uncertainty of less than 2%. Relevant experimental data for liquid viscosities and interfacial tensions were also collected.

The measured data and the collected experimental data were compared to calculated values from NeqSim and PVTsim. These tools utilize similar empirical methods to calculate liquid viscosities. Interfacial tensions are calculated by the Firoozabadi Ramey Method in PVTsim. NeqSim offers several calculation methods for interfacial tension. These include the Firoozabadi Ramey Method, the Parachor Method, Linear Gradient Theory, Gradient Theory Simple and Gradient Theory. NeqSim proved to predict the most accurate liquid viscosity values. In regard to interfacial tensions, Gradient Theory in NeqSim provided the most accurate results.

A parameter study was conducted in OLGA to establish how liquid viscosity and interfacial tensions affects the simulations of multiphase flow. The simulations were conducted using field data provided by Statoil of the Åsgard transport pipeline. The simulations were conducted using both the standard OLGA module and the OLGA HD module. It was shown that alterations in liquid viscosity and interfacial tensions have small impacts on the simulations. Increasing the mass flow of TEG did impact the simulations. The impact was negligible with the standard OLGA module, but significant with the OLGA HD module. It is concluded that the OLGA HD module results in more accurate simulations of the Åsgard transport pipeline. It is also concluded that both NeqSim and PVTsim calculates sufficiently accurate property values to be used in the current OLGA version 7.3.5.

The development of NeqSim as a property generator is a continuous process. There are still areas where NeqSim can be improved. These are discussed in the final chapter, and include further improvements in the calculations of liquid viscosity and interfacial tension and the generation of wax property tables.

Sammendrag

Langdistansetransport av flerfasestrømning er en viktig teknologi i utviklingen av olje- og gassfelt. Å forutsi faseoppførsel i lange rørledninger er en krevende og komplisert prosess. For å realistisk simulere disse situasjonene er industrien avhengig av programvare som kan kalkulere presise fluidegenskaper. Det mest brukte simuleringsverktøyet idag er et dataprogram kalt OLGA (OiL and GAs simulator). OLGA behøver innmating i form av en tabell med fluidegenskaper for å utføre simuleringene. Disse tabellene er genererert av verktøy som PVTsim (Pressure, Volume and Temperature simulator) og NeqSim (Non-Equilibrium Simulator). Hensikten med denne masteroppgaven var å videreutvikle og forbedre programvaren NeqSim som en tabellgenerator. Oppgaven var spesifikt rettet mot væskesviskositet og overflatespenning av vannholdig TEG (TriEthylene Glycol). Disse egenskapene er ansett blant de mest innflytelsesrike parametrene for fluidoppførsel.

Eksperimentelt arbeid ble utført for å måle overflatespenning av TEG og metan under høyt trykk. Det er liten tilgjengelighet på slike data i litteraturen. Målingsmetoden som ble benyttet var "pendant drop"-metoden. Overflatespenningene ble målt med en usikkerhet på mindre enn 2%. Relevant eksperimentell data for væskeviskositet og overflatespenning har ble også innhentet.

De målte verdiene og de innhentede eksperimentelle data ble sammelignet med beregnede verdier fra NeqSim og PVTsim. Programvarene benytter lignende empiriske metoder for å beregne væskeviskositet. Overflatespenning blir beregnet med Firoozabadi Ramey-metoden i PVTsim. NeqSim tilbyr flere beregningsmetoder for overflatespenning. Dette inkluderer Firoozabadi Ramey-metoden, Parachor-metoden, "Linear Gradient Theory", "Gradient Theory Simple" og "Gradient Theory". NeqSim beregnet mest nøyaktige verdier for væskeviskositet. Med hensyn til overflatespenning beregnet "Gradient Theory" i NeqSim de mest nøyaktige verdiene.

En parameterstudie ble gjennomført i OLGA for å etablere hvordan væskeviskositet og overflatespenning påvirker simuleringer av flerfasestrømning. Simuleringene ble utført ved bruk av feltdata fra Statoil av Åsgard transport rørledningen. Simuleringene ble utført både med standard OLGA-modulen og med OLGA HD-modulen. Det ble vist at endringer i væskeviskositet og overflatespenning har liten påvirkning på simuleringene. Økning av massestrømmen av TEG påvirket simuleringene. Effekten var neglisjerbar med standard OLGA-modulen, men betydelig med OLGA HD-modulen. Det er konkludert at OLGA HD-modulen resulterer i mer nøyaktige simuleringer av Åsgard transport rørledningen. Det er også konkludert at både NeqSim og PVTsim beregner tilstrekkelig nøyaktige egenskapsverdier til å brukes i den nåverende OLGA versjonen 7.3.5.

Utviklingen av NeqSim som en tabellgenerator er en kontinuerlig prosess. Det finnes fremdeles områder hvor NeqSim kan forbedres. Disse er diskutert i det siste kapittelet, og omhandler ytterligere forbedringer i beregningene av væskeviskositet og overflatespenning, samt generering av egenskapstabeller for voks.

Contents

List of Figures

List of Tables

Abbreviations

CPA	-	Cubic Plus Associating
DEG	-	Diethylene glycol
EG	-	Ethylene glycol
EoS	-	Equation of State
GC	-	Gas chromatograph
LBVC	-	Lohrenz-Bray-Clark
MEG	-	Monoethylene glycol
Mole%	-	Mole percentage
MSm^3	-	Million standard cubic meter
NeqSim	-	Non-Equilibrium simulator
OH	-	Hydroxyl
OLGA	-	Oil and gas simulator
PFCT	-	Pedersen-Fredenslund-Christensen-Thomassen
PR	-	Peng-Robinson
PVTsim	-	Pressure, Volume and Temperature simulator
RK	-	Redlich-Kwong
SAFT	-	Statistical Associating Fluid Theory
SRK	-	Soave-Redlich-Kwong
TEG	-	Triethylene glycol
T_4EG	-	Tetraethylene glycol
VDW	-	van der Waals
wt%	-	Weight percentage

Nomenclature

Symbol	Description	Unit
α	Phase fraction	-
A	Area	m^2
β	Bond number	-
C_p	Heat capacity	J
D	Pipe diameter	m
e	Empirical interaction parameter	-
E_η	Viscosity coefficient	-
ε	Surface roughness	m
f	Friction factor	-
g	gravity	m/s^2
G	Excess free energy	J
H	Enthalpy	J/kg
k	Thermal conductivity	W/m·K
κ	Friction coefficient	-
l	Length	m
m	Mass transfer	kg/m·s
M	Molecular weight	kg/mol
η	Dynamic viscosity	mPa·s
ρ	Density	kg/m^3
P	Pressure	bar
P_i	Parachor value	-
q	Interfacial heat flux	J/m·s
Q	Heat flux	J/m·s
R	Universal gas constant	J/mol·K
R	Radius	m
Re	Reynolds number	-
R_s	Gas mass fraction	-
s	Cross section	m
S	Entropy	J/K
τ	Shear stress	N/m^2
t	Thickness	m
T	Temperature	K
u	Velocity	m/s
U	Internal energy	J
μ	Chemical potenial	J/mol
υ	Kinematic viscosity	m^2/s
W	Work	J
x	Mole fraction	-
ξ	Viscosity reducing parameter	-
y	Mole fraction	-
γ	Interfacial tension	mN/m
Φ	Grand potential	J
θ	Angle	°

Chapter 1

Introduction

1.1 Multiphase Flow

Multiphase flow is present in many processes surrounding us, both environmental and industrial. In fluid mechanics, multiphase flow is simultaneous flow of various phases in contact. It is usually gases and liquids appearing together, but there can also be solids present. The subject has been of growing interest in the Norwegian petroleum industry the last decades. Long distance transport of unprocessed natural gas in the same pipeline means less transport expenditures and the possibility of processing the mixture onshore. This constitutes a significant economical advantage.

Fluids transported in rich gas transport pipelines, such as Åsgard transport, will eventually reach seabed temperature of close to 0°C. At low temperatures and high pressures, hydrates can form if liquid water is present. Hydrates are solid particles which can cause severe operating problems in downstream equipment. Because hydrocarbons in reservoirs contain water, one option is to remove the water from the hydrocarbons before transportation. TEG (TriEthylene Glycol) is among the most used liquid solvents for absorption of water.

The consequence of using TEG as a solvent is that small amounts of it will be transported within the rich gas. This influences properties like liquid viscosity and interfacial tension, which are among the most influential parameters for fluid behaviour. These properties have considerable effects on fluid flow characteristics and consequently capacity and processing aspects. To determine size and design of the transport pipelines and downstream process equipment accurate simulation models are needed to describe the behaviour of the multiphase flow. The computer program OLGA (OiL and GAs simulator) is a modelling tool for multiphase flow. It was commercialized by the Schlumberger company SPT Group, and is the most used simulation tool today. Multiphase flow technology is highly advanced and challenging, and is a process in development.

Multiphase flow simulators comprise advanced fluid mechanical and numerical models. As input it needs a property table comprising various thermodynamic and physical properties for the fluid. The property table is generated by a property generation tool which calculates properties for a set amount of temperature and pressure points. An example of a property table generator is PVTsim (Pressure, Volume and Temperature simulator), which calculates fluid properties using a classical equation of state. These equations calculate accurate property values for fluids containing hydrocarbons, but struggle when applied to polar components like water and TEG. Another option is to generate property tables using NeqSim (Non-Equilibrium Simulator), which is developed at the Department of Refrigeration and Air Conditioning, at the Norwegian University of Science and Technology. NeqSim calculates fluid properties using the Cubic Plus Association Equation of State, which is more compatible with polar components.

1.2 Thesis Specification

NeqSim comprise several mathematical models for predicting viscosity and interfacial tensions. The accuracy of these models when applied to TEG are however uncertain. The aim of this master's thesis is to evaluate the models used for property generation and to compare generated data with experimental data for aqueous TEG and methane.

The following tasks are to be considered:

1. Review of experimental data of interfacial tension and viscosity of TEG/water solutions.
2. Experimental measurement of interfacial tension of high pressure TEG and natural gas.
3. Status and further development of NeqSim as a property generation tool for multiphase flow simulators.
4. Simulation of a rich gas pipeline (Åsgard transport) with a free liquid glycol phase. Comparison of the effect of various property generation models and tools.

1.3 Report Structure

Chapter 2, 3 and 4 in the study are theoretical chapters. Chapter 2 includes aspects of dehydration, hydrates and glycols. Chapter 3 focuses on conservation laws and closure relations for multiphase flow. Chapter 4 describes the properties liquid viscosity and interfacial tension along with the models for calculating them. Chapter 5 gives an introduction to the software OLGA, NeqSim and PVTsim. Chapter 6 presents a review of existing experimental data on viscosity and interfacial tension of TEG, water and methane. Methods for measuring interfacial tension are also presented in this chapter. Chapter 7 describes the experimental set up, apparatus and procedure of the laboratory work conducted in this study. Chapter 8 presents the

experimental results obtained in this study along with an uncertainty analysis. Chapter 9 compares experimental data and generated properties from NeqSim and PVTsim. It also compares the obtained measured interfacial tension values to the measured values obtained in a similar study. Chapter 10 presents a parameter study simulated in OLGA of the Åsgard transport pipeline. Chapter 11 is the discussion of our work. Chapter 12 presents the conclusion to our thesis and recommendations for further work. The thesis ends with bibliography and appendices.

Chapter 2

Dehydration

2.1 Hydrates

The formation of hydrates is one of the most common problems in multiphase flow pipelines. Hydrates are ice-like structures where the water molecules form crystalline structures which are held together by hydrogen bonding. The structures are stabilized by light natural gas compounds such as methane. The formation can occur if liquid water is present in the flow. According to Anyadiegwu et al. (2014) the temperature must be below the gas dew point temperature and the pressure above the gas dew point pressure, meaning they can form at higher temperatures than ice. The high pressure and low temperatures in rich gas transport pipelines make them susceptible to hydrate formation.

Hydrates can cause several operating problems, the most severe being partial or complete blockages of pipes and downstream equipment. Hydrate plugs large enough to block a pipeline completely can form within minutes (Kidnay et al., 2011). Other problems are erosion of expanders and fouling and plugging of heat exchangers (Rojey, 1997). To prevent the formation of hydrates the usual solution is to strip the water content from the flow. In order to remove and control the water content of the natural gas, a dehydration process is utilized.

2.2 Absorption

There are several ways to achieve dehydration. Examples are absorption, adsorption, gas permeation and refrigeration. The most widely used method in oil and gas processing is absorption. Absorption is a process where a gas (or liquid) is contained within a liquid solvent to remove specific compounds. Physical absorption is the transfer of mass from one phase to another.

In oil and gas processing, water is usually removed from the natural gas by absorption dehydration, using a liquid solvent. The contact is normally accomplished in tray or packed towers. To

achieve viable absorption, a low cost solvent with strong affinity for water is favoured.

2.3 Glycols

Glycols are the common name for dihydric alcohols, which are alcohols containing two hydroxyl (–OH) groups. They are considered among the more effective liquid solvents and are commonly used in oil and gas processing. Dehydration by absorption using glycol is usually economically more attractive than dehydration by a solid desiccant (Anyadiegwu et al., 2014). The OH-bonds have a strong affinity for water molecules and will extract water from the natural gas when the gas is exposed to the liquid glycol. Glycols used for dehydrating natural gas are ethylene glycol (EG), diethylene glycol (DEG), triethylene glycol (TEG), and tetraethylene glycol(T_4EG). Normally a single type of pure glycol is used in a dehydrator, but sometimes a glycol blend is economically attractive (Guo and Ghalambo, 2005).

2.3.1 TEG

TEG (TriEthylene Glycol) is the most used glycol for natural gas dehydration. It provides the best combination of dew point depression, operating cost and reliability (Guo and Ghalambo, 2005). It is an odourless viscous liquid. The advantages of TEG is the ease of regeneration and operation, minimal losses of drying agent during operation, high affinity for water and chemical stability. TEG has been successfully utilized to dehydrate natural gases over wide ranges of operating conditions (Anyadiegwu et al., 2014). The physical and chemical properties of triethylene glycol are given in Table 2.1.

Parameter	**Unit**	**Properties**
Empirical formula	-	$C_6H_{14}O_4$
Molecular weight	g/mol	150.17
Density at 25 °C	g/cm^3	1.120
Flash point	°C	176
Ignition point	°C	371
Boiling point at 1 atm	°C	287.7
Freezing point	°C	-4.3
Critical Temperature	°C	440
Critical Pressure	kPa	3313.3
Viscosity at 20 °C	mPa ·s	49.0
Vapor pressure at 20 °C	kPa	<0.001

Table 2.1: Physical and chemical properties of TEG, Company (2007)

2.3.2 TEG Content in Gas Phase

The loss of TEG from the dehydration unit to the transport pipeline (carryover of TEG) occurs in two ways:

- **Mechanical TEG carryover:** Small droplets carried over into the pipeline mechanically.
- **TEG vaporization:** TEG vaporizes and is solved in the gas. Normally, this amount is considerably higher than the mechanical carryover. The amount is dependant on the operation conditions of the TEG contactor.

Over time, liquid TEG can accumulate within the pipeline. Condensed liquid may cause slug formation in a pipeline with transient conditions, or cause an undesirably high pressure drop along the pipeline. The condensed TEG and water may cause long-term corrosion on the inside of the wall of the pipeline if the water content is high enough (Kordabadi and Dinon, 2013).

Chapter 3

Properties Needed for Multiphase Flow Simulation

In fluid mechanics, multiphase flow is simultaneous flow of various phases in contact. It is usually gases and liquids appearing together, but there can also be solids present. In oil and gas production, it is crucial to account for the occurring multiphase flow. The wells produce gas, water and oil at the same time, which leads to three phase flow. In addition, methanol and glycol is often injected in the well stream to avoid hydrate formation in the pipelines. Flow models play a major part in predicting accurate production rates and flow assurance, but calculation models have historically been inaccurate. Even the best equations of state have their limitations.

However, technology for transporting multiphase flow have advanced rapidly in recent decades. New calculation models like SAFT (Huang and Radosz, 1990) and CPA-EoS (Kontogeorgis et al., 1996) provide significantly better simulation models. This has already had an enormous economical impact on several offshore developments. Multiphase flow pipelines have in some places replaced topside offshore installations. In the development of future oil and gas fields, long-distance multiphase transport of gas, water, oil and chemicals will be an important feature. This chapter is based on material written by Solbraa (2002), Bratland (2010) and Bjortuft (2014). It will be limited to a two phase flow scenario consisting of one gas phase and one liquid phase.

Two phase flow can generally be treated as separated flow or dispersed flow. Separated flow regimes, such as stratified or annular flow, has a well defined interface. This may not be the case when dealing with the more complex interface of dispersed flow regimes, like bubble/droplet or slug flow. However, simulation of two phase pipe flow can be done using the same mathematical models for both flow regimes. The respective closure relations on the other hand, will have to differ. The next sections will discuss the conservation laws and closure relations for the mentioned two phase system. It will describe the thermodynamic and physical properties needed in

multiphase flow simulators.

In Section 3.1, the basic equations for the two fluid model are described. Section 3.2 limits the model to a simple situation of stratified flow for simplicity. Section 3.3 includes some general comments on closure relations.

3.1 Conservation Laws

The model presented in this section uses a transient and one dimensional basis for all conservation laws. Only the x-axis is applied. An introduction to one dimensional modelling of two phase flow was given by Wallis (1969). Ishii (1975) presented the basic theory and equations for the two fluid model.

In transient single phase flow, three conservation equations are sufficient to describe the main conservation principles - mass conservation, momentum conservation, and energy conservation. The same equations apply for multiphase flow, one set of equations for each phase. The conservation equations for mass, momentum and energy will be given in the following sections, both for gas phase and for liquid phase. In Figure 3.1 by Solbraa (2002) some of the characteristic parameters used in the two fluid model are presented. Table 3.1 presents the symbols and units used in the conservation equations.

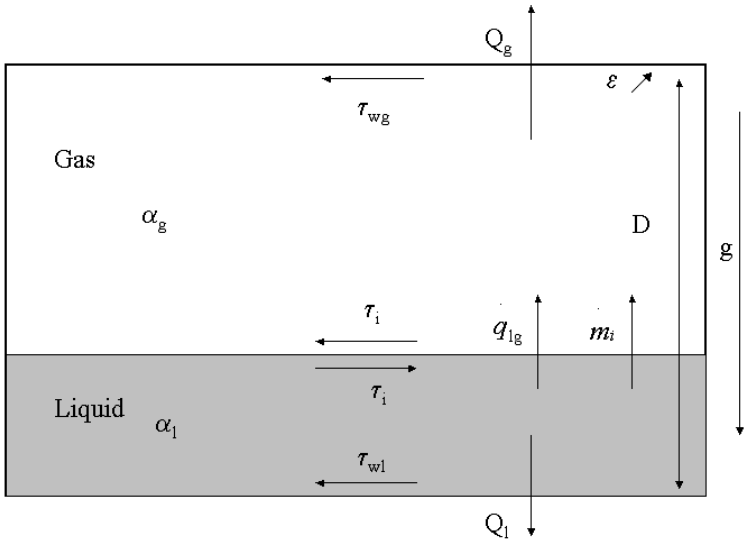

Figure 3.1: Illustration of symbols used in the conservation equations of the two fluid model, Solbraa (2002)

Variable	Description	Unit
m	Mass transfer	$kg/m \cdot sec$
τ_i	Interfacial liquid-gas shear stress	N/m^2
τ_{wg}	Wall-gas shear stress	N/m^2
τ_{wl}	Wall-liquid shear stress	N/m^2
α_l	Liquid phase fraction (holdup) $\left({}^{A_l}/_{A}\right)$	-
α_g	Gas phase fraction $\left({}^{A_g}/_{A}\right)$	-
Q	Heat flux from surroundings	$J/m{\cdot}sec$
q_{lg}	Interfacial heat flux	$J/m{\cdot}sec$
D	Pipe diameter	m
ε	Surface roughness	m
g	Gravity	m/sec^2

Table 3.1: Table of symbols and units used in the conservation equations of the two phase model

3.1.1 Mass Conservation

The conservation equations of mass for the gas and the liquid are given as

$$\frac{\partial(\alpha_g \rho_g A)}{\partial t} + \frac{\partial(\alpha_g \rho_g u_g A)}{\partial x} = m_{lg} - m_{gw} \tag{3.1}$$

$$\frac{\partial(\alpha_l \rho_l A)}{\partial t} + \frac{\partial(\alpha_l \rho_l u_l A)}{\partial x} = -m_{lg} - m_{lw} \tag{3.2}$$

where ρ is the density, A is the Area, and u is the velocity. α is the phase fraction defined as

$$\alpha_k = \frac{A_k}{A} \tag{3.3}$$

m_{lg} is the mass transfer between the phases, and m_{kw} is the mass transfer between phase k and other sources, such as inflow perforations in the pipe wall. The equations assume mass transfer from the liquid phase to the gas phase, which makes m_{lg} negative in the liquid equation. Also, the gain of one phase, must be the loss of the other, as phase change cannot result in altered total mass

$$\sum_{k=1}^{N} m_{ki} = 0 \tag{3.4}$$

Another useful relation follows from the definition of what a fraction is. The sum of all phase fractions must equal 1 to fill the cross section of the pipe

$$\sum_{k=1}^{N} \alpha_k = 1 \tag{3.5}$$

3.1.2 Momentum Conservation

The conservation equations of momentum for the gas and the liquid are given as

$$\frac{\partial(\alpha_g \rho_g u_g A)}{\partial t} + \frac{\partial(\alpha_g \rho_g u_g^2 A)}{\partial x} = m_{lg} u_i - m_{gw} u_g - \alpha_g A \frac{\partial P_g}{\partial x} - \alpha_g \rho_g A g sin\theta - s_{gw} \tau_{gw} - s_i \tau_i \quad (3.6)$$

$$\frac{\partial(\alpha_l \rho_l u_l A)}{\partial t} + \frac{\partial(\alpha_l \rho_l u_l^2 A)}{\partial x} = -m_{lg} u_i - m_{lw} u_l - \alpha_l A \frac{\partial P_l}{\partial x} - \alpha_l \rho_l A g sin\theta - s_{lw} \tau_{lw} + s_i \tau_i \quad (3.7)$$

where g is the gravity, and s is the cross sectional contact length between the phases or the wall. τ_{kw} is a frictional term for the wall, and τ_i is the interfacial friction. In the same manner as for the mass conservation equations, the interfacial friction term appears with opposite signs in the two equations.

3.1.3 Energy Conservation

The conservation equations of energy for the gas and the liquid are given as

$$\frac{\partial \alpha_g \rho_g A\left(U_g + \frac{u_g^2}{2} g z_g\right)}{\partial t} + \frac{\partial \alpha_g \rho_g u_g A\left(H_g + \frac{u_g^2}{2} + g z_g\right)}{\partial x} = q_{lg} + Q_g \quad (3.8)$$

$$\frac{\partial \alpha_l \rho_l A\left(U_l + \frac{u_l^2}{2} g z_l\right)}{\partial t} + \frac{\partial \alpha_l \rho_l u_l A\left(H_l + \frac{u_l^2}{2} + g z_l\right)}{\partial x} = -q_{lg} + Q_l \quad (3.9)$$

where z is a vertical coordinate, U is internal energy, H is enthalpy, and Q is heat transfer from the surroundings. q_{lg} is heat transfer from the liquid to the gas, and is therefore negative for the liquid equation. Also, the heat gain of one phase, must be the equal heat loss of the other.

$$\sum_{k=1}^{N} q_{ki} = 0 \quad (3.10)$$

3.2 Stratified Two Phase Flow

All equations in the previous section are general in their presented form. There are not brought in any fluid specific properties, such as how viscosity, density, surface tension and specific enthalpy varies with pressure and temperature. The equations presented are valid for any fluid, but they are not complete in this sense. To describe friction or heat, other correlations must be added. They are often referred to as closure relations, as they are needed to fulfil the equation set. With the help of these correlations, we are able to match the number of unknowns with the

number of equations.

To avoid getting lost in details a relatively simple situation is considered. There are only two fluids, one gas and one liquid. The pressures and temperatures are such that there is no evaporation or condensation. The gas does not dissolve in the liquid (which in real life is never quite true), and there are no perforations in the pipe. The flow is strictly stratified. To make the energy conservation equation redundant, the flow is assumed to be isothermal. These assumptions might seem unreasonable, but the mass transfer terms are often insignificant in cases where the rate of mass transfer is small compared to the flow rate of the phases. For long multiphase pipelines containing oil and gas this is usually the case, as pressures and temperatures change gradually.

3.2.1 Simplified Conservation Laws

In the given situation there are zero mass transfer between the phases, and also no mass transfer through the walls of the pipe. The mass conservation equations for the gas and the liquid, Equations 3.1 and 3.2, reduce to

$$\frac{\partial(\alpha_g \rho_g)}{\partial t} + \frac{\partial(\alpha_g \rho_g u_g)}{\partial x} = 0 \tag{3.11}$$

$$\frac{\partial(\alpha_l \rho_l)}{\partial t} + \frac{\partial(\alpha_l \rho_l u_l)}{\partial x} = 0 \tag{3.12}$$

with Equation 3.5 reduced to

$$\alpha_g + \alpha_l = 1 \tag{3.13}$$

As pressure variations due to different elevation of the two phases are neglected, the pressure on the interface can be defined as P. This reduces the momentum conservation equation for the gas and the liquid, Equations 3.6 and 3.7, to

$$\frac{\partial(\alpha_g \rho_g u_g A)}{\partial t} + \frac{\partial(\alpha_g \rho_g u_g^2 A)}{\partial x} = \alpha_g A \frac{\partial P}{\partial x} - \alpha_g \rho_g A g sin\theta - s_{gw}\tau_{gw} - s_i \tau_i \tag{3.14}$$

$$\frac{\partial(\alpha_l \rho_l u_l A)}{\partial t} + \frac{\partial(\alpha_l \rho_l u_l^2 A)}{\partial x} = \alpha_l A \frac{\partial P}{\partial x} - \alpha_l \rho_l A g sin\theta - s_{lw}\tau_{lw} + s_i \tau_i \tag{3.15}$$

As already mentioned, the energy conservation equations, Equations 3.8 and 3.9, are not needed in this case.

3.2.2 Closure Relations - Interfacial Shear

The closure relations which needs to be established for this particular situation is the interfacial shear, and the shear between the phases and the wall. The wall-gas shear can be calculated from

$$\tau_{wg} = f_{wg}\rho_g \frac{u_g^2}{8} \tag{3.16}$$

where f_{wg} is the Darcy friction factor. Similarly the wall-liquid shear can be calculated from

$$\tau_{wl} = f_{wl}\rho_l \frac{u_l^2}{8} \tag{3.17}$$

The interfacial shear can be calculated from

$$\tau_i = f_i\rho_g \frac{(u_g - u_i)^2}{8} \tag{3.18}$$

where u_i is the interfacial velocity. For simplicity the interfacial velocity can be assumed to be the same as the liquid velocity. f_i is the Darcy friction factor on the interface. To estimate the friction factor between a fluid and the wall the correlation presented by Haaland (1983) can be used

$$\frac{1}{\sqrt{f_w}} = -1.8\log_{10}\left[\frac{6.9}{Re} + \left(\frac{\varepsilon}{3.7D_h}\right)^{1.11}\right] \tag{3.19}$$

where Re is the Reynolds number, D_h is the hydraulic diameter, and ε is the roughness of the pipe wall. The interfacial friction factor can be estimated from an empirical correlation given by Wallis (1969)

$$\frac{f_i}{f_{wg}} = 1 + 0.75\alpha_l \tag{3.20}$$

where α_l is the liquid phase fraction (holdup). The Reynolds number is defined as

$$Re = \frac{uD_h\rho}{\eta} \tag{3.21}$$

where η is the viscosity. The hydraulic diameter is calculated from

$$D_h = \frac{4A}{O} \tag{3.22}$$

where A is the cross section area, and O is the wetted perimeter. The Haaland (1983) equation is an approximation of the implicit Colebrook equation. As described above the frictional factor in fully developed turbulent pipe flow depends on the Reynolds number and the relative pipe roughness $\frac{\varepsilon}{D}$. A functional form of this dependence cannot be obtained from a theoretical analysis, and the available results are obtained from experiments. The results are presented in tabular, graphical and functional form obtained by curve-fitting experimental data. Cyril F.

Colebrook combined the available data for transition and turbulent flow in smooth and rough pipes into the Colebrook equation given by

$$\frac{1}{\sqrt{f}} = -2.0log\Big(\frac{\varepsilon/D}{3.7} + \frac{2.51}{Re\sqrt{f}}\Big) \tag{3.23}$$

The graphical visualization of the Darcy friction factor led to the forming of the famous **Moody chart** which is one of the most widely accepted and used charts in engineering today (Cengel and Cimbala, 2014).

3.3 Other Properties for Closure Relations

Generally, more closure relations than shear stress are needed to complete a set of equations for multiphase flow. Examples are heat capacity, entropy and thermal conductivity. Simulation models rely on these properties to generate results. Table 3.2 presents the properties generated in NeqSim to use in simulation tools.

Variable	Description
ρ	Density
R_s	Gas mass fraction
η	Viscosity
C_p	Heat capacity
H	Enthalpy
k	Thermal conductivity
γ	Surface tension
S	Entropy

Table 3.2: Table of properties produced in NeqSim

Chapter 4

Theoretical Concepts

The critical concepts in this study are liquid viscosity and surface tension/interfacial tension. These are influential properties for fluid behaviour. This chapter will describe the properties as well as the models used to calculate them. There are numerous calculation models. We will focus on the models that are available in NeqSim and PVTsim, which are the software we will use to generate properties. NeqSim and PVTsim will be described in the next chapter.

In Section 4.1 the concept of liquid viscosity is described. Section 4.2 describes the models to calculate liquid viscosity. Section 4.3 describes the concept of surface tension, and section 4.4 describes the models used to calculate surface tension.

4.1 Liquid Viscosity

Liquid viscosity is the measure of a liquids internal resistance to flow. It is a function of temperature and pressure, and can be termed a drag force. Viscosity determines the hydrodynamic characteristics of fluids, such as flow rate and pressure drop. Because of this, liquid viscosities are critical for simulating pipeline flow. Pipeline design, pump characteristics, injection and transportation design heavily depend on liquid viscosity. The overall pressure drop is also essential to the hydraulic capacity of the pipeline.

There are two distinct forms of viscosity: Dynamic viscosity and kinematic viscosity. Dynamic viscosity is often simply referred to as viscosity in the literature and is the focus of this study. The SI-system utilizes the unit Pa·s for dynamic viscosity, where 1 Pa·s = 1 N·s/m^2 = 1 kg/(m·s). For practical use it is common to specify viscosity in milliPascal second or centipoise (1 mPa·s = 1 cP) as this gives more practical numerical values. Dynamic viscosity is defined by Viswanath et al. (2007) as "the tangential force per unit area required to slide one layer against another layer when the two layers are maintained at a unit distance". This means that dynamic viscosity is the ratio of the shear stress to the strain rate.

$$\eta = \tau \frac{x}{v} \tag{4.1}$$

where η is viscosity, τ is shear stress, x is length and v is velocity. Kinematic viscosity is the ratio of the dynamic viscosity of a fluid to its density.

$$v = \frac{\eta}{\rho} \tag{4.2}$$

where v is kinematic viscosity and ρ is density. Polling et al. (2001) establishes that liquid viscosity decreases with increasing temperatures and increases with increasing pressures.

4.2 Models to Calculate Liquid Viscosity

Historically the theoretical methods to calculate liquid viscosity have been inaccurate. This is due to the high complexity of liquid molecular structures and interactions. This has led the studies of viscosity to mainly focus on experimental measurements, and the establishment of empirical and semi-empirical formulas.

Theoretical models based on the corresponding state principle, the absolute rate theory of Eyring and the free volume theory have been developing in parallel. The book "Viscosity" by Touloukian et al. (1975) published several theories and models. Accurate theoretical models have emerged the last decades by combining these models with the cubic equations of state (EoS). The newly emerged friction theory, which is partially based on empirical formulas, is able to give good predictions for liquid viscosity. This section will give a brief introduction the mathematical models available in NeqSim and PVTsim, starting with the empirical models.

4.2.1 Empirical Models

Pure Compounds

For simplicity, it is often desirable to determine liquid viscosity from experimental data. There have been published numerous compilations of compound parameters that correlate these data. Arrhenius proposed in 1899 an equation which acts as a formula for the temperature dependence of reaction rates. In the case of liquid viscosity it is given by

$$\eta = \eta_0 e^{-E_\eta/(RT)} \tag{4.3}$$

where η_0 is the viscosity at some reference temperature, T is the temperature, E_η is the temperature coefficient for viscosity and R is the universal gas constant (Laidler, 1984). Equation 4.3 is an empirical relationship with numerous modifications and alterations developed over the years. Different datasets utilize empirical equations often based on the Arrhenius equation to

correlate their data. NeqSim utilizes a compound parameter list including empirical equations developed by Statoil, which is described in Section 5.2.2.

Grunberg and Nissan

Grunberg and Nissan (1949) established the one-parameter equation for correlating the liquid viscosity of nonpolar mixtures. It is based on the Arrhenius equation, Equation 4.3, but includes an additional term. It is given by

$$ln(\eta_{1,2}) = x_1 ln(\eta_1) + x_2 ln(\eta_2) + e x_1 x_2 \tag{4.4}$$

where x is the mole fraction of the respective compounds and e is an empirical interaction parameter.

LBC Correlation

The Lohrenz-Bray-Clark (LBC) correlation by Lohrenz et al. (1964) proposed an empirical correlation for the prediction of liquid viscosity of hydrocarbon mixtures based on their composition. According to Young et al. (2007) it is the most widely used viscosity model in reservoir engineering. This is due to its simplicity, consistency and flexibility. It is based on the empirical residual concept and the general structure of the LBC correlation is given by

$$\left((\eta - \eta_0)\xi + 10^{-4}\right)^{1/4} = a_0 + a_1\rho_r + a_2{\rho_r}^2 + a_3{\rho_r}^3 + a_4{\rho_r}^4 \tag{4.5}$$

where η_0 is the dilute gas limit viscosity, ξ is the viscosity reducing parameter and ρ_r is the reduced density of the fluid. The model predicts reasonable gas viscosities, but the oil viscosities are not accurate. Because of this it is necessary to tune the calculated viscosities.

PFCT Correlation

A popular correlation based on north sea oil is the Pedersen-Fredenslund-Christensen-Thomassen (PFCT) correlation by Pedersen et al. (1984). The model uses a parameter α to account for molecular size and density effects. It is given by

$$\eta_{mix}(P,T) = \left(\frac{T_{c,mix}}{T_{c,o}}\right)^{-1/6}\left(\frac{P_{c,mix}}{P_{c,o}}\right)^{2/3}\left(\frac{M_{mix}}{M_o}\right)^{1/2}\left(\frac{\alpha_{mix}}{\alpha_o}\right)\eta_o(P_o,T_o) \tag{4.6}$$

where o refers to the reference component, T is temperature, P is pressure, M is molecular weight and α is given by

$$\alpha_{mix} = 1 + 7.747x10^{-5}{\rho_r}^{4.265}{M_{mix}}^{0.8579} \tag{4.7}$$

$$\alpha_o = 1 + 8.374x10^{-4}{\rho_r}^{4.265} \tag{4.8}$$

where ρ_r is the reduced density of the reference fluid. The mixture molecular weight is given by

$$M_{mix} = 0.291(\overline{M}_w - \overline{M}_n) + \overline{M}_n \tag{4.9}$$

where $\overline{M}_w$ and $\overline{M}_n$ are the weight average and number average molecular weights. Pedersen et al. (1984) established that this model predicted the experimental viscosities with an error of less than 1 %. An improved version of this correlation was presented by Pedersen and Fredenslund (1987). The modified parameter α is given by

$$\alpha_{mix} = 1 + 7.378x10^{-3}{\rho_r}^{1.847}{M_{mix}}^{0.5173} \tag{4.10}$$

$$\alpha_o = 1 + 0.031x10^{-3}{\rho_r}^{1.847} \tag{4.11}$$

where the mixture molecular weight is now given by

$$M_{mix} = 1.304x10^{-}4(\overline{M}_w{}^{2.303} - \overline{M}_n{}^{2.303}) + \overline{M}_n \tag{4.12}$$

It was established that the predictions of light component liquid viscosities were markedly improved using the modified expression.

4.2.2 Friction Theory

Proposed by Quinones-Cisneros et al. (2000) the friction theory representd a new approach to the modelling of viscosity. Instead of regarding the viscosity of dense fluids as a transport property, it is now viewed as a mechanical property. The method is based on the friction concepts of classical mechanics and the van der Waals theory of fluids. The mechanical approach effectively separates the total viscosity into a dilute gas term and a friction term. It is given by Quinones-Cisneros et al. (2001) as

$$\eta = \eta_0 + \eta_f \tag{4.13}$$

where η_0 is the dilute gas term and η_f is the friction term. The friction term is linked to the Van der Waals attractive and repulsive pressure terms by analogy with the Amontons-Coulomb law of friction.

$$\eta_f = \kappa_r p_r + \kappa_{rr}{p_r}^2 + \kappa_a p_a \tag{4.14}$$

where κ_r, κ_{rr} and κ_a are temperature dependent friction coefficients, p_r is the repulsive term and p_a is the attractive term. To find the dilute gas viscosity term the model proposed by Chung et al. (1988) is used. The model can predict accurate dilute gas viscosities for several polar and nonpolar fluids over wide ranges of temperature. It is based on the Chapman-Enskog theory (Chapman and Cowling, 1970) and is given as

$$\eta_0 = 40.785 \frac{\sqrt{MT}}{{v_c}^{2/3}\Omega^*} F_c \tag{4.15}$$

where M is the molecular weight, v_c is the critical volume, Ω^* is the empirically determined reduced collision integral and F_c is another empirically determined factor. Originally the friction theory were restricted to use equations of state (EoS) explicitly consisting of a repulsive and an attractive term. This meant the use of EoS of the van der Waals type, such as the Soave-Redlich-Kwong EoS or the Peng-Robinson EoS. This limited the number of usable equations as well as the accuracy of the predicted viscosities. Quinones-Cisneros and Deiters (2006) extended the theory to all types of EoS, both theoretical and empirical. In combination with empirical EoS the friction theory was established to be able to predict experimental viscosity data with an accuracy as high as that of the requirements for reference models. This was concluded for several liquids, including water.

4.3 Surface Tension

At the interface between two phases there exist a contractile force which will try to minimize the area of the interface. Surface tension or interfacial tension is a quantitative measure of this force (Mork, 2004). The term *surface tension* is often used for single phase liquids, whilst *interfacial tension* is used for the interface of two immiscible liquids. In the literature the expressions are used interchangeably (Polling et al., 2001). In this theoretical section we will use to the term *surface tension* to simplify the explanations. However, *interfacial tension* is the preferred term in the oil and gas sector today, where the liquid usually consists of two or more substances. This is the term we will be utilizing later in the study when describing results and experimental work.

4.3.1 Attractive Intermolecular Forces

Between molecules in liquid and gas there is an imbalance of intermolecular forces. A molecule in the liquid bulk phase is symmetrically surrounded by other molecules in a way that makes the sum of all the attractive intermolecular forces equal to zero. This is displayed in Figure 4.1.

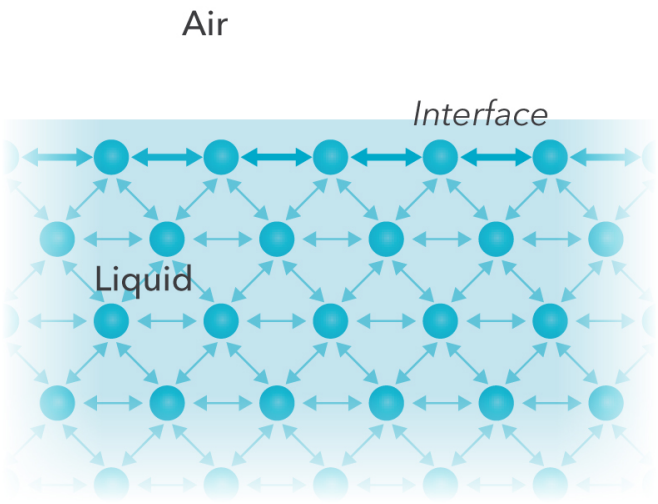

Figure 4.1: Intermolecular forces

The molecules at the liquid surface on the other hand is only affected by the attractive forces on the liquid side, since there are so "few" molecules in the gas phase that the interaction across the interface is negligible. The molecules at the surface are therefore exposed to a net force directed towards the liquid phase. In other words, the surface is trying to reduce its own area. The result of this is that the surface is in a constant state of tension, which is the reason why the force is named **surface tension** (γ). It can be defined as the **force per unit of length** which is acting perpendicular on any line on the liquids surface. To discourage the reduction of the surface area, a force F must be applied, $F = 2(\gamma \cdot L)$. The reason it is multiplied by 2 is that the film has two sides (front and back), each of which contributes equally to the force. This leads to

$$\gamma = \frac{F}{2L} \tag{4.16}$$

In the SI-system the unit for γ is N/m. It is common to specify γ in milliNewton per meter (1 mN/m = 10^{-3} N/m = 1 dyn/cm) as this gives more practical numerical values (Mork, 2004).

4.3.2 Excess Surface Free Energy

An alternative, and sometimes better method to quantify surface tension is to regard it as the cause of excess surface free energy. The surface tension leads to a demand of energy to increase the surface area. If the surface area is increased in the x-direction, dx, the total area increase of the surface (front and back) will be $dA = 2Ldx$. The work (dW) being done will be "stored" as an excess surface free energy (dG) given by:

$$dW = dG = Fdx = \gamma \cdot (2L)dx = \gamma dA \tag{4.17}$$

From Equation 4.17 we can see that surface tension can be expressed as

$$\gamma = \left(\frac{dG}{dA}\right)_{T,P} \tag{4.18}$$

i.e γ equals the **increase in surface free energy** (J/m^2) when the surface increases with one unit of area. This definition is equivalent with the "*force per unit length*" definition because $J/m^2 = N/m$, though the free energy-expression have the advantage of being easier to apply to the conventional thermodynamic (Norgaard and Nygaard, 2014).

4.3.3 Forces on a Curved Surface

When investigating surface tensions it is important to consider the mechanics of fluid surfaces. On a droplet there are forces acting upon the curved surfaces. This is illustrated in Figure 4.2.

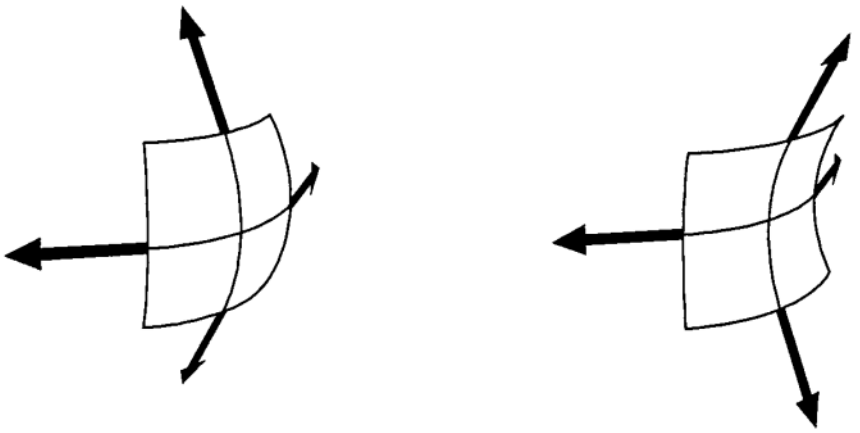

Figure 4.2: Forces on a curved surface, Norgaard and Nygaard (2014)

In the left picture of Figure 4.2 surface tension forces pull the surface towards the concave side. This means the pressure must be higher on the concave side of the surface. In the picture to the right the surface tension forces oppose each other, and therefore reduce the difference in pressure along the surface. The mean curvature of a two-dimensional surface is specified in terms of the two principal radii R1 and R2. A mechanical analysis shows that the pressure change across the surface is directly proportional to the surface tension, and to the mean curvature of the surface. This relationship is known as the Young-Laplace equation. The pressure change across the interface is named the Laplace pressure. The Young-Laplace equation is given by

$$P_A - P_B = \gamma\left(\frac{1}{R_1} + \frac{1}{R_2}\right) \tag{4.19}$$

The Young-Laplace equation can be written as coupled first-order differential equations in terms

of the coordinates of the surface as given by Norgaard and Nygaard (2014)

$$\frac{dx}{ds} = \cos\theta \tag{4.20}$$

$$\frac{dz}{ds} = \sin\theta \tag{4.21}$$

$$\frac{d\theta}{ds} = \frac{2}{R_0} + \left(\frac{\Delta\rho g}{\gamma}\right)z - \frac{\sin\theta}{x} \tag{4.22}$$

where Δp is the density difference, x and z is the horizontal and vertical coordinates, θ is the angle between the surface tangent and the horizontal plane, s is the arc length, R_0 the radius of the curvature at the drop apex and g is gravity. Figure 4.3 shows a pendant drop using the same coordinates as the Young-Laplace equation (Nilsen, 2001).

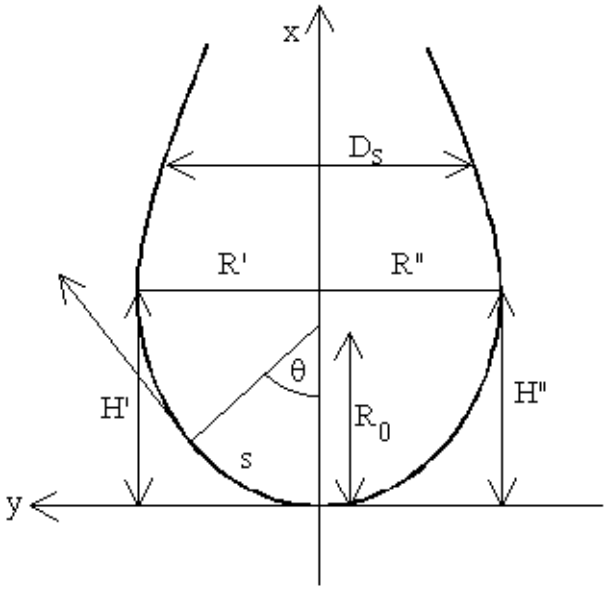

Figure 4.3: A Pendant drop, Norgaard and Nygaard (2014)

The drop has a neck at the top, which causes the two principal radii to have opposite denotations. The two radii have the same denotation at the bottom of the drop, which results in a larger mean curvature. If desired, the parameters in the Young-Laplace equation can be made dimensionless. This results in only one parameter β, the bond number, also called the shape factor

$$\beta = \Delta\rho g R_0^2/\gamma \tag{4.23}$$

4.4 Models for Calculating Surface Tension

There are several methods and models described in the literature to calculate surface tension. This chapter will focus on the methods available in NeqSim and PVTsim.

4.4.1 Parachor Method

There are several versions of the Parachor Method described in the literature. The most well known is the one presented by Weinaug and Katz (1943). It is based on Sugden's method for pure components from 1924, but is also expanded to mixtures. The surface tension heavily depends on the liquid density and the parachor value. The parachor value is defined by Negi and Anand (1985) as *the molar volume of a liquid at a temperature where its surface tension is unity*. The parachor values are computed from surface tension data, densities at equilibrium and molecular weights. The surface tension values are obtained by

$$\gamma^{1/4} = \sum_{i=1}^{N} P_i \left(\frac{\rho_l}{M_l} x_i - \frac{\rho_v}{M_v} y_i \right) \tag{4.24}$$

where P_i is the parachor value, M_v and M_l is molecular weight of the vapor and liquid phase respectively, ρ_v and ρ_l is the vapor and liquid density, y_i is the mole fraction of constituent i in the gas phase and x_i is the mole fraction of constituent i in the liquid phase

4.4.2 Firoozabadi and Ramey

Firoozabadi and Ramey (1988) developed a method to calculate surface tension between non-polar hydrocarbons and water. Ramey introduced an earlier version, but this one had troubles when applied to gas phase regions. The correlation was developed from experimental data which allows the interfacial tension to be calculated from the input of water and hydrocarbon densities and the reduced temperature of the hydrocarbon component.

$$\gamma^{1\backslash 4} = \frac{a_1 \Delta\rho^{(1-b_1)}}{T_r^{0.3125}} \tag{4.25}$$

where $\Delta\rho$ is the density difference between water and the hydrocarbons, T_r is a pseudo-reduced temperature for the hydrocarbon phase, and a_1 and b_1 are constants which depend on the $\Delta\rho$-value.

4.4.3 Gradient Theory

In this section the theoretical background of the Gradient Theory will be described briefly. The section is based on Nilsen (2008). Imagine there is a planar interface between vapour and liquid bulk phases. The interface thickness is denoted by z and equals the distance normal to the

interface. According to Gradient Theory, in the absence of external potentials, the differential equation that governs the density distribution $\rho(z)$ through the planar interface is given by

$$\sum_{j=1}^{N} \frac{d}{dz}\left(\kappa_{ij}\frac{d\rho_j}{dz}\right) - \frac{1}{2}\sum_{j=1}^{N}\sum_{k=1}^{N}\frac{\partial c_{jk}}{\partial \rho_i}\frac{d\rho_j}{dz}\frac{d\rho_k}{dz} = \frac{\partial \Phi(\rho)}{\partial \rho_i} \tag{4.26}$$

where κ denotes the influence parameter of the inhomogeneous fluid at the interface, and $\Phi(\rho)$ is the grand thermodynamic potential defined by

$$\Phi(\rho) = f^0(\rho) - \sum_i \rho_i \mu_{iB} \tag{4.27}$$

$$f^0(\rho) = \rho\mu(\rho) - P(\rho) \tag{4.28}$$

where f^0 is the local *Helmholtz free energy* density of homogeneous fluid at the interface grid of density $\rho(z)$ and μ_{iB} is the chemical potential of the component i in the bulk phase. Considering a planar interface between two bulk phases, the Gradient Theory states that the surface tension of a mixture is:

$$\gamma = \int_{-\infty}^{+\infty} \kappa_{ij}\frac{d\rho_i}{dz}\frac{d\rho_j}{dz}dz \tag{4.29}$$

To avoid solving a boundary value problem on the infinite interval $[-\infty,+\infty]$, a density variable ρ is defined to eliminate the position coordinate variable z, as z moves from $-\infty$ to $+\infty$ the density variable ρ will increase monotonically from ρ^I to ρ^{II}. To do this, the following equations are used

$$\frac{d\rho_i}{dz} = \frac{d\rho_i}{d\rho}\frac{d\rho}{dz} \tag{4.30}$$

$$\frac{d^2\rho_i}{dz^2} = \frac{d(\frac{d\rho_i}{d\rho})}{d\rho}\frac{d\rho}{dz}\frac{d\rho}{dz} + \frac{d\rho_i}{d\rho}\frac{d(\frac{d\rho}{dz})}{d\rho}\frac{d\rho}{dz} = \frac{d^2\rho_i}{d\rho^2}\left(\frac{d\rho}{dz}\right)^2 + \frac{d\rho_i}{d\rho}\frac{d\rho}{dz}\frac{d}{d\rho}\left(\frac{d\rho}{dz}\right) \tag{4.31}$$

where dz can be written as

$$dz = \sqrt{\frac{\sum_i\sum_j \kappa_{ij}\frac{d\rho_i}{d\rho}\frac{d\rho_j}{d\rho}}{2[\Phi(\rho)-\Phi_B]}}d\rho \tag{4.32}$$

The equation 4.29 can be rewritten in the following form by using the independent density variable ρ

$$\gamma = \int_I^{\rho^{II}} \sqrt{(2(\Phi(\rho)-\Phi_B)\sum_i\sum_j \kappa_{ij}\frac{d\rho_i}{d\rho}\frac{d\rho_j}{d\rho}}d\rho \tag{4.33}$$

Linear Gradient Theory

The Gradient Theory is quite complicated and time-consuming. A set of either algebraic or differential equations have to be solved by numerical methods before interfacial tensions in mixtures can be calculated. This makes it difficult to apply Gradient Theory to multicomponent mixtures and reservoir simulations.

Zuo and Stenby (1996) developed a Linear Gradient Theory. It is assumed that the densities of each component, $\rho_i(z)$, are linearly distributed across the interface with width h, between a liquid phase and gas phase given by

$$\frac{d\rho_i(z)}{dz} = D_i, \qquad D_i = \frac{\Delta}{\rho}_i h = \frac{\rho_{iL} - \rho_{iV}}{h} \tag{4.34}$$

where D_i is a constant for component i. According to the densities of component i in the coexisting vapor and liquid phases (boundary conditions) , the density of component i at position z can be uniquely determined. This makes it unnecessary to solve a set of differential or algebraic density profile equations.

Chapter 5

Software

This chapter describes the software utilized for this Master's thesis. The description is based on material from the OLGA 7 user manual (Schlumberger, 2013), Solbraa (2002) and the PVTsim technical overview (Calsep, 2016).

The multiphase flow simulator OLGA comprise advanced fluid mechanical and numerical models. A property table generation tool, such as NeqSim or PVTsim, generates the thermodynamic and physical properties needed for the simulations. In general, all fluid properties can be expressed in terms of pressure, temperature and composition. Given a fluid composition for a certain temperature and pressure range, a property table is generated. Based on the received properties, OLGA is able to simulate the multiphase flow for various situations. This means that the simulation in OLGA is only as good as the properties it is given.

In Section 5.1 the multiphase flow simulator tool OLGA is described. Section 5.2 describes the process simulator NeqSim, and Section 5.3 describes the simulation program PVTsim.

5.1 OLGA

OLGA is a three fluid model. This means that separate conservation equations are applied for the gas, the oil and the water phase. The fluids are coupled through interfacial mass transfer in a similar way as the described two fluid model in Section 3.1. The velocity of any liquid droplets in the gas phase is given by a slip relation.

One mixture energy equation is applied, assuming that all phases are the same temperature. This yields seven conservation equations and one equation of state to be solved. The seven conservation equations are three equations for mass and momentum, one for each phase, and one for energy. The equation of state is for the pressure calculations.

5.1.1 OLGA HD

OLGA HD is a module available in OLGA 7.3.5. The module is described as a high-definition stratified flow model. The model is developed to provide more consistent, scalable and accurate predictions of pressure drop and holdup for systems dominated by stratified and large wave flow regimes. It can be used for all simulations, but will only be beneficial for these flow regimes.

The OLGA HD module is a friction model. The module applies a parametrized two-dimensional velocity distribution to obtain frictions and velocity shape factors in the cross section. Combining the two-dimensional velocity distribution with the one-dimensional conservation equations, described in Section 3.1, results in a three-dimensional representation of a slowly evolving flow. The velocity distribution in each layer is given by a generic layer model, which determines the frictions and the momentum flux terms. This makes the traditional closure relations of one-dimensional models redundant (D.Biberg et al., 2015). The model can handle one to three phase layers. Figure 5.1 illustrates the case of three phase layers.

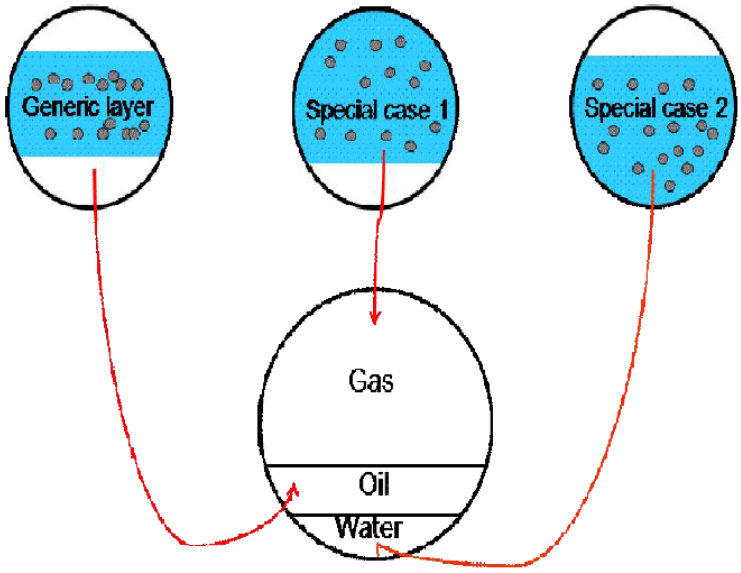

Figure 5.1: Illustration of the generic layer model utilized in OLGA HD, Schlumberger (2013)

The generic model is utilized for all three layers. Coupling the layers yields a full three phase model. This constitutes an analytic expression for the velocity distribution in the generic layer. Dispersions are assumed to travel with the same velocity as the continuous phase, i.e. there is assumed local no-slip. Non uniform distributions yield a profile slip (bulk slip).

Pre-integration yields a generic wall friction law formulated as a generalized friction factor relation. In the case of single phase flow it reduces to the Colebrook equation, Equation 3.23.

Continuity in forces and velocities across the interfaces is used to find generic expressions for the interface friction. In the case of two- and three-phase flow the module is highly complex. A brief description of the calculation method is given in Appendix A.

5.2 NeqSim: A General Non-Equilibrium Simulator

NeqSim (Non-Equilibrium Simulator) was developed by Solbraa (2002). It is described as a dynamic process simulator especially designed to handle non-equilibrium situations. Common non-equilibrium processes include absorption, drying processes, hydrate formation and multiphase flow in pipelines. NeqSim is also capable of solving normal equilibrium process calculations.

NeqSim utilizes a method developed by Michelsen and Mollerup (1986) which makes it possible to build a thermodynamic library where it is easy to change and implement different thermodynamic models. NeqSim has a large library of different models to utilize for calculations. This includes the modern and accurate SRK-CPA equation of state, which gives accurate predictions even for polar components.

5.2.1 Property Simulation

The thermodynamic and physical property models available in NeqSim has the potential to make it a great property simulation tool. The development of NeqSim as a property table generator was started by Solbraa (2002) and continued by Bjortuft (2014). This Master's thesis is a continuation of a project thesis conducted in the fall of 2015. The project thesis compared the performance of NeqSim to the performance of PVTsim. It was demonstrated that NeqSim showed a similar capability to PVTsim, both for two phase simulations and three phase simulations.

One of the recommendations for further work was developing and evaluating the calculation models for interfacial tension between hydrocarbons and glycol as well as the effect of TEG on the liquid viscosity. NeqSim has the earlier mentioned benefit of utilizing many of the modern calculation models available today. The calculation models for viscosity and interfacial tension available in NeqSim includes the ones described in Chapter 4.

5.2.2 Viscosity

All the models described in Section 4.2 are available in the NeqSim library. However, only the Grunberg and Nissan (1949) theory is developed enough to be utilized by the software at the time of this study. Compounds are listed with four liquid viscosity parameters in the Statoil

database. The compounds are also given a specific number which decides the empirical equation to calculate their liquid viscosity. The parameters are tuned in cohesion with their respective equation and the liquid viscosity calculation model is automatically generated by NeqSim. The four different equations in use are given by

$$\eta = A \cdot T^B \tag{5.1}$$

$$\eta = e^{(A+B/T)} \tag{5.2}$$

$$\eta = e^{(A+B/T+C\cdot T+D\cdot T^2)} \tag{5.3}$$

$$\eta = 10^{A\cdot(1/T+1/B)} \tag{5.4}$$

where A, B, C and D are the liquid viscosity parameters and T is the temperature. The equation utilized to calculate the liquid viscosities of TEG, water and methane is Equation 5.3. To correlate the viscosity of mixtures the Grunberg and Nissan (1949) mixing rule is applied.

5.2.3 Interfacial Tension

Interfacial tension can be calculated using the models described in Section 4.4. The interfacial tension model can be manually decided in NeqSim. The Parachor and the Firoozabadi Ramey methods are available in full. All compounds in the Statoil database is given its own parachor parameter to calculate accurate values. The Gradient Theory is available in a simple version, a more advanced version and as Linear Gradient Theory. The full Gradient Theory is being developed, but is not ready to be utilized at the time of this study.

5.3 PVTsim

PVTsim (Pressure, Volume and Temperature simulator) was developed by Calsep. It is described as a *"versatile equation of state modelling software that allows the user to simulate fluid properties and experimental PVT data"*(Calsep, 2016). PVTsim is an established property generator in the market today. It calculates fluid properties using classical equations of state, such as the SRK-EoS (Soave-Redlich-Kwong)or the PR-EoS (Peng-Robinson). These equations give good predictions for mixtures only involving hydrocarbons. However, they struggle when dealing with more complex polar components, like water and TEG.

5.3.1 Viscosity

To calculate liquid viscosity values of aqueous solutions PVTsim utilizes a similar approach as NeqSim. Compounds are listed with viscosity parameters in the PVTsim database, and the empirical equation is automatically generated. After the viscosity of the pure compounds are calculated, the mixing rule of Grunberg and Nissan (1949) is applied to correlate the mixture viscosity.

5.3.2 Interfacial Tension

Interfacial tensions between a water phase and a hydrocarbon phase is calculated by the Firoozabadi Ramey Method, described in Section 4.4.2. This includes calculations with TEG.

Chapter 6

Collected Experimental Data

Experimental data relevant to this study has been collected. Section 6.1 presents the data gathered for viscosity. Section 6.2 presents the data gathered for interfacial tension. A summary of the gathered experimental data are presented in Table 6.1.

Description	Components	Pressures	Reference
Viscosity	TEG, water	Atmospheric	Sun and Teja (2003), Tsai et al. (2009), Guo et al. (2011), Sagdeev et al. (2011), Begum et al. (2012)
	TEG, water, methane	High	Ng et al. (2009)
Interfacial tension	TEG, water	Atmospheric	Begum et al. (2012)
	Water, methane	High	Kashefi (2012)
	TEG, water, methane	High	Ng et al. (2009)

Table 6.1: Presentation of collected experimental data

6.1 Viscosity

6.1.1 Viscosity of TEG

Several studies have been conducted for mixtures comprising up towards 100 wt% TEG. The study Sagdeev et al. (2011) was conducted using aqueous TEG consisting of 98,5 wt% TEG. The other studies chosen all comprise more than 99.5 wt% TEG. The data claims to have an uncertainty of between 0.3 % and 2 %. Experimental values for viscosity at atmospheric pressure are plotted in Figure 6.1 as a function of temperature. The different datasets are in good agreement and shows a clear tendency of decrease in viscosity with the increase of temperature.

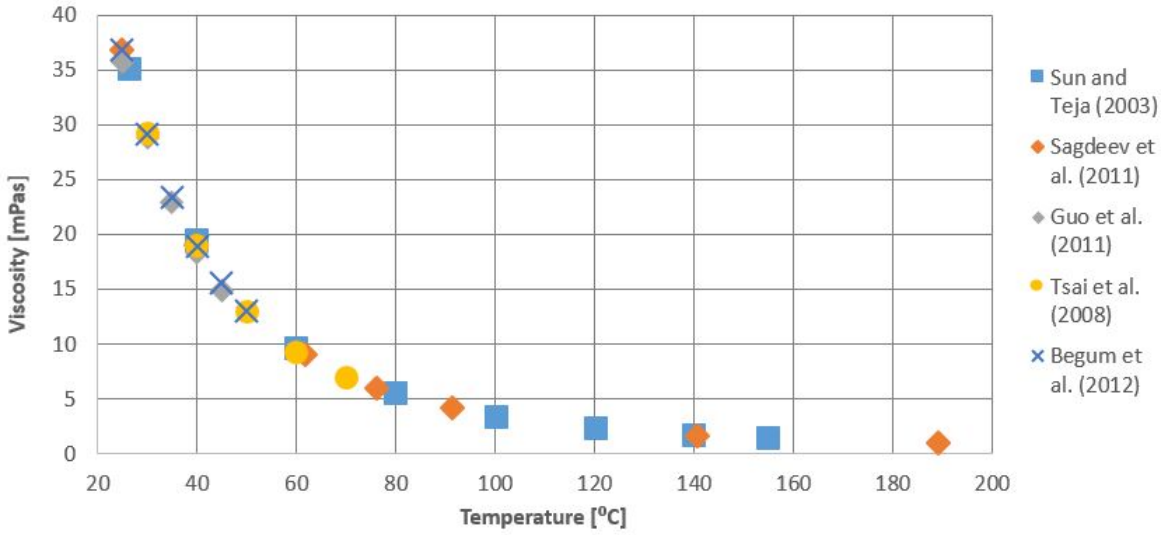

Figure 6.1: Experimental data of the viscosity of TEG at atmospheric pressure and temperatures 25 - 190 °C.

6.1.2 Viscosity of Aqueous TEG

Figure 6.2 plots the experimental values from Sun and Teja (2003) for viscosity of four aqueous solutions containing various amounts of TEG as a function of temperature. The reported uncertainty of the study is 2%. The pure TEG utilized is specified to comprise a minimum of 99.9 wt% TEG. The study established a decrease in viscosity with the increase of temperature for all weight fractions of TEG.

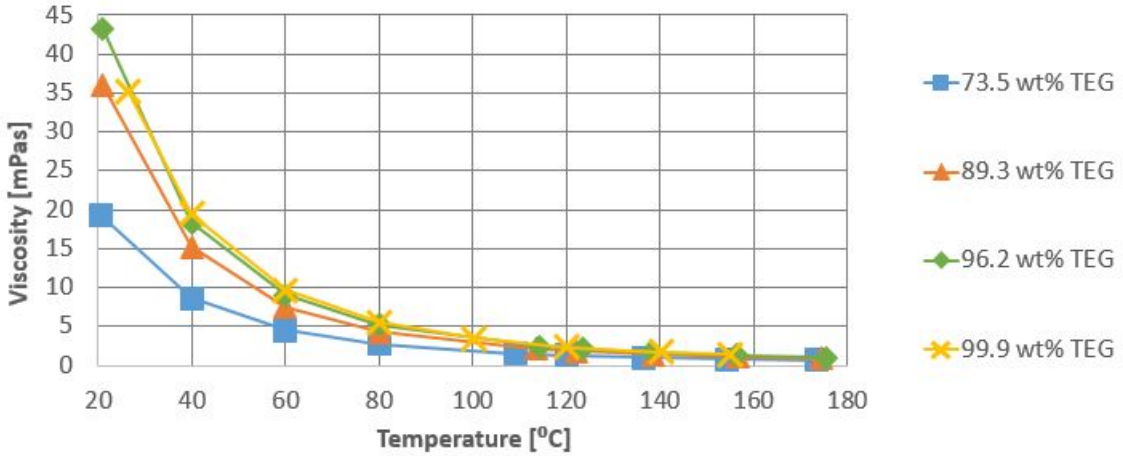

Figure 6.2: Experimental data of the viscosity of aqueous TEG at atmospheric pressure and temperatures 20 - 180 °C, Sun and Teja (2003).

Figure 6.3 plots the viscosity values of aqueous mixtures at five different temperatures as a function of weight fractions of TEG, obtained from Begum et al. (2012). The study reported an un-

certainty in the viscosity measurements of up to 0.04 mPas. The pure TEG utilized in this study is specified to comprise up towards 99,9 wt% TEG. The study shows an increase of viscosity with the increase of TEG weight fraction for all temperatures.

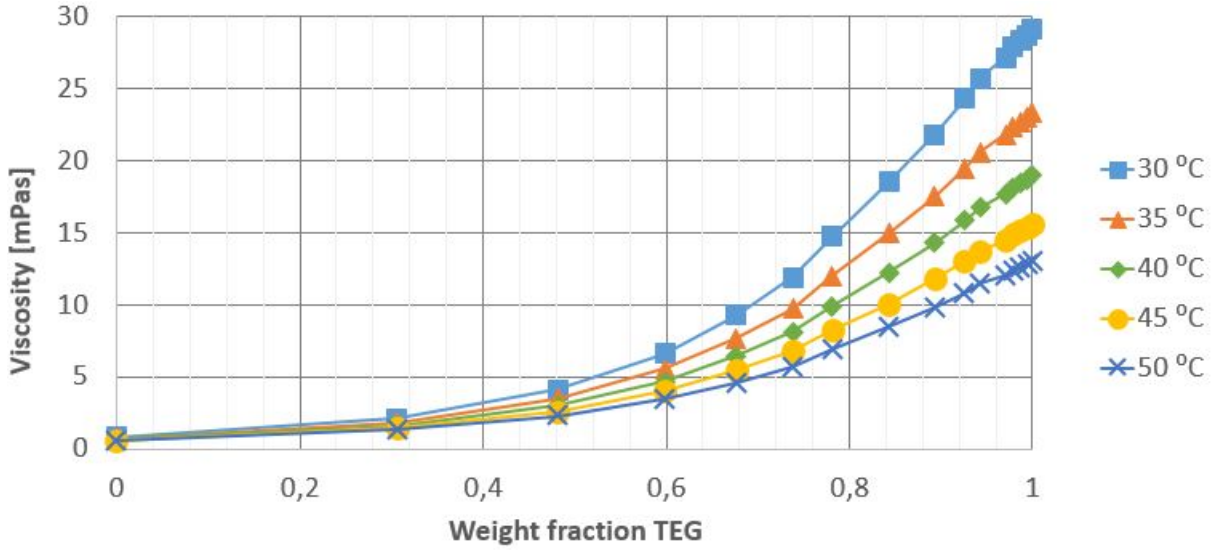

Figure 6.3: Experimental data of the viscosity of aqueous TEG at atmospheric pressure and weight fractions 0 to 1, Begum et al. (2012).

6.1.3 Viscosity of Aqueous High Pressure TEG and Methane

There exists one study with experimental data for viscosity of aqueous TEG in methane. The study is conducted by Ng et al. (2009) utilizing a Cambridge Electromagnetic Viscometer (EMV) and has a claimed uncertainty of 1 %. The aqueous TEG used in the study consisted of 98 wt% TEG and 2 wt% water. Experimental values for viscosity of the mixture in equilibrium are plotted in Figure 6.4 as a function of pressure. The study concluded that the viscosity remains relatively constant as a function of pressure at a given temperature.

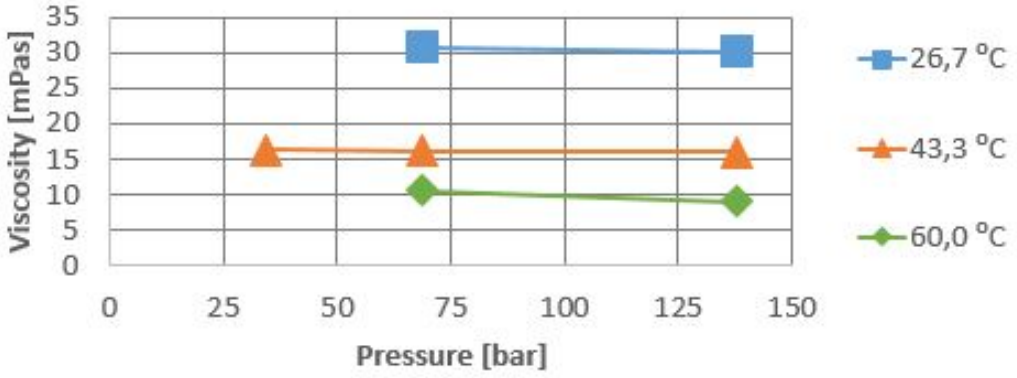

Figure 6.4: Experimental data for the viscosity of TEG containing methane in equilibrium at pressures 34 - 138 bar, Ng et al. (2009).

6.2 Interfacial Tension

6.2.1 Measurement Methods

The Wilhelmy Plate Method

The measurement is conducted by immersing a thin plate into a liquid. After it is immersed, the plate is pulled back up. The interfacial tension between the plate and the liquid will hold the plate back. The additional force needed, F, to pull the plate level with the liquid surface is related to the surface tension and given by Webster (1999) as

$$F \cdot cos\theta = 2\gamma(l + t) \tag{6.1}$$

where θ is the contact angle, often zero, l is length of the plate, t is the thickness and γ is the interfacial tension.

Pendant Drop Method

A liquid droplet (heavier phase) is suspended in the equilibrated vapor or liquid (lighter phase). The bubble is created by the use of a needle mounted on the top of the cell which the liquid flows through. The shape of the droplet is determined by the interfacial tension and gravity. The interfacial tension tries to minimize the surface area and get the droplet into a spherical shape, while gravity stretches the droplet. This is what gives the droplet the typical pear-like shape. By utilizing this method it is possible to calculate the interfacial tension from a shadow image of the pendant droplet using a shape analyser. The analysis is based on the Young-Laplace equation mentioned in Section 4.3 (Webster, 1999).

Rising Bubble Method

A bubble of the lighter phase is upward in the equilibrated denser phase. The bubble is created by the use of a needle mounted in the bottom of the cell. The gas rises through the needle. The analysis procedure of the bubble is similar to that of the pendant drop method, using the Young-Laplace equation mentioned in Section 4.3 (Webster, 1999).

6.2.2 Interfacial Tension of Aqueous TEG and Air

The study Begum et al. (2012) conducted experimental research using the Wilhelmy paper plate method, which is described in Section 6.2.1, at atmospheric pressure. Each measurement was conducted six times and the average was taken. The reported error of the study is up to 0.51 mN/m. Figure 6.5 plots the experimental values of the interfacial tension of the solution and air as a function of weight fraction of TEG in the aqueous solution. The study was conducted at 303.15 K and concluded that an initially sharp decrease in surface tension was observed with the addition of TEG to the water. Most of the total decrease occurs within 0.2 weight fraction of glycol. Increasing weight fractions leads to the interfacial tension decreasing slowly towards the value of pure TEG. The pure TEG is specified to comprise up towards 100 wt% TEG.

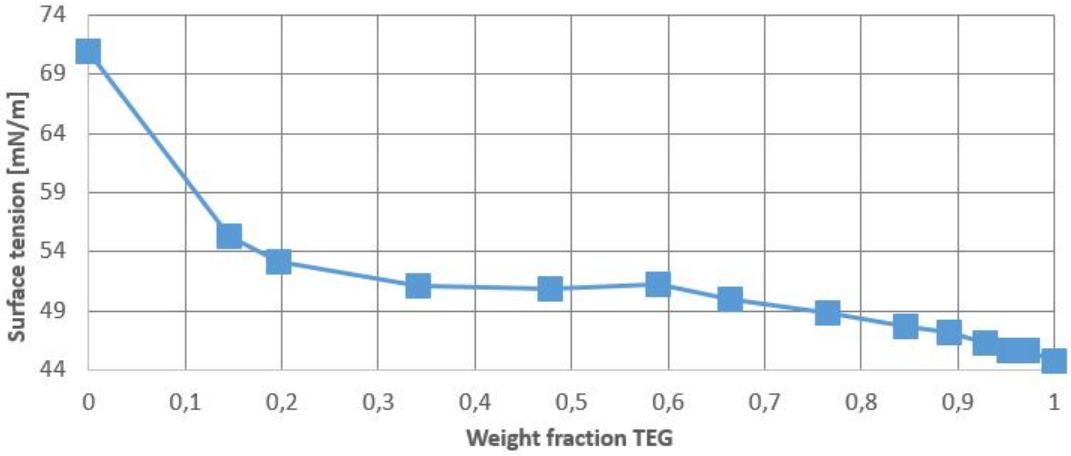

Figure 6.5: Experimental data of interfacial tension of aqueous TEG and air at 30 °C, Begum et al. (2012).

6.2.3 Interfacial Tension of High Pressure Water and Methane

The study Kashefi (2012) conducted high pressure interfacial tension measurements of water and methane. The measurements was conducted using the rising bubble method at 37.8°C and the pendant drop method at temperatures 100, 150 and 200°C. The study did not report uncertainties. The study established a sharp decreasing trend with the increase of pressures

up to about 275 bar for all temperatures. Figure 6.6 plots experimental values of the interfacial tension as a function of pressure.

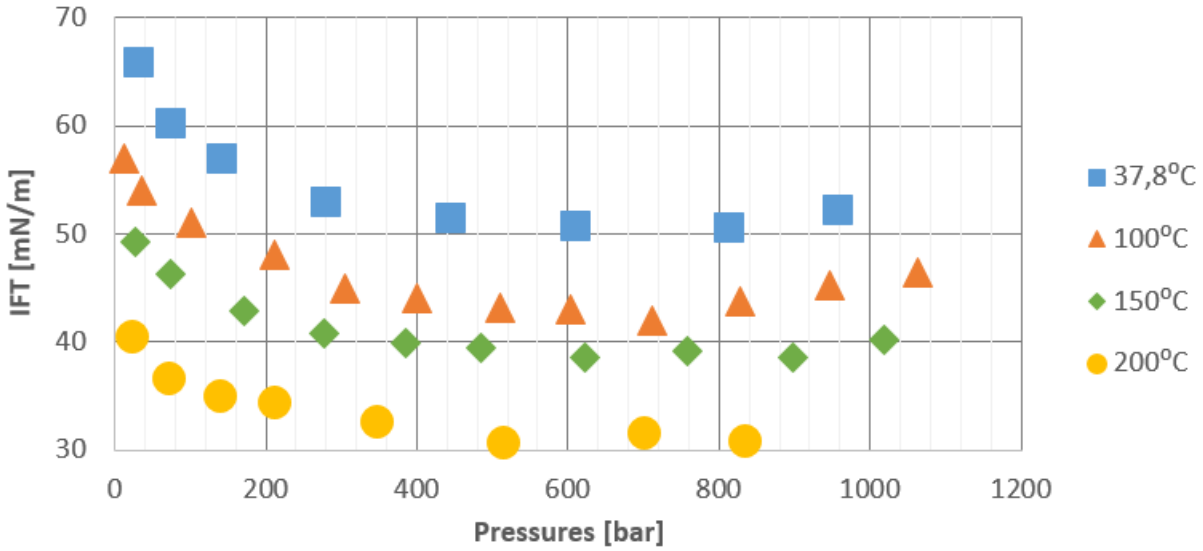

Figure 6.6: Experimental data of the interfacial tension of water and methane in equilibrium at pressures 12 - 1064 bar, Kashefi (2012).

6.2.4 Interfacial Tension of High Pressure Aqueous TEG and Methane

One study exists which conducted high pressure interfacial tension measurements of aqueous TEG and methane. The study was conducted by Ng et al. (2009) using the pendant drop method described in Section 6.2.1. The interfacial tension is claimed to be known within an error of 4%. The aqueous TEG used in the study consisted of 98 wt% TEG and 2 wt% water. The study concluded that the interfacial tensions of the system exhibited a decrease with increasing pressure. Figure 6.7 plots experimental values of the interfacial tension as a function of pressure. The values at 43.3°C and 60°C are very similar. The values at 26,7°C are noticeably higher.

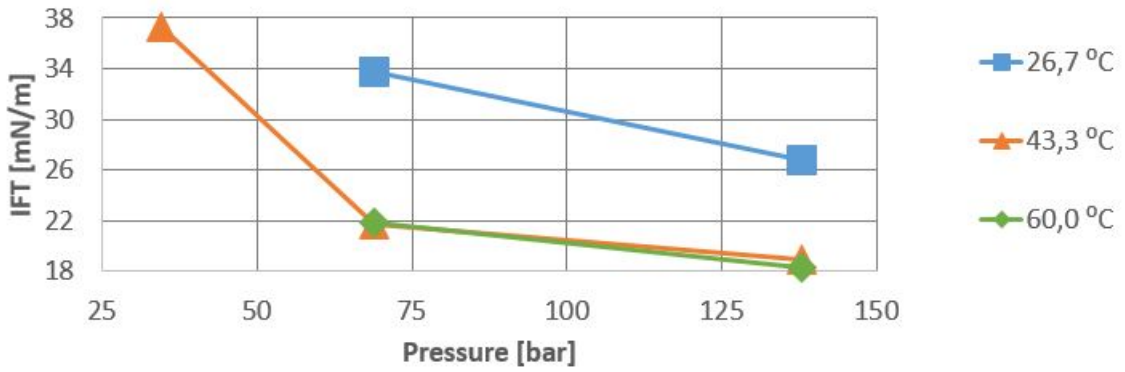

Figure 6.7: Experimental data of the interfacial tension of aqueous TEG and methane in equilibrium at pressures 34 - 138 bar, Ng et al. (2009).

Figure 6.8 plots experimental values of the interfacial tension as a function of temperature. The values are decreasing with the increase of temperature between 26.7 and 43.3°C.

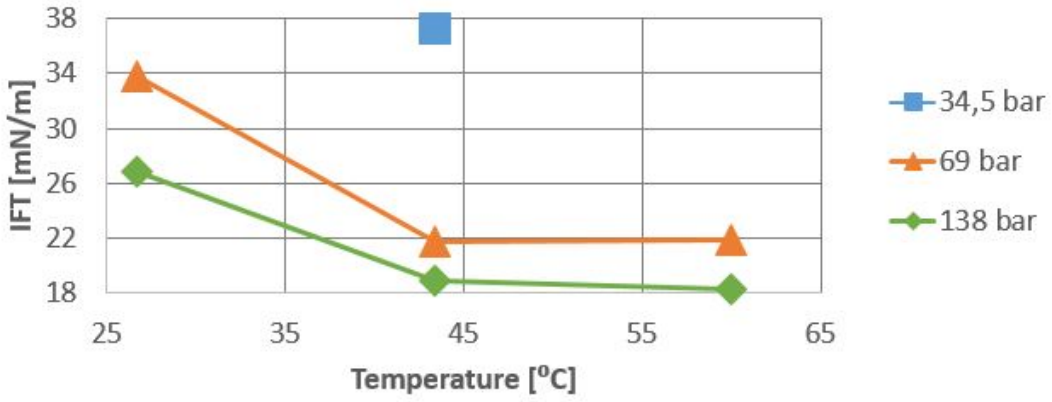

Figure 6.8: Experimental data of the interfacial tension of aqueous TEG and methane in equilibrium at temperatures 25-60 °C, Ng et al. (2009).

Chapter 7

Experimental Setup

Section 7.1 describes the apparatus utilized for this study and Section 7.2 the procedure. Section 7.3 specifies the fluid utilized.

7.1 Experimental Apparatus

7.1.1 Temperature Test Chamber

To conduct high pressure measurements of interfacial tension, it is important to be able to set a specific temperature which remains constant during the measurements. The temperature test chamber model VT^3 7150 from Vötsch Industrietechnik was utilized for the laboratory work. Figure 7.1 shows the climate chamber model VC^3 4034 which looks similar and is of the same series as the one utilized in this study. Nearly every part of the system was placed inside the chamber which provided constant temperatures during the measurements.

Figure 7.1: Climate Test Chamber VC^3 4034

7.1.2 Schematic Overview

A flow sheet of the vapour and liquid flow path is presented in Figure 7.2. The blue dotted line illustrates the temperature chamber, and the devices within this line is placed inside the chamber. The Gas Chromatograph (GC) and the accompanying liquid and gas sampling valves illustrated in the flow sheet were not utilized for the measurements. The equipment is presented in detail below, and technical information is provided in Table 7.1

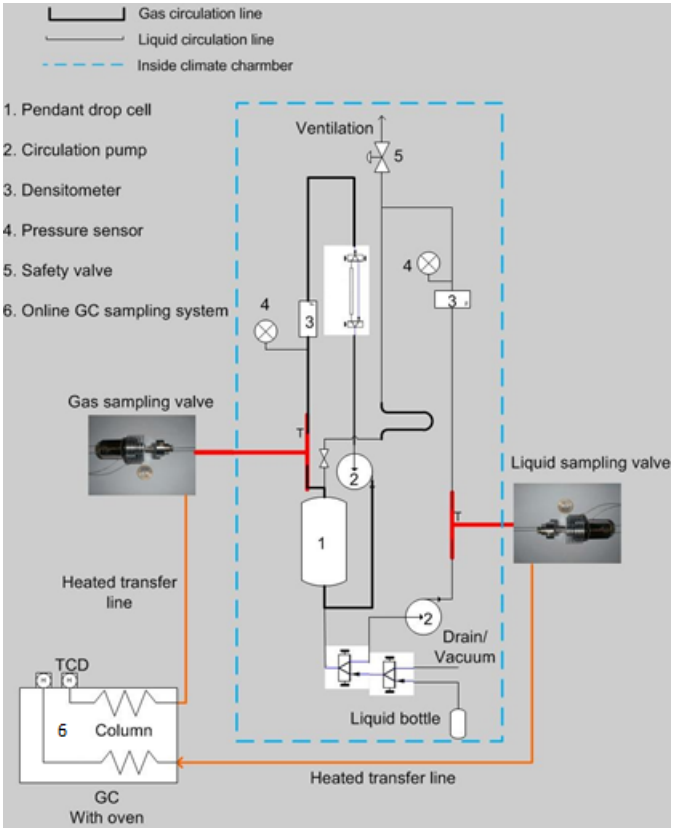

Figure 7.2: Flow sheet of High Pressure Interfacial Tension Rig,(Norgaard and Nygaard, 2014)

.

7.1.3 Pendant Drop Cell

The measurements were conducted using the pendant drop method described in Section 6.2.1. The pendant drop cell is where the measurements are conducted. Within the pressure and temperature range of the cell, experiments can be done safely and accurately. Inside the cell the liquid droplets are formed at the tip of a needle. The droplet is surrounded by gas. A two-stem valve is used to control the drop formation. The cell is transparent. A video microscope is used to view the formation of the droplet and to measure the droplet dimensions. The measurements and calculations are done automatically using an image analysis software. (Tem, 2004)

7.1.4 Densitometer

There are two densitometers of the the type Anton Paar DMA HPM. One is measuring liquid densities and the other one gas densities. The external cells of the densitometers measure the period of harmonic oscillation of the built-in U-tube, which contains the mixture. The period of oscillation is converted into the densities of the mixture by an evaluation unit (Paar, 2004). More information regarding the evaluation unit is given in Table 7.1.

7.1.5 Pressure Sensors

There are two pressure sensors which measures the liquid and gas pressures separately. A quartz crystal temperature signal is provided to thermally compensate the calculated pressure and achieve high accuracy over a broad range of temperatures (Paroscientific, 2005).

7.1.6 Circulation Pump

A high pressure liquid pump is utilized to circulate the liquid from the pendant drop cell through the needle. It is important to insure that the stem valve in the drop cell is open to avoid liquid pressure build-up. The liquid pump is a key apparatus to obtain a stable phase equilibrium in the cell.

Name	Description
Climate Test Chamber	Provider: Vötsch Industrietechnik. Type: VT^3 7150 Temperature Range: -75° C - 180°C Max Pressure: 150 bar
Pendant Drop Cell	Provider: Temco, Inc. Model: IFT-10 Pressure Range: 0-690 bar Max Temperature:177°C Cell Volume: 41.5 cm^3
Video Camera	Provider: Ramé-Hart Instrument Co. Lens: Cosmicar Television lens; 50mm, 1:1.8 Software: Drop Image
Liquid Circulation Pump	Provider: Eldex Laboratories, Inc. Type: ReciPro® Liquid Metering Pumps Model: B - 100 - S - 2CE Flow Rate: Flow rate: 0.2 - 8 ml/min Temperature Range: 5°C-35°C Pressure Range: 0-344.7 bar Serial Number: 17742
Pressure Sensor	Provider: Paroscientific, Inc. Type: Digiquartz® Pressure Transducer Model: 410KR-HHT-101 Instrument Number: 3172 Temperature Range = 0°C-177°C Pressure Range: 0 - 689.5 bar
Densitometer	Provider: Anton Paar GmbH External measuring cell: DMA HPM Number:80309444 Evaluation unit: mPDS 2000V3 Instrument Number:3116 Pressure Range: 0-1400 bar Temperature Range: $-10°C$ - 200°C
Light source	Model: BODSON GBE 75 Microscope Ligth Source.

Table 7.1: Technical Equipment Information

7.2 Experimental Procedure

The experiment procedure includes three parts. The process of filling the rig with gas and liquid, the mixing process and the measurements.

7.2.1 Filling the Rig

The gas in use for the experiments is enclosed in a container outside of the climate test chamber. To fill gas, a pressure level is set from the tank by using a constant pressure valve. The amount of gas is decided by the desired measurement pressure, and is not measured in this experiment. The valve marked "Drain/Vacuum" in the flow sheet in Figure 7.2 is opened, allowing the gas to flow into the system.

The liquid is stored in a liquid cylinder inside the climate test chamber. The cylinder can be seen in the bottom of the flow sheet marked "Liquid bottle". The cylinder is connected to a volume displacement pump outside of the chamber. The pump is set to a higher pressure than the pendant drop cell pressure to push the liquid into the cell. Again, the pressure of the pump is decided by the desired measurement pressure.

7.2.2 Mixing Process

The circulation pump is turned on to let the gas and liquid circulate the system. The circulation provides the physical contact needed between the liquid and gas phase for the mixture to reach equilibrium. Liquid is evaporated and transferred into the gas phase. The gas is diffused into the liquid phase. In the beginning the mass transfer rate between the phases is fast, and the pressure is rapidly reduced. Figures 7.3 and 7.4 displays the pressure stabilization process for liquid and gas respectively for 100 wt% TEG and 20°C over the course of 24 hours.

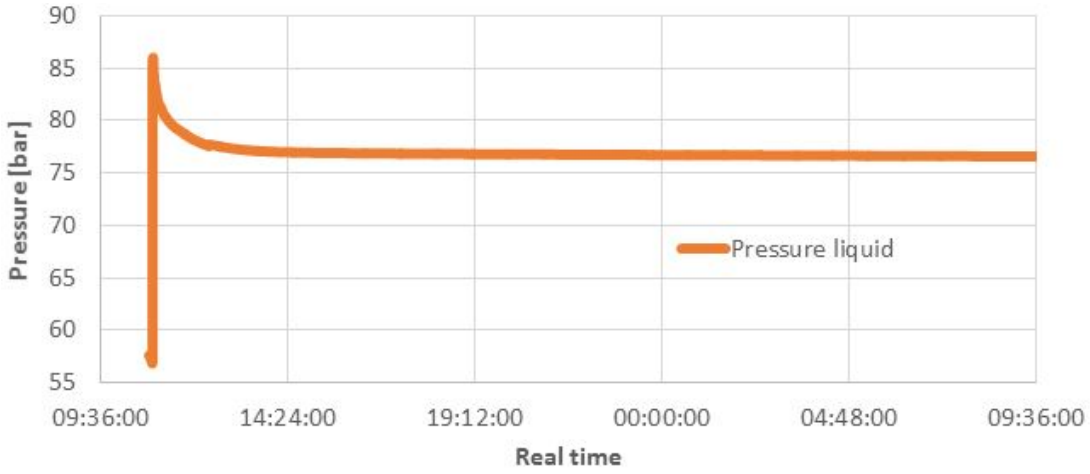

Figure 7.3: Pressure stabilization process of the liquid phase for 100 wt% TEG and methane at 20 °C.

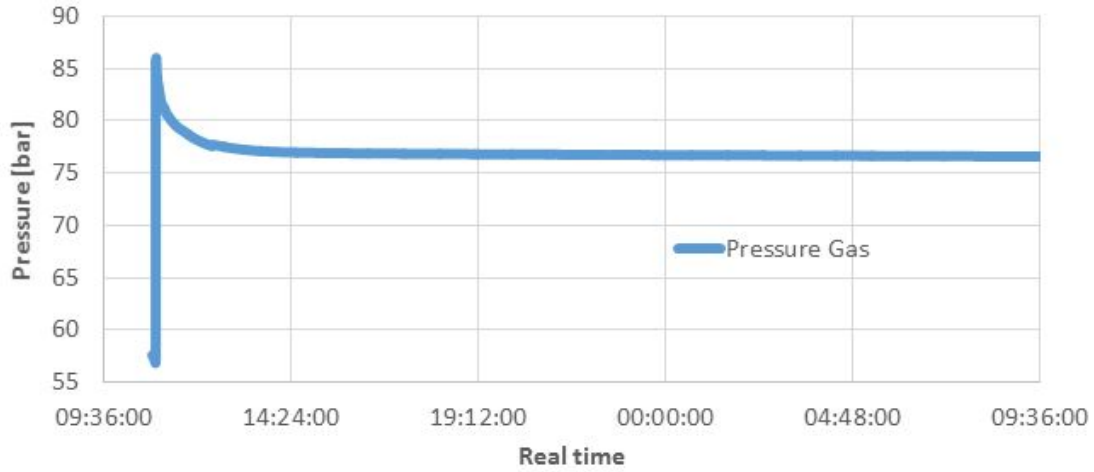

Figure 7.4: Pressure stabilization process of the vapor phase for 100 wt% TEG and methane at 20 °C.

As displayed in Figures 7.3 and 7.4 the pressure stabilizes at a lower value than the filling pressure. This means achieving the desired measurement pressure is a difficult task. The filling pressure is always set higher than the desired measurement pressure due to the pressure decreasing as the system reaches equilibrium.

7.2.3 Measurements

The liquid and gas densities, temperatures and pressures are measured by the equipment described in Section 7.1. The circulation pump is turned off, and the stem valve is used to form a droplet inside the cell. The drop hangs from the needle, and the camera takes pictures of it. The

shape is related to the interfacial tension by the shape parameters R_0 and β, described in Section 4.3.3. These parameters are determined from the drop profile, and DropImage Advanced uses them to calculate the interfacial tension values. To obtain stable values, the measurements are conducted when the shape of the drop has stabilized, about a minute after it is formed. Ten drops are formed and analysed at each temperature and pressure level. The software takes a hundred pictures of each droplet, which leads to one thousand measurements at each condition. Figure 7.5 shows an image of a droplet used for measurement.

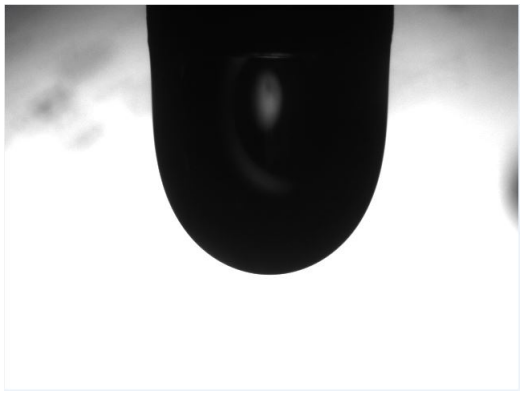

Figure 7.5: Picture of droplet from DropImage Advanced. 20 °C, 90 wt% TEG and 196.6 bar.

7.3 Fluid Specification

The methane utilized in the laboratory work is provided by Air Liquide Norway AS. It is specified as Methane: N55, which means it has a standard purity of 99.9995 mole%.

The TEG used is provided by Merck Schuchardt OHG with CAS number: 112-27-6. The exact measured weight composition of the utilized liquid mixtures is given in Table 7.2.

Mixture	**TEG [wt%]**	**Water [wt%]**
100 wt% TEG	99.85	0.15
90 wt% TEG + 10 wt% water	90.05	9.95

Table 7.2: Compostition of TEG/water mixtures

Chapter 8

Experimental Results

The experimental conditions are presented in Section 8.1. The data obtained from our experimental work are presented in Section 8.2. The uncertainty analysis of the interfacial tension measurements conducted is given in Section 8.3.

8.1 Experimental Conditions

Interfacial tension are measured at three temperature levels (4.3°C, 20°C and 41.5°C) and three pressure points (50, 100, 200 bar) for both liquid mixtures described in Section 7.3. As described in Section 7.2, achieving the desired pressure is a difficult task. Because of this the measurements are conducted at pressures similar to the specified pressures. Also, some temperature levels have more than three pressure measurements.

8.2 Experimental Results

The results of our experimental laboratory work are presented in Table 8.1.

Liquid composition	Temperature [°C]	Pressure [bar]	Interfacial tension [mN/m]	Liquid density [g/cm^3]	Vapor density [g/cm^3]
100 wt% TEG	4.3	54.3	**34.0**	1.1355	0.0439
		76.2	**29.8**	1.1339	0.0646
		96.5	**27.5**	1.1316	0.0847
		192.8	**21.3**	1.1373	0.1768
	20	57.7	**34.2**	1.1227	0.0434
		95.5	**27.3**	1.1266	0.0757
		172.5	**22.0**	1.1204	0.1429
		218.6	**21.0**	1.1233	0.1760
	41.5	52.6	**34.7**	1.1050	0.0362
		101.8	**29.7**	1.1032	0.0724
		197.8	**23.0**	1.1011	0.1427
90 wt% TEG + 10 wt% water	4.3	54.5	**34.9**	1.1312	0.0629
		106.4	**29.4**	1.1306	0.1100
		209.9	**23.5**	1.1313	0.1899
	20	55.6	**36.2**	1.1198	0.0420
		108.4	**28.1**	1.1185	0.0874
		196.6	**25.2**	1.1190	0.1594
	41.5	53.2	**36.6**	1.1032	0.0382
		96.9	**31.5**	1.1014	0.0699
		189.2	**25.6**	1.1021	0.1381

Table 8.1: Experimental matrix

8.2.1 100 wt% TEG

Figure 8.1 plots experimental values of the interfacial tension as a function of pressure for 100 wt% TEG.

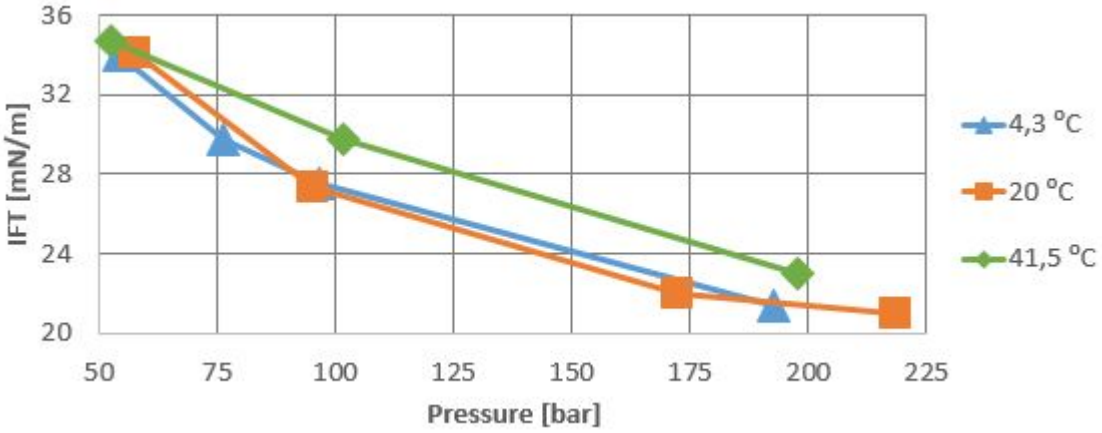

Figure 8.1: Experimental data of the interfacial tension of methane and TEG in equilibrium at pressures 50-225 bar, 100 wt% TEG

The interfacial tension values decreases with the increase of pressure. The values at 4.3°C and 20°C are very similar for all pressures. The values at 41.5°C are similar to the rest at 50 bar, but is somewhat higher at increased pressures. It appears that the interfacial tension slightly increases with the increase of temperature between 20 and 41.5°C.

8.2.2 90 wt% TEG

Figure 8.2 plots experimental values of the interfacial tension as a function of pressure for 90 wt% TEG.

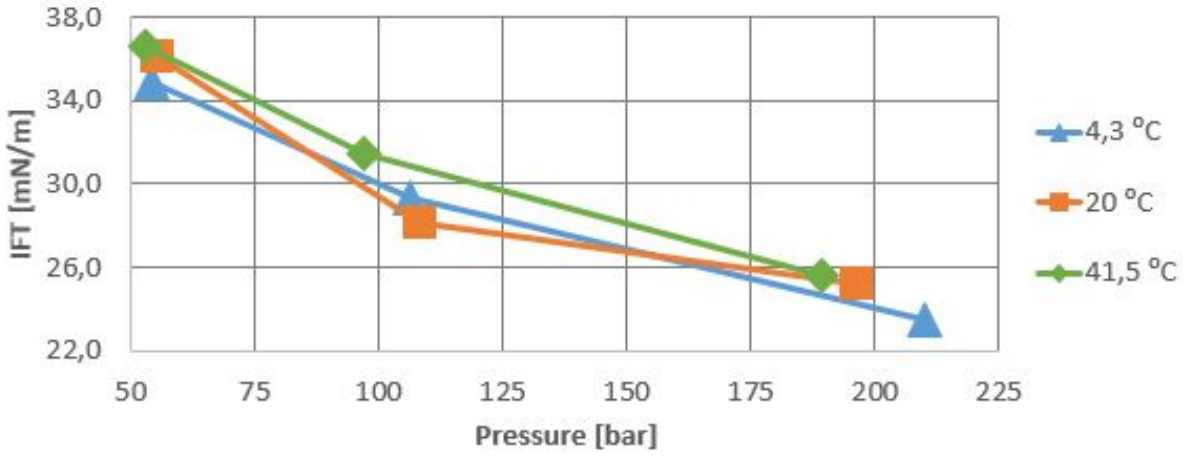

Figure 8.2: Experimental data of the interfacial tension of methane and aqueous TEG in equilibrium at pressures 50-210 bar, 90 wt% TEG.

The interfacial tension values decreases with the increase of pressure. The values at 41.5°C are consistently higher than those of 4.3°C, and the shapes of the lines are very similar. It appears

that the interfacial tension slightly increases with the increase of temperature between 4.3 and 41.5°C. The values at 20°C are close to that of the other two temperature levels, but with a different slope. The interfacial values at around 50 and 200 bar are very similar to that of 41.5°C, while the values at around 100 bar are lower.

8.2.3 Comparing Values of Liquid Mixtures

Figures 8.3, 8.4 and 8.5 plots experimental values of the interfacial tension for both liquid mixtures as a function of pressure at temperatures 4.3°C, 20°C and 41.5°C.

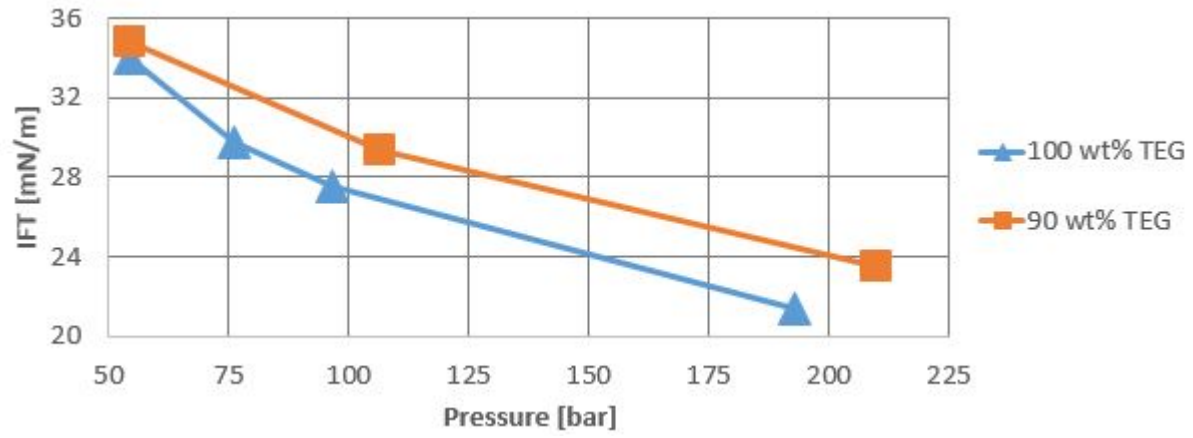

Figure 8.3: Experimental data of the interfacial tension of methane and aqueous TEG in equilibrium at pressures 50-220 bar and 4.3°C.

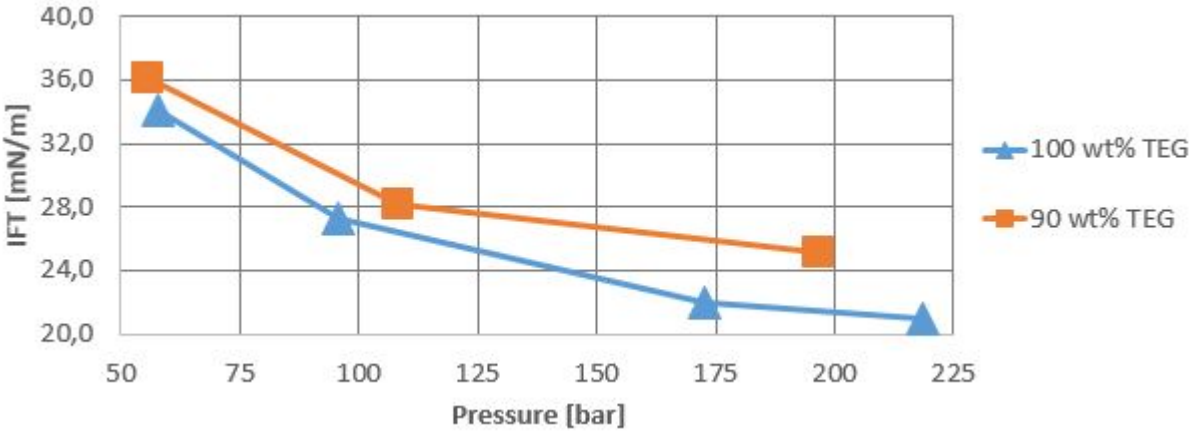

Figure 8.4: Experimental data of the interfacial tension of methane and aqueous TEG in equilibrium at pressures 50-220 bar and 20°C.

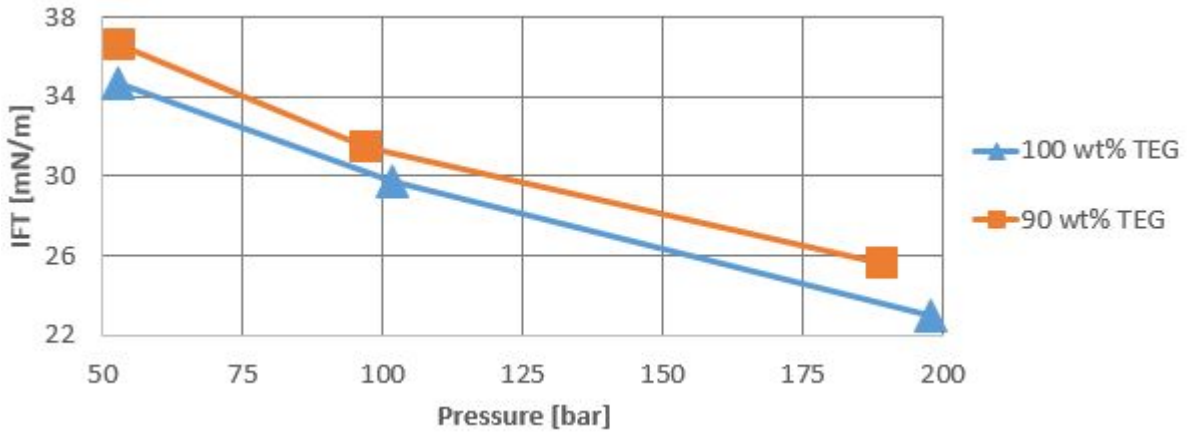

Figure 8.5: Experimental data of the interfacial tension of methane and aqueous TEG in equilibrium at pressures 50-200 bar and 41.5°C.

Figures 8.3, 8.4 and 8.5 display consistently higher interfacial tension values for the aqueous solution containing 90 wt% TEG. This seems logical given that water has a higher surface tension than TEG, as shown in Section 6.2.2. The difference appear to increase slightly with pressure.

8.3 Uncertainty Analysis

When evaluating experimental data the overall uncertainty of the measurements has to be considered. This is the sum of the uncertainty of the drop shape analysis, $e_1(\gamma)$, and the uncertainty of the measured conditions, $e_2(\gamma)$. The data measured for 100 wt% TEG at 4.3°C is used as an example of how the calculation is conducted. The total uncertainty is given at the end of this section.

The gas pressure gauge and temperature sensors are calibrated by the manufacturer. The temperature sensors are integrated in the high pressure densitometers. The uncertainties of the density measurements and the other measuring equipment are given in Table 8.2.

Condition	Uncertainty
Temperature	±0.1° C
Pressure	0.01 %
Liquid density, $e(\rho_{liq})$	±4.2472 x $10^{-3} g/cm^3$
Vapor density, $e(\rho_{vap})$	±4.4252 x $10^{-3} g/cm^3$
Methane composition	0.0005 mole%

Table 8.2: Uncertainty of measured conditions

8.3.1 Drop Shape Analysis

At each temperature and pressure condition ten droplets were made. 100 pictures were taken of each droplet over the course of 20 seconds to obtain accurate measurements of the interfacial tension. The uncertainty of the drop shape analysis is related to the camera and the software used for the measurements. The uncertainty can be calculated by obtaining the standard deviation of the interfacial tension values in our experimental data. The standard deviation is given by

$$e_1(\gamma) = \sqrt{\frac{1}{N}\sum_{i=1}^{N}(\gamma_i - \overline{\gamma})^2} \tag{8.1}$$

where N is the total number of measurements taken at every experimental condition. e_1 is the average deviation for one droplet and is revealed by the fluctuations of the interfacial tension values. Figure 8.6 plots the measured interfacial tension values of the tenth droplet for the different pressures at 100 wt% TEG and 4.3°C over time. The stable interfacial tension values measured shows that there was good equilibrium in the experimental conditions during the measurement process.

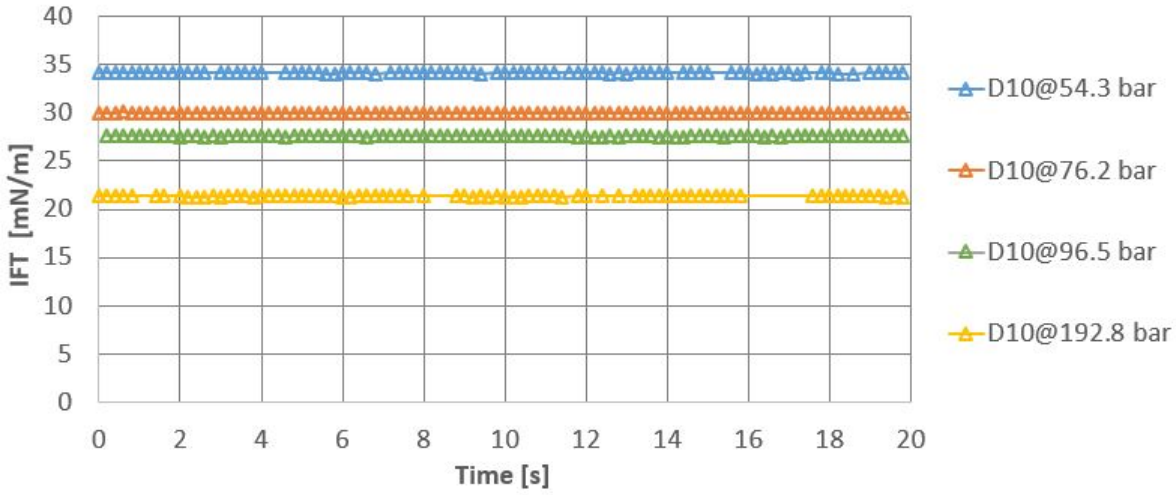

Figure 8.6: Experimental interfacial tensions over time for 100 wt% TEG at 4.3°C

8.3.2 Measured Conditions

The uncertainty of the measured conditions is the combined deviation related to the measured phase densities, shape factor and apex radius. To calculate the uncertainty of the measured conditions we have utilized the combined standard uncertainty calculation of the measured interfacial tension provided by ISO (2008) given as

$$e_2(\gamma) = \sqrt{\left(\frac{\partial\gamma}{\partial\rho_{liq}}e(\rho_{liq})\right)^2 + \left(\frac{\partial\gamma}{\partial\rho_{vap}}e(\rho_{vap})\right)^2 + \left(\frac{\partial\gamma}{\partial\beta}e(\beta)\right)^2 + \left(\frac{\partial\gamma}{\partial R_0}e(R_0)\right)^2} \tag{8.2}$$

where β is the shape factor and R_0 is the apex radius. $e(\beta)$ and $e(R_0)$ is the respective standard deviations of our measured values and $e(\rho_{liq})$ and $e(\rho_{vap})$ are given in Table 8.2. The partial derivatives can be found by

$$\frac{\partial\gamma}{\partial\rho_{liq}} = \frac{g{R_0}^2}{\beta} \tag{8.3}$$

$$\frac{\partial\gamma}{\partial\rho_{vap}} = -\frac{g{R_0}^2}{\beta} \tag{8.4}$$

$$\frac{\partial\gamma}{\partial\beta} = -\frac{(\rho_{liq}-\rho_{vap})}{\beta^2}g{R_0}^2 \tag{8.5}$$

$$\frac{\partial\gamma}{\partial R_0} = 2\frac{(\rho_{liq}-\rho_{vap})}{\beta}gR_0 \tag{8.6}$$

where g is gravity. The input variables of Equation 8.2 for 100 wt% TEG at 4.3°C are listed in Table 8.3.

Pressure [bar]	ρ_{liq}	ρ_{vap}	β	$e(\beta)$	R_0	$e(R_0)$	g
54.3	1.1355	0.0439	0.583	0.00234	1.361	0.00201	9.81
76.2	1.1339	0.0646	0.617	0.00181	1.324	0.00099	9.81
96.5	1.1316	0.0847	0.629	0.00513	1.299	0.00486	9.81
192.8	1.1373	0.1768	0.653	0.00585	1.216	0.00484	9.81

Table 8.3: Input variables to Equation 8.2

8.3.3 Overall Uncertainty

The calculated results for the overall uncertainty of 100 wt% TEG at 4.3°C is given in Table 8.4. The total uncertainty is the sum of e_1 and e_2. It is given both in [mN/m] and in percentage of the value of the average interfacial tension at the given pressure.

Pressure [bar]	Interfacial tension [mN/m]	e_1 [mN/m]	e_2 [mN/m]	e_{tot} [mN/m]	e_{tot} [%]
54.3	34.03	0.117	0.256	0.373	1.10
76.2	29.77	0.101	0.197	0.298	1.00
96.5	27.54	0.067	0.345	0.412	1.50
192.8	21.33	0.037	0.290	0.327	1.53
Average					**1.28**

Table 8.4: Uncertainties for 100wt% TEG at 4.3°C

The total average uncertainty for both mixtures utilized in the experiments at different temperature levels are given in Table 8.5.

Mixture	Temperature [°C]	e_{tot}[%]
100 wt% TEG	4.3	1.28
	20	2.12
	41.5	1.73
	Average	1.71
90 wt% TEG	4.3	2.88
	20	1.47
	41.5	1.17
	Average	1.84
Average		**1.78**

Table 8.5: Experimental uncertainty

It can be noted that the uncertainties are well distributed. The uncertainties for the mixture of 90 wt% TEG is somewhat higher than that of 100 wt% TEG, but the difference is negligible. There seems no systematic error exists in our experimental process.

Chapter 9

Comparison of Experimental and Simulated Data

Simulated values from NeqSim and PVTsim are compared to experimental data in this chapter. In Section 9.1 the comparison of simulated values against the collected experimental viscosity data in Section 6.1 is presented. Section 9.2 presents the comparison of simulated values against the collected interfacial tension data in Section 6.2. Section 9.3 compares simulated interfacial tension and density values to experimental data obtained in this study. Section 9.4 compares experimental interfacial tension values obtained in this study to those of Ng et al. (2009). Section 9.5 evaluates the different simulation tools.

9.1 Collected Viscosity Data Compared to Simulated Data

9.1.1 Viscosity of TEG

NeqSim calculates liquid viscosity as described in Section 5.2.2. The viscosity is calculated using Equation 5.3 and NeqSim applies the Grunberg and Nissan (1949) mixing rule described in Section 4.2.1. PVTsim calculates the liquid viscosity as described in Section 5.3, also utilizing the Grunberg and Nissan (1949) mixing rule. The liquid viscosity values obtained in NeqSim and PVTsim will be compared to the collected experimental data in this section.

The study Sun and Teja (2003) was conducted using aqueous TEG specified to comprise a minimum of 99.9 wt% TEG with a claimed uncertainty of 2%. In practical terms, this is as close to pure TEG as possible. Simulations were conducted for pure TEG. The obtained values are compared to the experimental data in Figure 9.1.

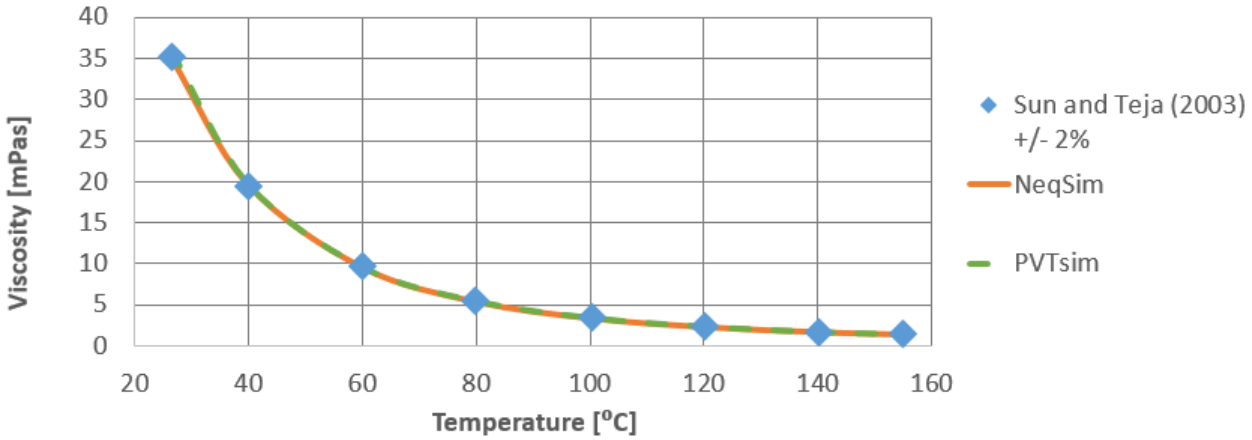

Figure 9.1: Calculated liquid viscosities of TEG compared to experimental data at atmospheric pressure and temperatures 25 - 160 °C, Sun and Teja (2003).

The results are in good agreement. The average deviation of the values in NeqSim is 1.3%, which is within the deviation range of 2%. The largest deviation is 3.1% at 80°C. The average deviation of the values in PVTsim is 1.0% and the largest deviation is 2.4% at 27°C. PVTsim is marginally more accurate than NeqSim in comparison to the experimental data.

9.1.2 Viscosity of Aqueous TEG

The study Sagdeev et al. (2011) was conducted using aqueous TEG consisting of 98,5 wt% TEG with a claimed uncertainty of 2%. Figure 9.2 displays the obtained simulated values of the mixture plotted against the experimental data.

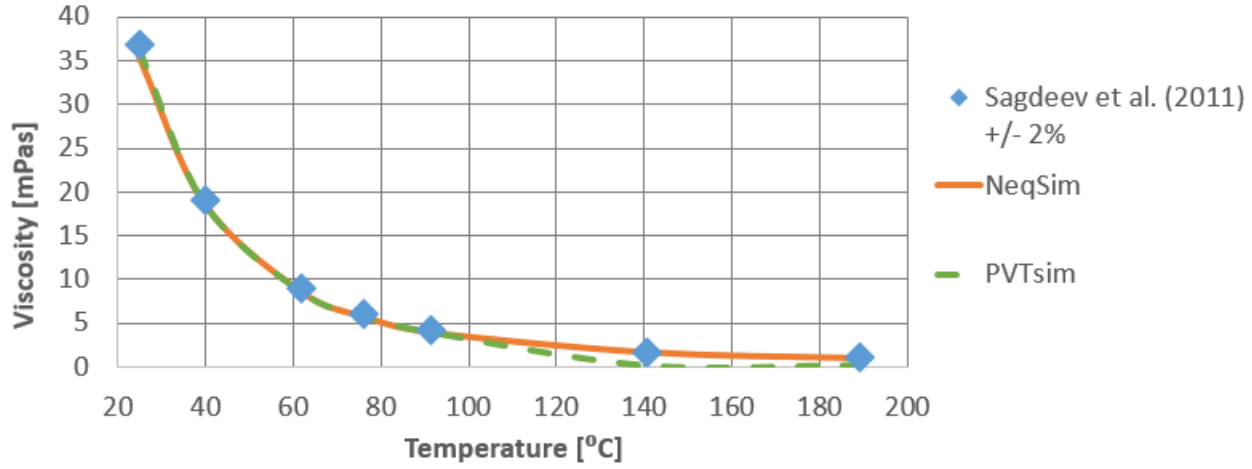

Figure 9.2: Calculated liquid viscosities of 98.5 wt% TEG in aqueous solution compared to experimental data at atmospheric pressure and temperatures 25 - 190 °C, Sagdeev et al. (2011).

The results are in good agreement. The average deviation of the values in NeqSim is 3.5%. The largest deviation is 5.1% at 91°C. The average deviation of the values in PVTsim is 24.9%. PVTsim

simulates accurate values at temperatures below 100°C, where the average deviation of the values is 2.3% compared to 3.7% in NeqSim. However, at 140 and 189°C the deviations in PVTsim are larger than 70%. Both property simulators experience larger deviations than with pure TEG. PVTsim is slightly more accurate at temperatures below 100°C, while NeqSim has a significantly better prediction at higher temperatures.

The study Begum et al. (2012) conducted measurements of the viscosity of various weight fractions of TEG in aqueous solution. The reported uncertainty of the study is 0.04 mPas. The pure TEG is specified to comprise up towards 100 wt% TEG. Figure 9.3 displays the obtained simulated values against the experimental data from the study at 30°C.

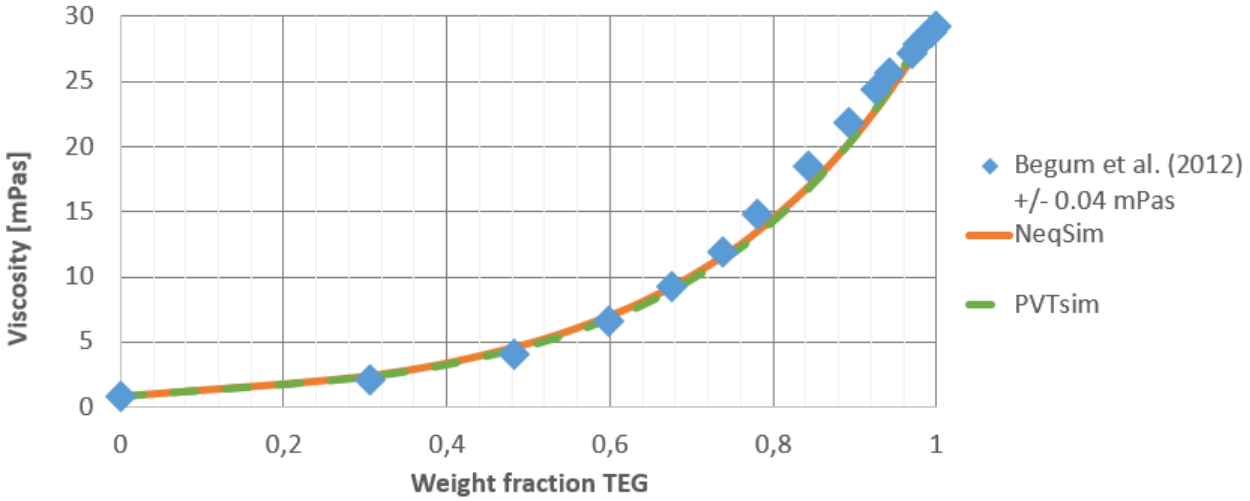

Figure 9.3: Calculated liquid viscosities of weight fractions 0 to 1 of TEG in aqueous solution compared to experimental data at atmospheric pressure and 30°C, Begum et al. (2012).

The results are in good agreement. The average deviation of the values in both NeqSim and PVTsim is 4.8%. The largest deviation in NeqSim is 13.5% at 0.3 weight fraction of TEG. The largest deviation in PVTsim is 10.4% at 0.78 weight fraction of TEG. The simulated values plotted against the experimental data at the other temperature levels of the study can be found in Appendix B.1.

Figure 9.4 displays the obtained simulated values in NeqSim as percentage of the experimental values for all temperatures in the study.

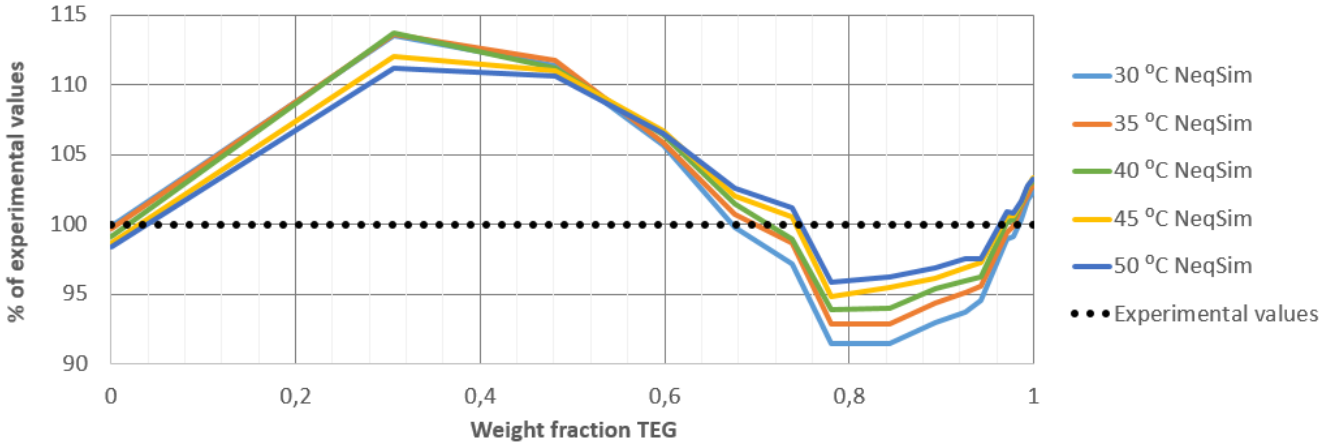

Figure 9.4: Calculated liquid viscosities in NeqSim of weight fractions 0 to 1 of TEG in aqueous solution as percentage of experimental data at atmospheric pressure, Begum et al. (2012).

The experimental values are plotted as a line with a constant value of 100%. Figure 9.4 displays an overestimation of the simulated values obtained in NeqSim up to 0.7 weight fraction of TEG. Between 0.7 and 0.98 weight fraction of TEG NeqSim underestimates the values. The average deviation of the numbers is 4.2%. The maximum average deviation is at 0.3 weight fraction of TEG with a value of 12.8%. The deviation is mildly decreasing with the increase of temperature. The average deviation is 4.8% at 30°C, 4.4% at 35°C, 4.2% at 40°C, 3.9% at 45°C and 3.7% at 50°C.

Figure 9.5 displays the obtained simulated values in PVTsim as percentage of the experimental values for all temperatures in the study.

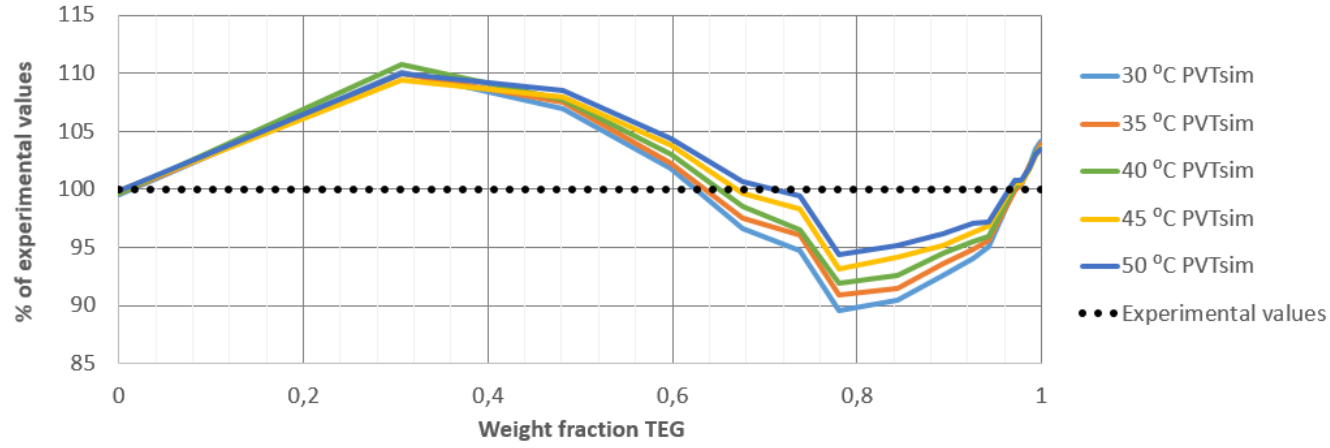

Figure 9.5: Calculated liquid viscosities in PVTsim of weight fractions 0 to 1 of TEG in aqueous solution as percentage of experimental data at atmospheric pressure, Begum et al. (2012).

The experimental values are plotted as a line with a constant value of 100%. Figure 9.5 is similar to Figure 9.4. It displays an overestimation of the simulated values obtained in PVTsim up to 0.7 weight fraction of TEG. Between 0.7 and 0.98 weight fraction of TEG, PVTsim underestimates

the values. The average deviation of the numbers is 4.0%. The maximum average deviation is at 0.3 weight fraction of TEG with a value of 10.0%. The deviation is mildly decreasing with the increase of temperature. The average deviation is 4.8% at 30°C, 4.3% at 35°C, 4.1% at 40°C, 3.6% at 45°C and 3.4% at 50°C. Compared to NeqSim, PVTsim has a similar but smaller deviation from the experimental values.

The study Sun and Teja (2003) conducted viscosity measurements for water containing 0.74, 0.89 and 0.96 weight fractions of TEG. The claimed uncertainty of the study is 2%. Figure 9.6 displays the obtained simulated values compared to the experimental data from the study at 0.74 weight fraction of TEG.

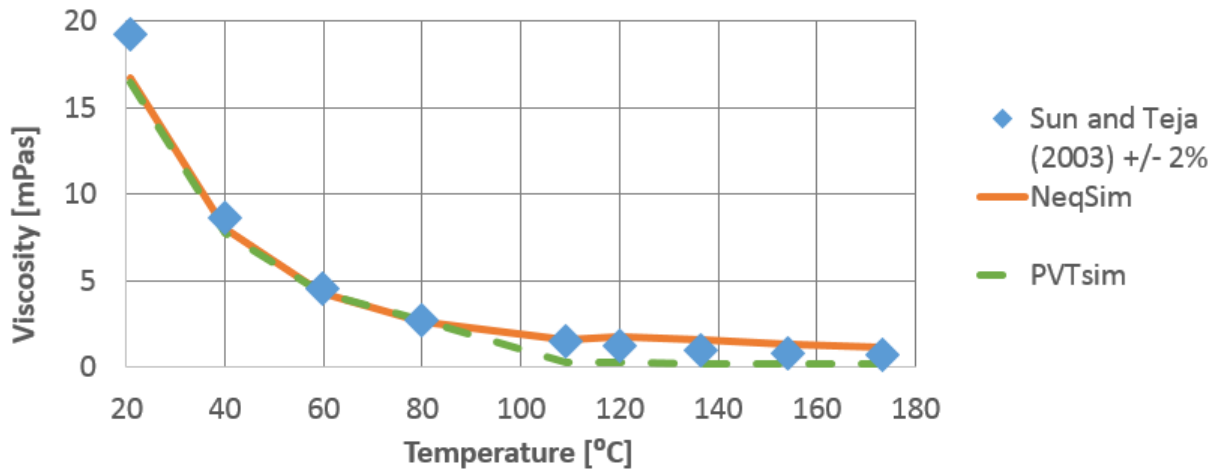

Figure 9.6: Calculated liquid viscosities of 0.74 weight fraction of TEG in aqueous solution compared to experimental data at atmospheric pressure and temperatures 20 - 175°C, Sun and Teja (2003).

The results are in good agreement at lower temperatures. The overall average deviation is smaller in NeqSim (28.7%) than in PVTsim (46.4%). The average deviation in NeqSim is 7.1% at temperatures 109°C and lower, but the deviation is 55.8% at higher temperatures. PVTsim has an average deviation of 7.7% at temperatures 80°C and lower, but an average deviation of 77.4% at higher temperatures. The simulated values plotted against the experimental data from the study at 0.89 and 0.96 weight fractions of TEG can be found in Appendix B.2.

Figure 9.7 displays the obtained simulated values in NeqSim as percentage of the experimental values for all weight fractions measured in the study.

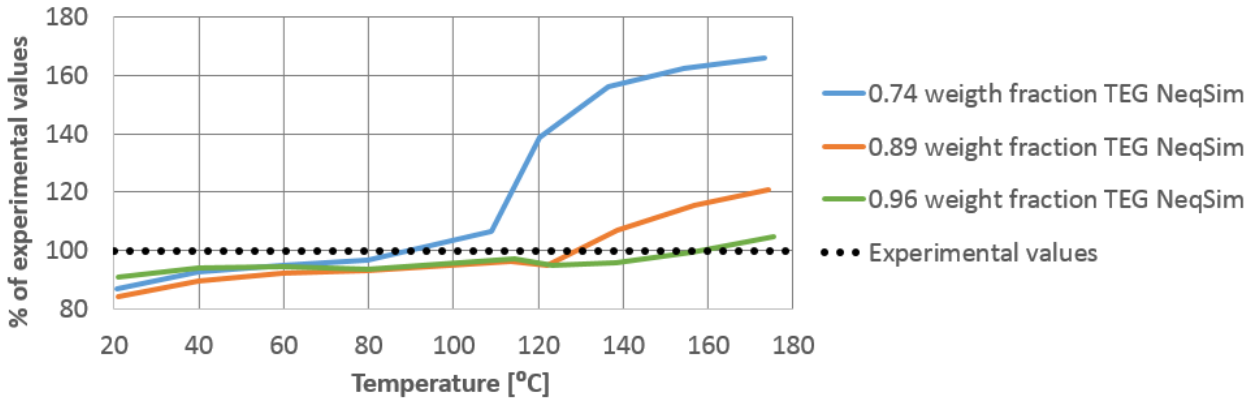

Figure 9.7: Calculated liquid viscosities in NeqSim of aqueous TEG as percentage of experimental data at atmospheric pressure and temperatures 20 - 175°C, Sun and Teja (2003).

The experimental values are plotted as a line with a constant value of 100%. Figure 9.7 displays the high simulated values obtained in NeqSim for high temperatures. The overall average deviation of the numbers is 14.7%. The deviations are noticeably smaller for higher weight fractions of TEG. The average deviation at 0.74 weight fraction TEG is 28.7%, at 0.89 weight fraction TEG it is 10.3% and at 0.96 weight fraction TEG it is 5.0%. The maximum deviation of 0.96 weight fraction TEG is 9.1% at 21°C. For 0.89 weight fraction it is 20.7% and for 0.74 weight fraction it is 66.2%, both at 173°C.

Figure 9.8 displays the obtained simulated values in PVTsim as percentage of the experimental values for all weight fractions measured in the study.

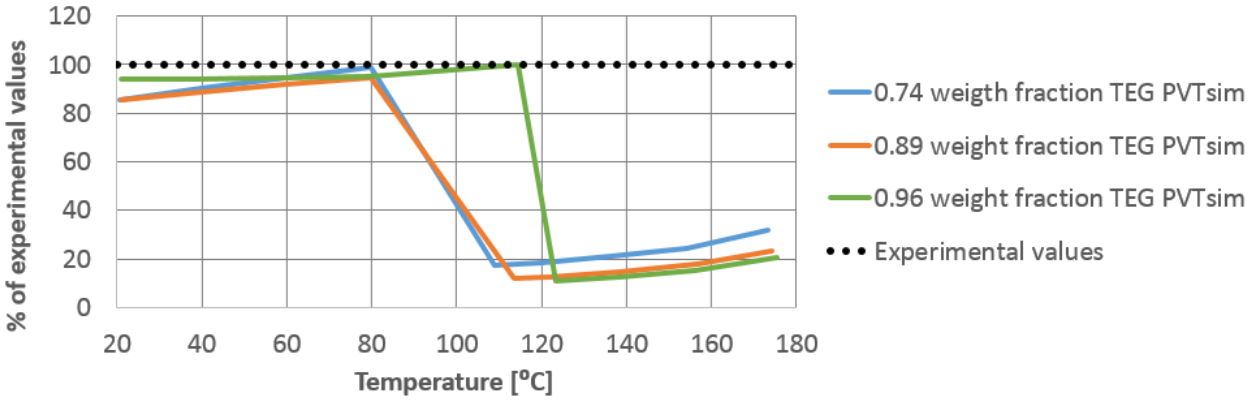

Figure 9.8: Calculated liquid viscosities in PVTsim of aqueous TEG as percentage of experimental data at atmospheric pressure and temperatures 20 - 175°C, Sun and Teja (2003).

The experimental values are plotted as a line with a constant value of 100%. Figure 9.8 displays the significantly low simulated values obtained in PVTsim for high temperatures. The overall average deviation of the numbers is 45.9%. The deviations are fairly similar for all weight fractions

of TEG. The average deviation at 0.74 weight fraction TEG is 46.4%, at 0.89 weight fraction TEG it is 50.9% and at 0.96 weight fraction TEG it is 40.4%.

NeqSim and PVTsim provide unsatisfactory results for liquid mixtures at high temperatures. The simulated viscosity values for pure TEG is satisfactory at all temperatures in both simulation programs, as shown in Figure 9.1. For liquid mixtures at temperatures 80°C and lower, PVTsim consistently provides the smallest deviations from the experimental data. The deviation of NeqSim at these temperatures is however only about 0.5% larger in average. Where PVTsim provides accurate results up to 80°C for liquid mixtures, NeqSim provides accurate results up to 109°C. At temperatures higher than this NeqSim overestimates the values, while PVTsim underestimates the values. NeqSim provide fairly accurate results for liquid mixtures containing up to 11 wt% water for all temperatures in the experimental experimental data. PVTsim struggles to provide accurate results for mixtures containing only 1.5 wt% water at high temperatures.

9.1.3 Viscosity of High Pressure Aqueous TEG and Methane

The study Ng et al. (2009) conducted viscosity measurements for aqueous TEG containing 2 wt% water and methane at high pressures. The reported uncertainty of the study is 1%. Figure 9.9 displays the obtained simulated values plotted against the experimental data from the study at 43.3°C.

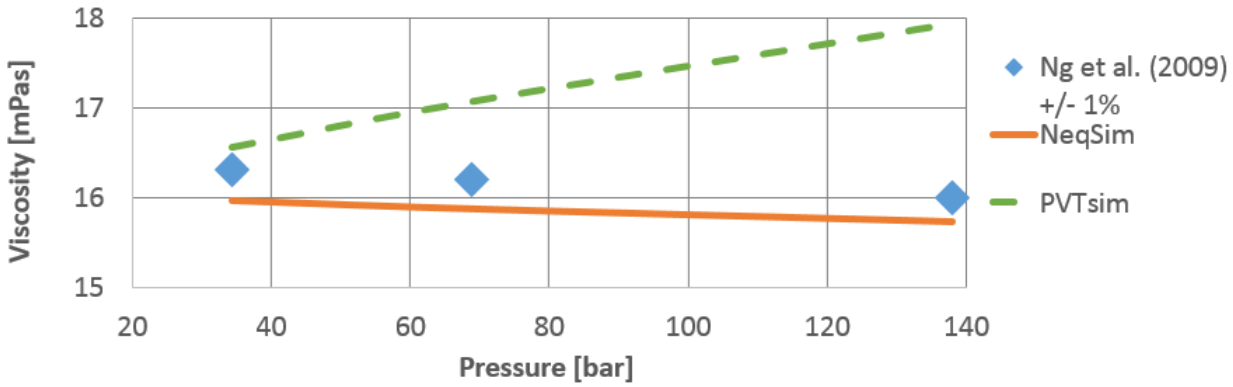

Figure 9.9: Calculated liquid viscosities of aqueous TEG and methane compared to experimental data at 43.3°C and pressures 34.5 - 138 bar, Ng et al. (2009).

The calculated values in NeqSim are in good agreement with the experimental data. The average deviation is 1.9% and the deviation is fairly constant independent of pressure. The average deviation of PVTsim is 6.4% and the deviation is increasing with the increase of pressure. At 138 bar the deviation is 12.1%. PVTsim calculates viscosity values which increase with the increase of pressure, while both the experimental data and the NeqSim values decrease with the increase of pressure. This pattern is repeated for experimental and simulated data for all temperature

levels in the study. The simulated values plotted against the experimental data from the study at 26.7 and 60°C can be found in Appendix B.3.

Figure 9.10 displays the obtained simulated values in NeqSim as percentage of the experimental values.

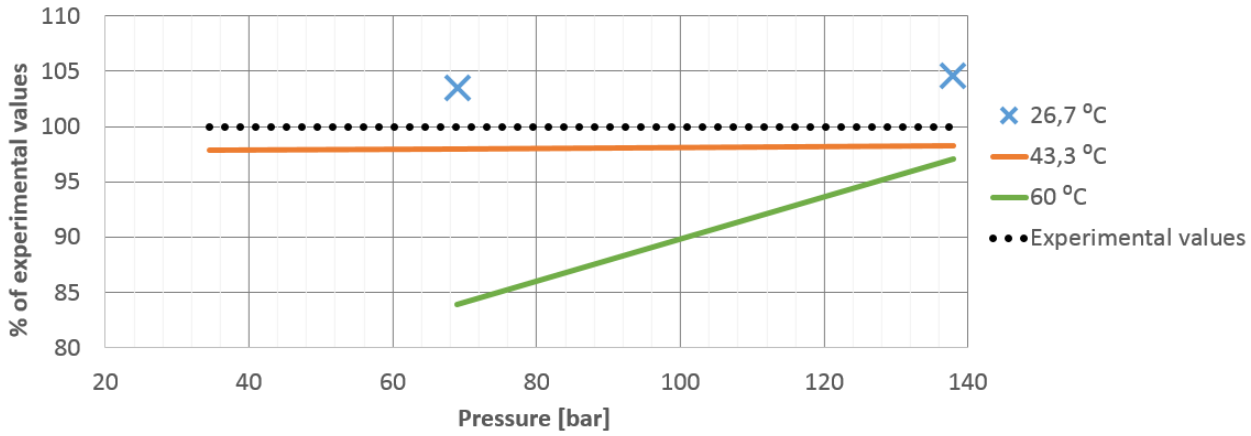

Figure 9.10: Calculated liquid viscosities in NeqSim of aqueous TEG and methane as percentage of experimental data at pressures 34.5 - 138 bar, Ng et al. (2009).

The experimental values are plotted as a line with a constant value of 100%. The overall average deviation of the numbers is 4.7%. The deviations are fairly consistent for the entire dataset, except for the deviation of 16% at 60°C and 69 bar. Disregarding this value the deviations appear to be fairly independent of pressure. NeqSim overestimates the values at 26.7°C and underestimates them at 43.3 and 60°C. The deviations might be explained by the amount of water in the aqueous TEG.

Figure 9.11 displays the obtained simulated values in PVTsim as percentage of the experimental values.

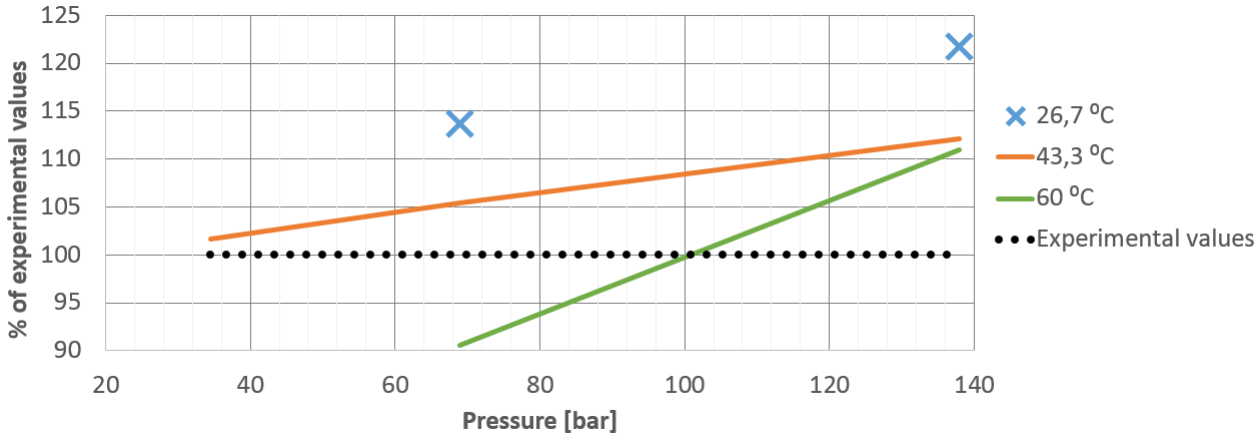

Figure 9.11: Calculated liquid viscosities in PVTsim of aqueous TEG and methane as percentage of experimental data at pressures 34.5 - 138 bar, Ng et al. (2009).

The experimental values are plotted as a line with a constant value of 100%. The overall average deviation of the numbers is 10.7%. The simulated values in PVTsim are higher than the experimental values for the entire dataset, except at 60°C and 69 bar. The deviations increase with the increase of pressure for all temperatures.

Figures 9.9, 9.10 and 9.11 show that NeqSim consistently predicts more accurate viscosity values at high pressures than PVTsim compared to the experimental values.

9.2 Collected Interfacial Tension Data Compared to Simulated Data

As described in Section 5.2.3 interfacial tension values can be calculated by several methods in NeqSim. PVTsim calculates interfacial tension values by using the Firoozabadi Ramey Method, as described in Section 5.3. The obtained simulated values from NeqSim for all methods and PVTsim will be compared to the collected experimental data in this section.

9.2.1 Interfacial Tension of Aqueous TEG and Air

The study Begum et al. (2012) conducted interfacial tension measurements of air and an aqueous solution containing various weight fractions of TEG at atmospheric pressure and 303.15°C. The reported error of the study is up to 0.51 mN/m. The pure TEG utilized is specified to comprise up towards 100 wt% TEG.

The solubility of gas at atmospheric pressure is low. This means that the experimental values of the solution-to-air interfacial tension acquired in Begum et al. (2012) will be similar to the

interfacial tension of methane and aqueous TEG at atmospheric pressure. Figure 9.12 plots the obtained simulated interfacial solution-to-methane tension values against the experimental data from the study as a function of TEG weight fraction.

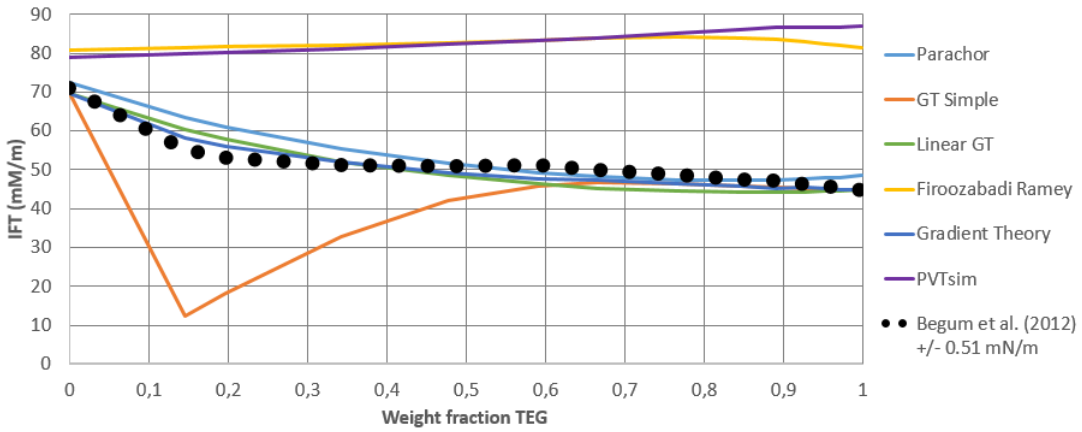

Figure 9.12: Calculated interfacial tensions of methane and aqueous TEG compared to experimental data at atmospheric pressure and 30°C, Begum et al. (2012).

Linear Gradient Theory and Gradient Theory calculate interfacial tension values which are within 10% deviation of the experimental data over the whole range. The Parachor Method calculates values which are within 15% deviation for the whole weight fraction range. The Gradient Theory Simple appears to overestimate the decrease in interfacial tension with the addition of TEG to the water, but calculates values within 15% deviation for 0.5 weight fraction of TEG and higher. The Firoozabadi Ramey Method in NeqSim calculates high values with an average deviation of 65.5%. The Firoozabadi Ramey Method in PVTsim calculates values very similar to this, with an average deviation of 68.5%. Both methods have their smallest deviation for pure water.

Figure 9.13 disregards the Firozabadi Ramey methods in NeqSim and PVTsim and the underestimation of the Gradient Theory Simple at low weight fractions of TEG. The figure displays the obtained simulated values in NeqSim as percentage of the experimental values.

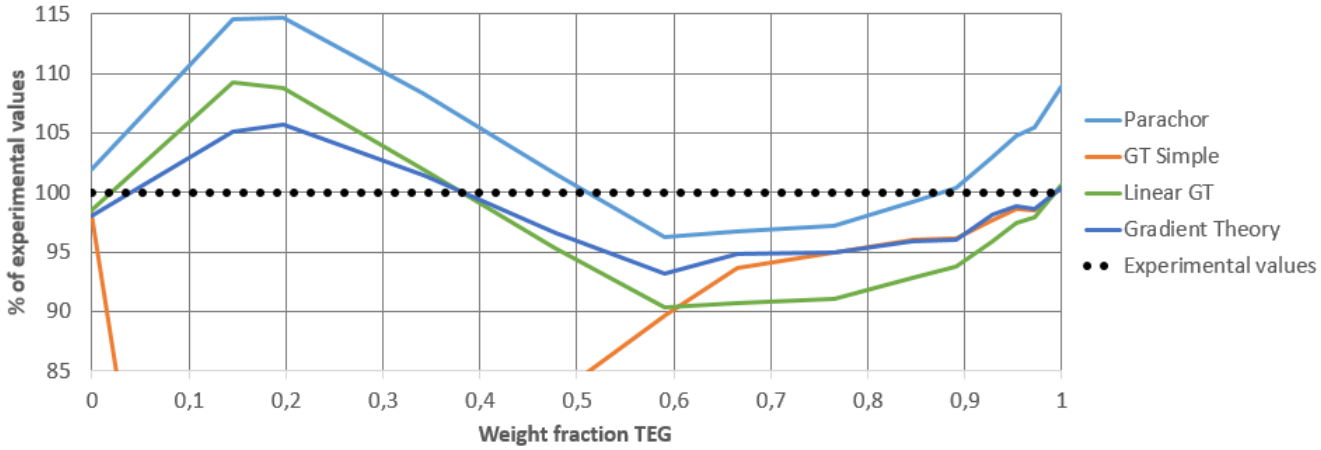

Figure 9.13: Calculated interfacial tensions of methane and aqueous TEG as a percentage of experimental data at atmospheric pressure and 30°C, Begum et al. (2012).

The experimental values are plotted as a line with a constant value of 100%. Most methods overestimate the interfacial tension for small weight fractions of TEG, and underestimate for higher weight fractions. The average deviation of the Parachor Method is 5.3% and it provides the best results of all methods from 0.45 TEG weight fraction to 0.9 TEG weight fraction. The Gradient Theory Simple calculates decent results at 0.5 TEG weight fraction and higher. The average deviation of the Gradient Theory Simple is 16.7%. Linear Gradient Theory provides good results over the entire range and an average deviation of 5.5%. Gradient Theory provides the smallest average deviation of all methods of 3.4%.

9.2.2 Interfacial Tension of High Pressure Water and Methane

Kashefi (2012) conducted high pressure interfacial tension measurements of water and methane. The measurements were conducted at temperatures 37.8 to 200°C and pressures 12 to 1064 bar. Pressures higher than 300 bar is not relevant for this study, and is disregarded. Figure 9.14 plots the obtained simulated interfacial tension values against the experimental data as a function of pressure at 100°C.

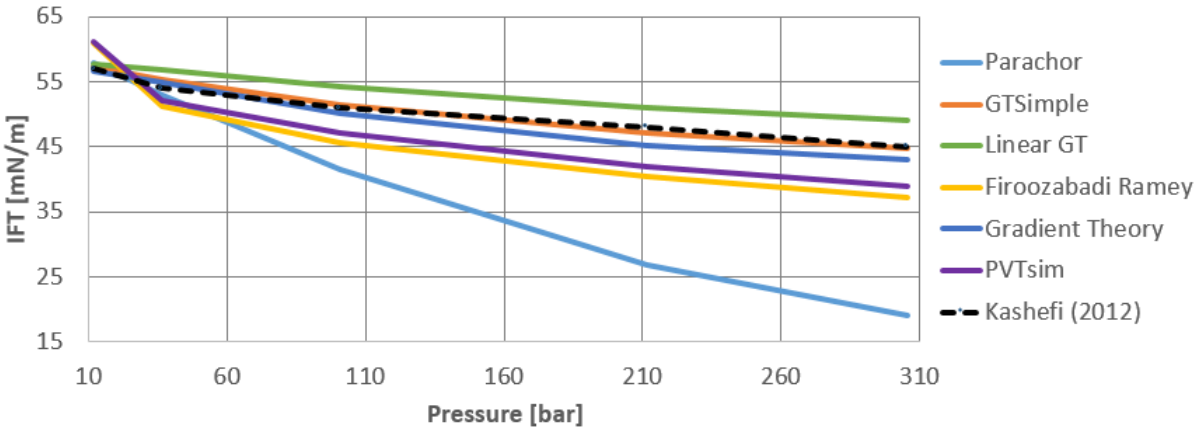

Figure 9.14: Calculated interfacial tensions of high pressure methane and water compared to experimental data at 100°C and pressures 12 - 305 bar, Kashefi (2012).

All methods simulate a decrease in interfacial tension values with the increase of pressure, which is in coherence with the experimental data. The three methods based on Gradient Theory predicts accurate values for the entire range. The Gradient Theory Simple provides values within 5% deviation while Linear Gradient Theory and Gradient Theory provide values within 10% deviation. Linear Gradient Theory is the only method that consistently overestimates the values. The Parachor Method provides the largest deviations. This pattern is repeated for all temperature levels measured in the study. The simulated values at the other temperature levels plotted against the experimental data from the study can be found in Appendix C.1.

The overall average deviation for all temperature levels in the study of the Gradient Theory Simple is 2.4%. The Linear Gradient Theory has an average deviation of 4.3% and Gradient Theory of 4.7%. PVTsim (9.6%) also predicts decent values. The Firoozabadi Ramey in NeqSim (19.2%) and the Parachor (25%) methods provide the largest deviations. The interfacial tension values of water and methane is not the most relevant numbers for this study. We confine ourselves to conclude that the methods based on Gradient Theory predicts the most accurate values.

9.2.3 Interfacial Tension of High Pressure Aqueous TEG and Methane

Ng et al. (2009) measured high pressure interfacial tensions of aqueous TEG and methane at temperatures 26.7 to 60°C and pressures 34.5 to 138 bar. The solution utilized was 98 wt% TEG and 2 wt% water. Simulations have been conducted for equivalent fluid compositions and conditions. Figure 9.15 plots the obtained simulated interfacial tension values against the experimental data as a function of pressure at 43.3°C.

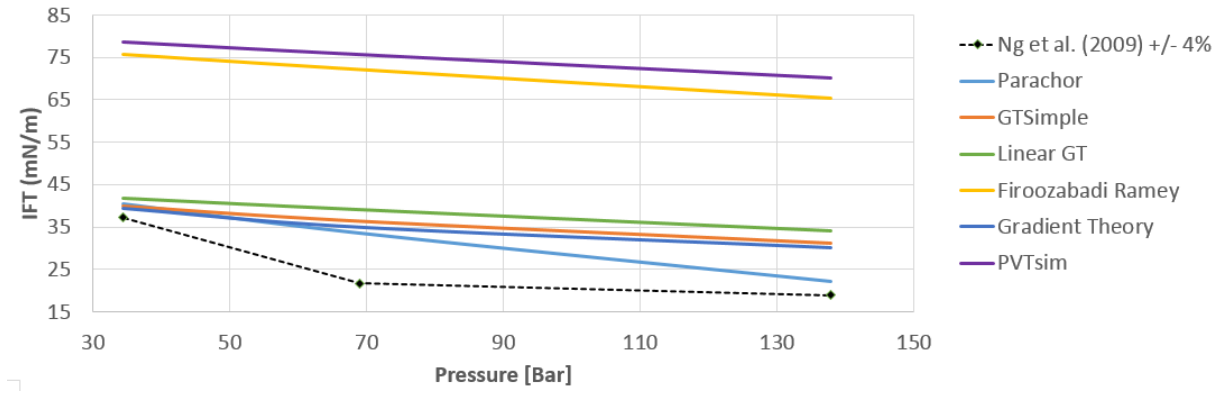

Figure 9.15: Calculated interfacial tensions of methane and aqueous TEG compared to experimental data at 43.3°C and pressures 34.5 - 138 bar, Ng et al. (2009).

The Firoozabadi Ramey methods in NeqSim and PVTsim simulate values more than twice as high as the experimental data. This is repeated at all conditions measured by Ng et al. (2009). The overall average deviation from the experimental data of the Firoozabadi Ramey Method in NeqSim is 187.4% and in PVTsim it is 204.4%. To easier compare the performance of the four methods which predict decent results, the Firoozabadi Ramey methods are disregarded for the rest of this section.

Figure 9.15 plots the obtained simulated interfacial tension values against the experimental data from the study at 43.3°C with the Firoozabadi Ramey methods omitted.

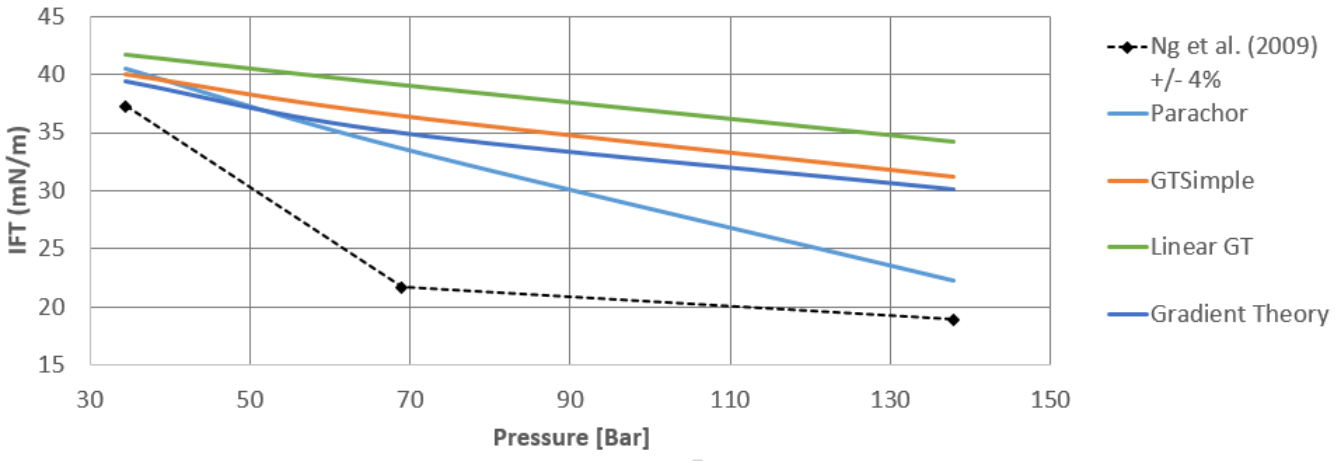

Figure 9.16: Calculated interfacial tensions of methane and aqueous TEG compared to experimental data at 43.3°C and pressures 34.5 - 138 bar, omitting the Firoozabdi Ramey methods, Ng et al. (2009)

All methods overestimate the interfacial tension compared to the experimental values. They all display a decrease of interfacial tension with the increase of pressure, which is in coherence with the experimental data. The three methods based on the Gradient Theory have a similar

slope, while the Parachor Method has steeper slope. At 34.5 bar the Gradient Theory provides the best results, with a deviation of 5.6 %. At this pressure the other methods also provide decent results, with a deviation ranging between 8.7% to 12%. All methods calculate their largest deviation at 69 bar, where Parachor provides the best results with a deviation of 55.2%. At 138 bar, the Parachor Method again has the smallest deviation of 17.8%. The other methods have a similar deviation at 69 and 138 bar, improving by approximately 3% at 138 bar. The Linear Gradient Theory consistently experience the largest deviations for all pressures, with an average of 57.8%. The comparisons between simulated and experimental data at 26.7°C and 60°C show similar results. The simulated values of the other temperature levels plotted against the experimental data from the study are presented in Appendix C.2.

Figure 9.17 plots the obtained simulated interfacial tension values from NeqSim against the experimental data as a function of temperature at 138 bar.

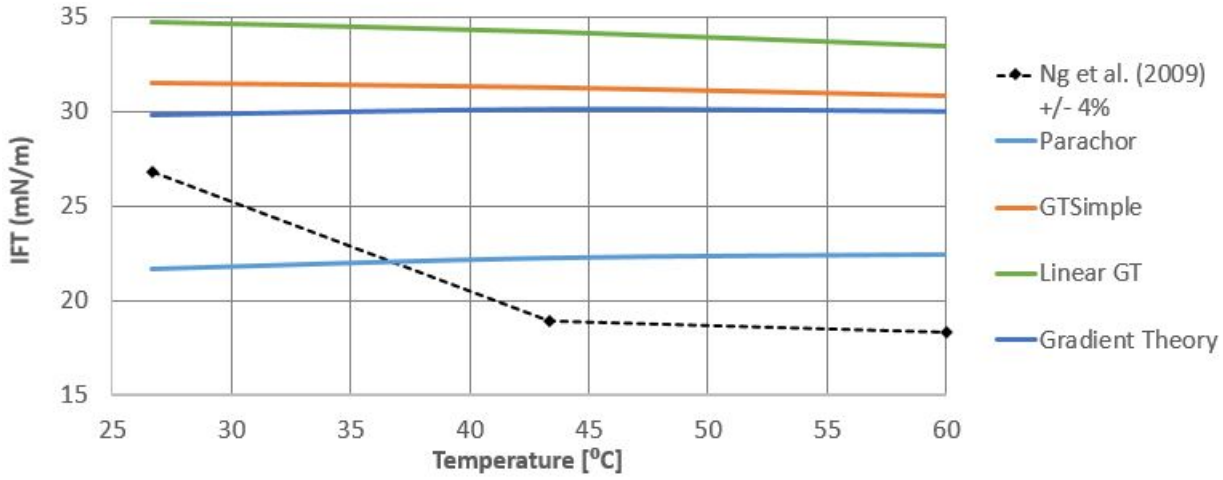

Figure 9.17: Calculated interfacial tensions of methane and aqueous TEG compared to experimental data at 138 bar and temperatures 26.7 - 60°, Ng et al. (2009)

All methods overestimate the interfacial tension compared to the experimental values. The only exception is the Parachor Method at 26.7°C. They all display fairly constant interfacial tension values independent of temperature, while the numbers from Ng et al. (2009) display a decrease in interfacial tension with the increase of temperature. At 26.7°C the Gradient Theory is the most accurate, with a deviation of 11.3%. At 43.3°C the Parachor Method has the smallest deviation of 17.8%. The other methods have deviations of between 59.3% and 81%. All methods experience their largest deviation at 60°C, approximately 4% higher than at 43.3°. At 34.5 bar there was conducted only one measurement, but the comparisons between simulated and experimental data at 69 bar show similar results, which are presented in Appendix C.2.

Figure 9.18 displays the total average deviation percentage of the methods for all conditions

measured by Ng et al. (2009) segregated by the different pressures.

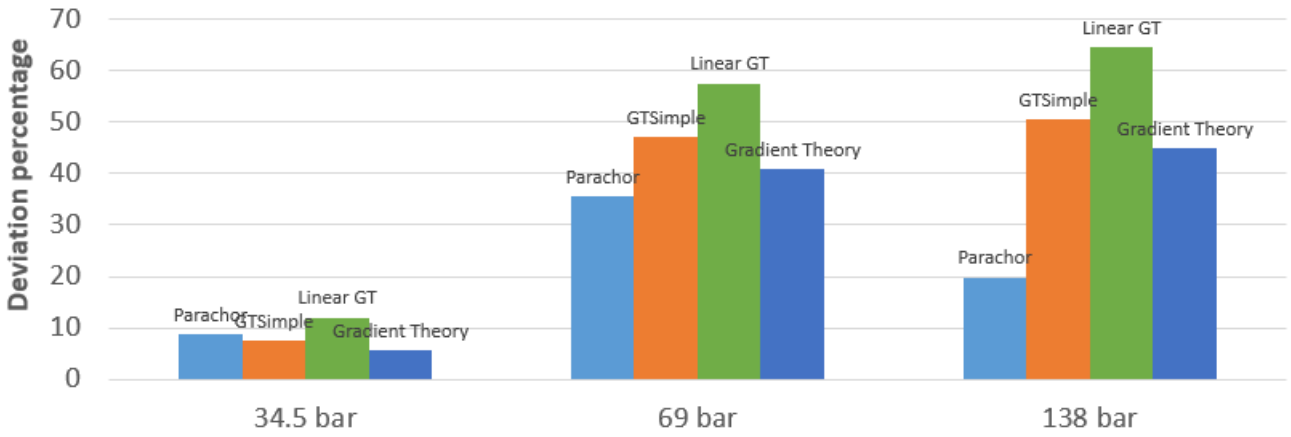

Figure 9.18: Average deviations of calculated and experimental interfacial tensions by pressure, Ng et al. (2009)

The deviations increase significantly with the increase of pressure. All methods have their smallest deviations at 34.5 bar. All methods except Parachor has their largest deviation at 138 bar, where Linear Gradient Theory has the largest of 64.5%. Parachor is significantly better than the other methods at this pressure. At 69 bar the Parachor Method and Gradient Theory have similar deviations. Linear Gradient Theory consistently provides the largest deviations from the experimental data.

Figure 9.19 displays the total average deviation percentage of the methods for all conditions segregated by the different temperatures.

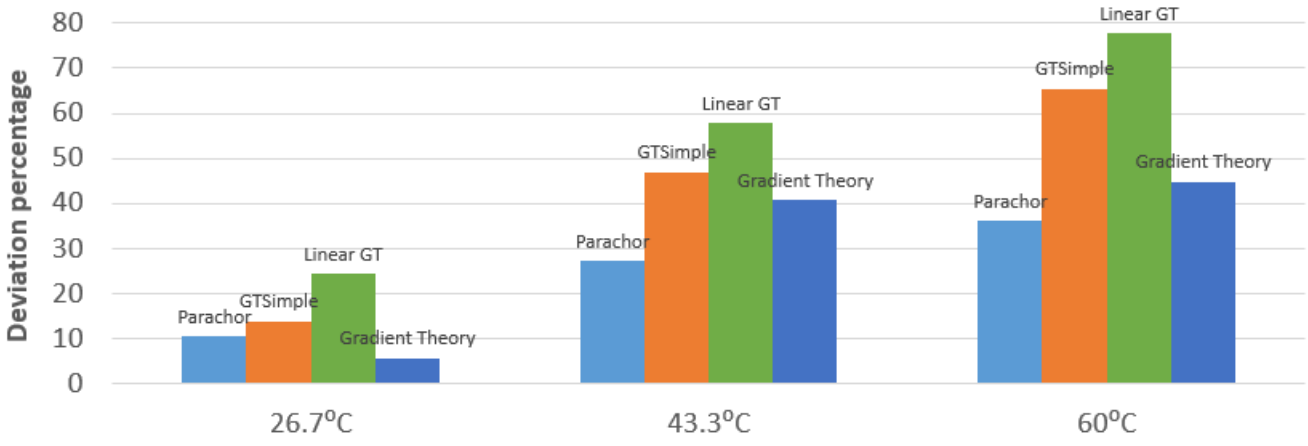

Figure 9.19: Average deviations of calculated and experimental interfacial tensions by temperature, Ng et al. (2009)

The deviations increase with the increase of temperature for all methods. At 26.7°C Gradient

Theory provides the smallest deviation of 7.7%. At 43.3 and 60°C the Parachor Method provides the smallest deviations. Linear Gradient Theory consistently provides the largest deviations and the Gradient Theory Simple the second largest.

The total average deviation percentage of the methods are presented in Figure 9.20.

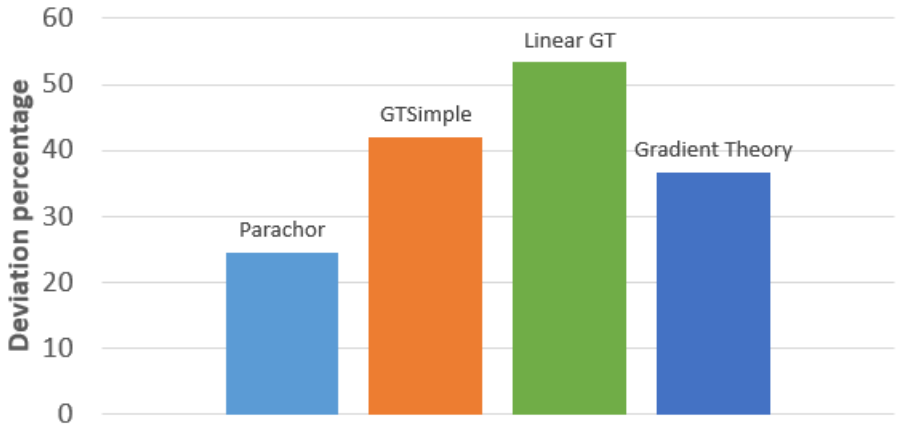

Figure 9.20: Average deviations of calculated and experimental interfacial tensions, Ng et al. (2009)

The Parachor Method has the smallest deviations of 24.6%. The Linear Gradient Theory has the largest deviations of 53.4%.

Figures 9.15, 9.16, 9.17, 9.18, 9.19 and 9.20 display simulated data which is consistently higher than the experimental data. The only exception is the Parachor Method at 138 bar and 26.7°C. The deviations appear to increase with the increase of both temperature and pressure. The Parachor Method provides the smallest deviations overall. The Gradient Theory provide the smallest deviations for low pressures and low temperatures. The largest deviations are provided by the Firoozabadi Ramey methods. This is no surprise, given that the Firoozabadi Ramey Method is mainly used for calculating interfacial tension of oil and water, and is not tuned for TEG. Of the methods which provide decent results, Linear Gradient Theory consistently provides the largest deviations for all conditions.

9.3 Measured Values of this Study Compared to Simulated Data

The Firoozabadi Ramey methods consistently simulates values more than twice as high as the experimental data. The average deviation of the Firoozabadi Ramey Method in NeqSim is 178.4% for 100 wt% TEG and 153.2% for 90 wt% TEG. PVTsim has an average deviation of 197.0% for 100 wt% TEG and 156.0% for 90 wt% TEG. To easier compare the performance of the other four methods, the Firoozabadi Ramey methods are disregarded for these comparisons.

9.3.1 Interfacial Tensions of 100 wt% TEG

Simulations in NeqSim have been conducted for equivalent fluid compositions and conditions. Figure 9.21 plots the obtained simulated interfacial tension values from NeqSim against experimental data obtained in this study as a function of pressure at 20°C.

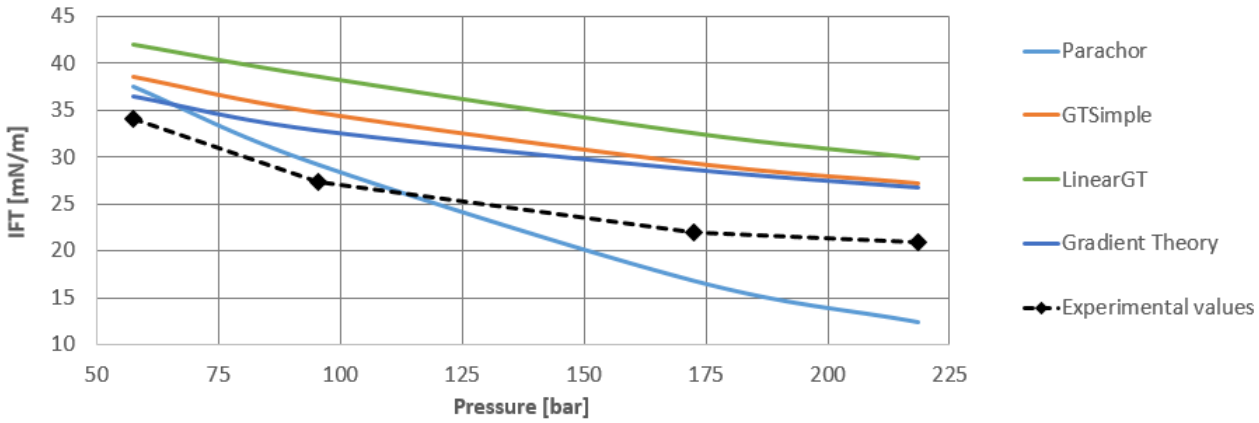

Figure 9.21: Calculated interfacial tensions of methane and TEG compared to the experimental results of this study at 20°C and pressures 57 - 219 bar.

The three methods based on Gradient Theory consistently overestimate the interfacial tension values compared to the experimental data. The Parachor Method overestimates the interfacial tension values at pressures below 100 bar, and underestimates the values at pressures higher than 100 bar. The three methods based on the Gradient Theory have a similar slope as the experimental data, while the slope of the Parachor Method is steeper. All methods display a decrease of interfacial tension with the increase of pressure, which is in coherence with results from this study. The Parachor Method provide the smallest deviations overall with an average of 20.5%. At 96 and 173 bar the Parachor Method provides the smallest deviations of 7% and 23.7% respectively. At 58 and 219 bar the Gradient Theory provide the smallest deviations of 6.6% and 27.9% respectively. The overall average deviation of the Gradient Theory is 21.2%. The Gradient Theory Simple provides an average deviation of 25.8%. The Linear Gradient Theory consistently provide the biggest deviations at all pressures, averaging 38.7% deviation. The comparisons between simulated and experimental data at 4.3°C and 41.5°C, which are presented in Appendix C.3, show similar results.

To easier identify the performance of the methods, we have divided the measured results into three different pressure groups: low (50 - 74 bar), medium (75 - 149 bar) and high (150 - 220 bar). Figure 9.22 displays the total average deviation percentage of the methods for all conditions measured segregated by pressure groups.

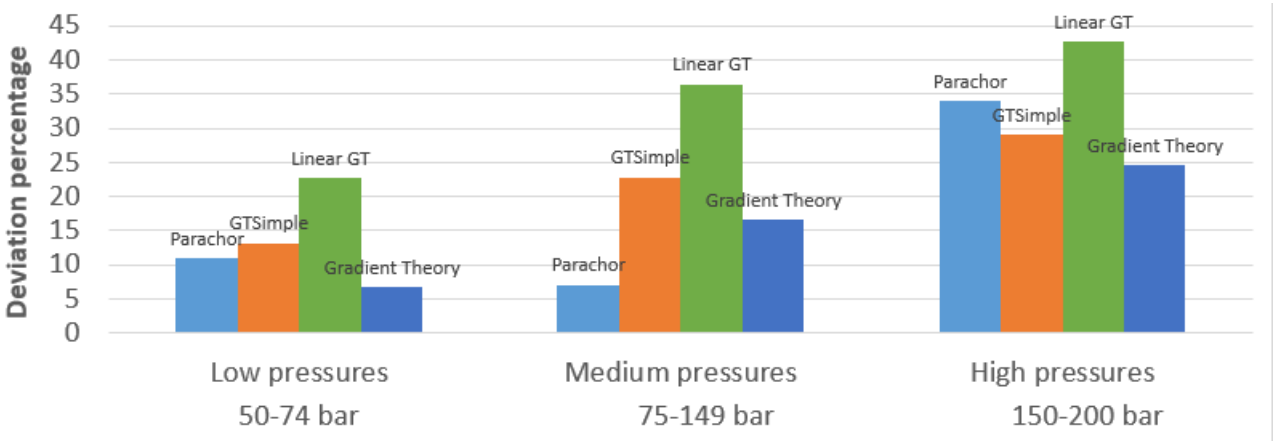

Figure 9.22: Average deviations of calculated and experimental interfacial tensions of this study by pressure groups

The deviations increase with the increase of pressure. The three methods based on Gradient Theory all have their minimum deviation at low pressures. The Parachor Method has its minimum deviation at medium pressures. The smallest deviations at low pressures is provided by the Gradient Theory of 6.7%. All methods have their largest deviations at high pressures, where Gradient Theory has the smallest. Parachor is significantly better than the other methods at medium pressures with a deviation of 7.1%. However, the Parachor Method experience noticeably high deviations at high pressures of 33.9%. Linear Gradient Theory consistently provides the largest deviations from the experimental data. It is worth noting that the Gradient Theory Simple is consistently providing results similar to the Gradient Theory, but approximately 5% more deviated.

Figure 9.23 displays the total average deviation percentage of the methods for all conditions segregated by the different temperatures.

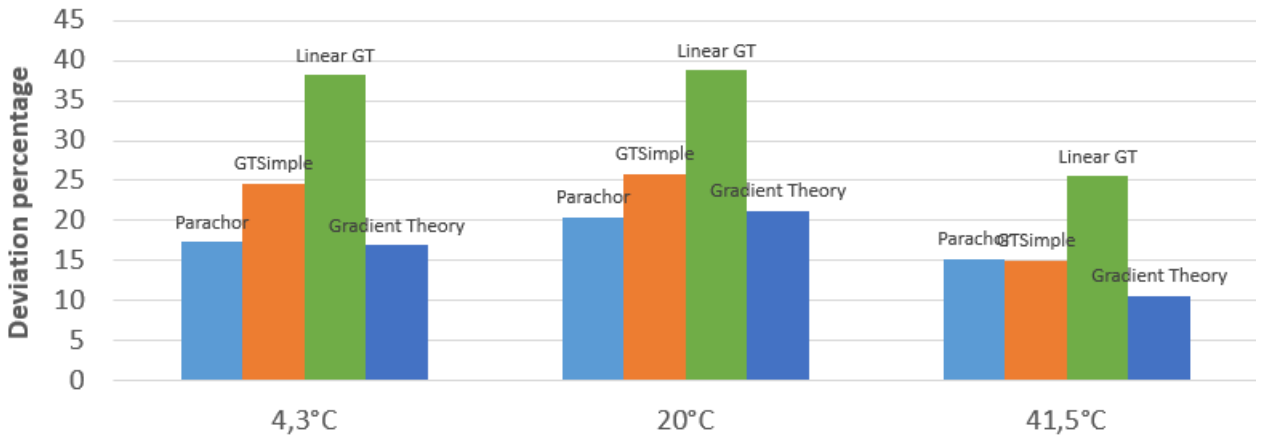

Figure 9.23: Average deviations of calculated and experimental interfacial tensions of this study by temperature

The deviations are similar at 4.3°C and 20°C, but smaller at 41.5°C for all methods. At 4.3°C Gradient Theory (17%) and Parachor Method (17.3%) provide almost similar deviations. Again, at 20°C the Gradient Theory (21.2%) and the Parachor Method (20.4%) have very similar deviations. At 41.5°C the Gradient Theory has the smallest deviations. Linear Gradient Theory consistently provides the largest deviations for all temperatures. It is worth noting that the Gradient Theory Simple is consistently providing results similar to the Gradient Theory, but approximately 5% more deviated.

The total average deviation percentage of the methods are presented in Figure 9.24.

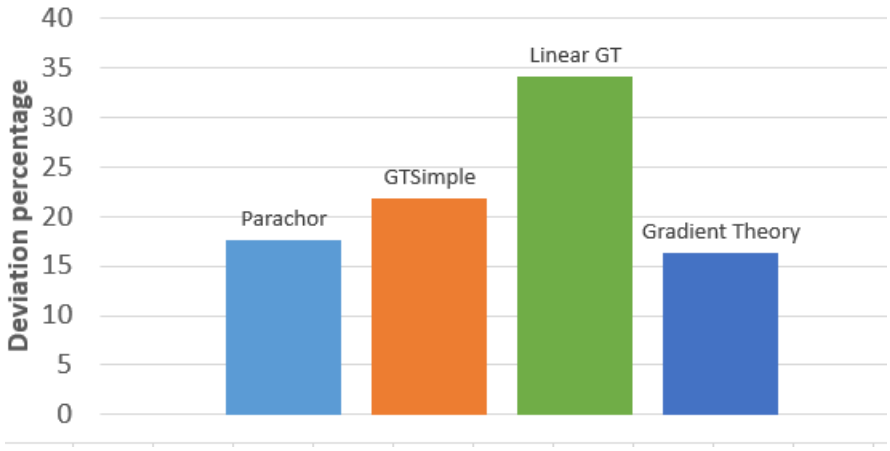

Figure 9.24: Average deviations of calculated and experimental interfacial tensions of this study

The Gradient Theory has the smallest deviations overall of 16.3%. The Parachor Method has an almost equal performance of 17.7% deviation. The Linear Gradient Theory provides the largest deviations.

Figures 9.21, 9.22, 9.23 and 9.24 display simulated data which for the three methods based on Gradient Theory is consistently higher than the experimental data. The Parachor Method display simulated data which is considerably lower than the experimental data for pressures higher than 100 bar. The deviations appear to increase with the increase of pressure, but decrease with the increase of temperature. The Parachor Method provides very small deviations for pressures below 150 bar. The Gradient Theory provide the smallest deviations overall. The Linear Gradient Theory consistently provides the largest deviations for all conditions.

9.3.2 Interfacial Tensions of 90 wt% TEG

Simulations in NeqSim have been conducted for equivalent fluid compositions and conditions. Figure 9.25 plots the obtained simulated interfacial tension values from NeqSim against the experimental data as a function of pressure at 4.3°C.

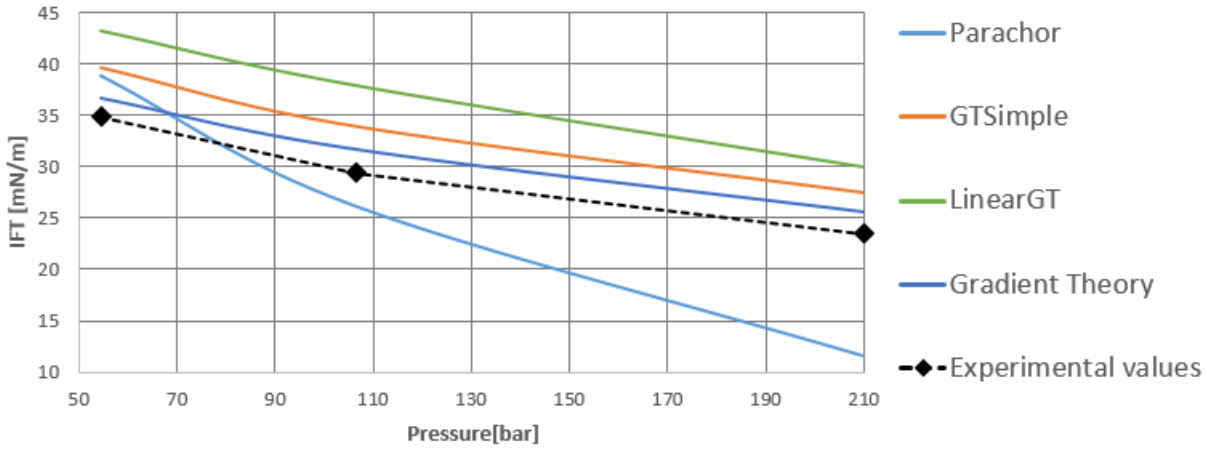

Figure 9.25: Calculated interfacial tensions of methane and aqueous TEG compared to the experimental results of this study at 4.3°C and pressures 55 - 210 bar

The methods based on Gradient Theory overestimate the interfacial tension values compared to the experimental data. The three methods based on the Gradient Theory have a similar slope to the experimental data, while the slope of the Parachor Method is steeper. All methods display a decrease of interfacial tension with the increase of pressure, which is in coherence with the values obtained in this study. The Gradient Theory consistently predicts the best results, with all calculated values within 9% deviation of the experimental data. All methods have their largest deviation at 210 bar, except the Linear Gradient Theory which has a slightly larger deviation at 106 bar. The methods based on Gradient Theory deliver decent results over the entire pressure range. The Parachor Method significantly underestimates the interfacial tension at 210 bar, with a deviation of 50.7%. The comparisons between simulated and experimental data at 20°C and 41.5°C, which are presented in Appendix C.4, show similar results.

Figure 9.26 displays the total average deviation percentage of the methods for all conditions measured segregated by pressure groups.

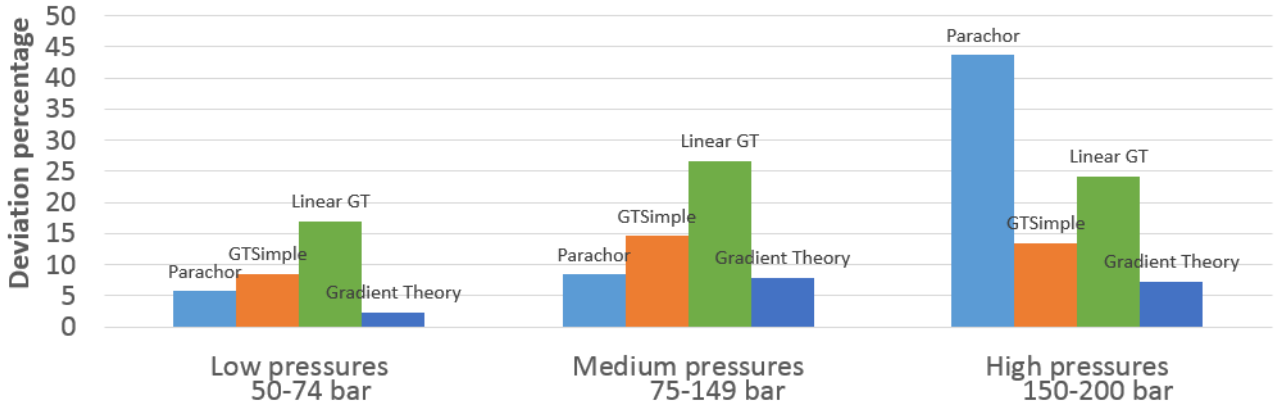

Figure 9.26: Average deviations of calculated and experimental interfacial tensions of this study by pressure groups

All methods have their minimum deviation at low pressures. The methods based on Gradient Theory have slightly larger deviations at medium pressures than at high pressures. The smallest deviations at low pressures is provided by the Gradient Theory of 2.3%. At medium pressures the Parachor Method (8.4%) and the Gradient Theory (8.0%) have similar deviations. However, the Parachor Method experience noticeably high deviations at high pressures of 43.7%. It is worth noting that the Gradient Theory Simple is consistently providing results similar to the Gradient Theory, but approximately 6% more deviated.

Figure 9.27 displays the total average deviation percentage of the methods for all conditions segregated by the different temperatures.

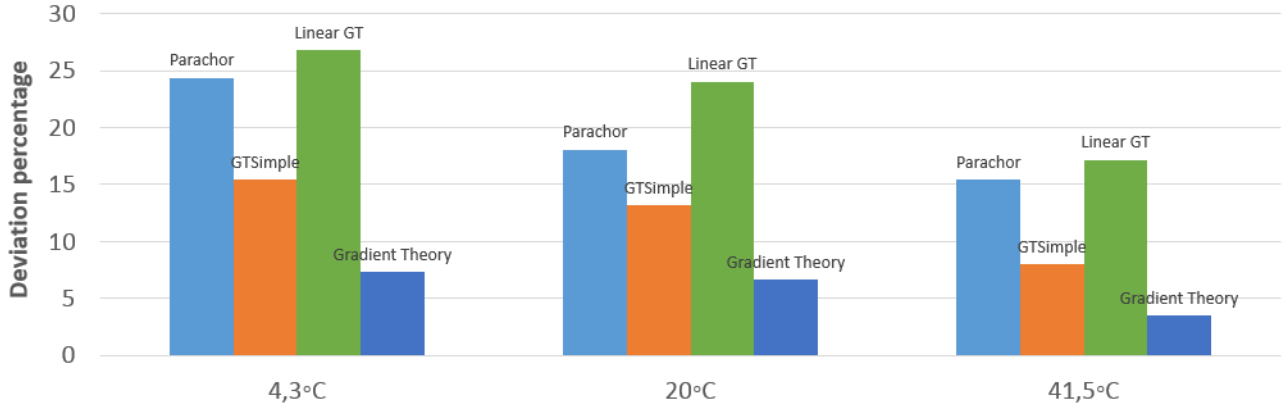

Figure 9.27: Average deviations of calculated and experimental interfacial tensions of this study by temperature

The deviations decrease with the increase of temperature for all methods. The Gradient Theory consistently provides the smallest deviations for all temperatures. The Gradient Theory Simple consistently provides the second smallest deviations, and Linear Gradient Theory consistently provides the largest deviations.

The total average deviation percentage of the methods are presented in Figure 9.28.

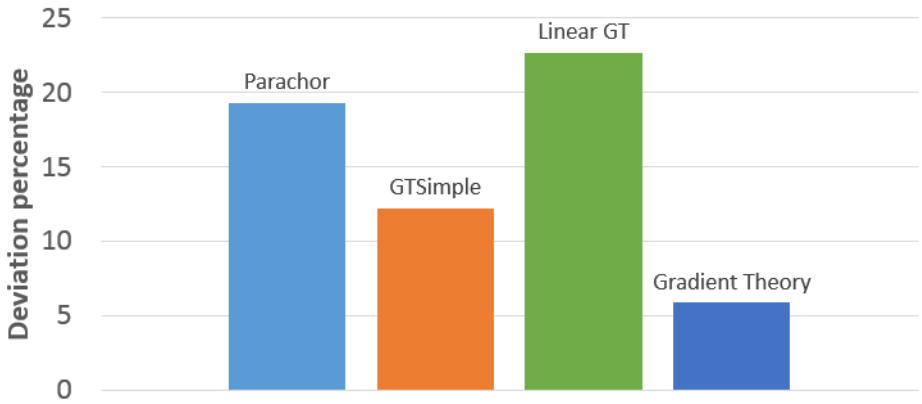

Figure 9.28: Average deviations of calculated and experimental interfacial tensions of this study

The Gradient Theory has the smallest deviations overall of 5.8%. The Parachor Method (19.2%) and the Linear Gradient Theory (22.6%) provide the largest average deviation.

Figures 9.25, 9.26, 9.27 and 9.28 display simulated data which for the three methods based on Gradient Theory is consistently higher than the experimental data. The Parachor Method simulates data which is considerably lower than the experimental data for pressures higher than 100 bar. The deviations appear to increase with the increase of pressure, but decrease with the increase of temperature. The Parachor Method provides the smallest deviations of the methods for pressures below 150 bar, but significantly large deviations at higher pressures. The Gradient Theory provides the smallest deviations overall. The Gradient Theory Simple provides the second smallest deviations.

9.3.3 Interfacial Tensions of both Liquid Mixtures

Figure 9.29 displays the total average deviation percentage of the methods for all conditions measured segregated by liquid mixtures.

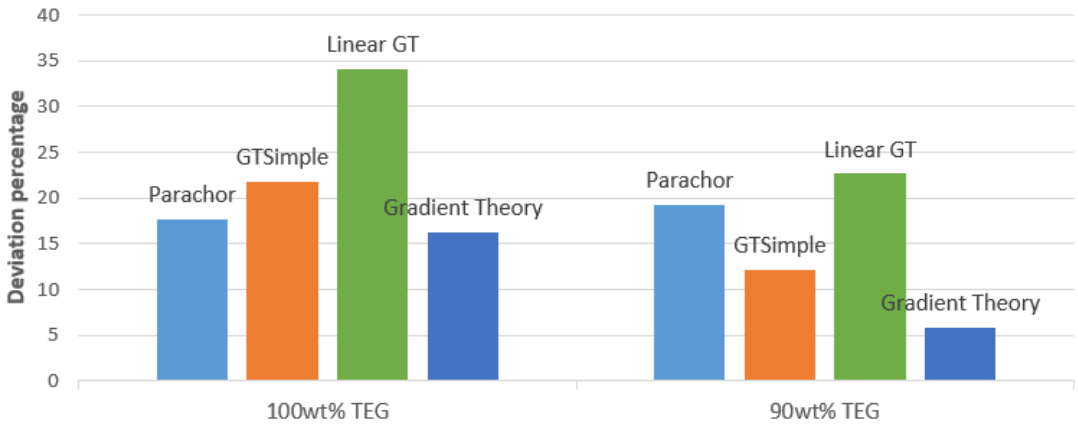

Figure 9.29: Average deviations of calculated and experimental interfacial tensions of this study by liquid mixtures

The deviations for the Parachor Method is higher for 90 wt% TEG than for 100 wt% TEG. As described in Section 5.2.3 the Parachor Method in NeqSim is calibrated for pure TEG. It therefore seems logical that the method predicts better values for 100 wt% TEG. The other methods have significantly lower deviations for 90 wt% TEG.

Figure 9.30 displays the total average deviation percentage of the methods for all conditions measured and both liquid mixtures segregated by pressure groups.

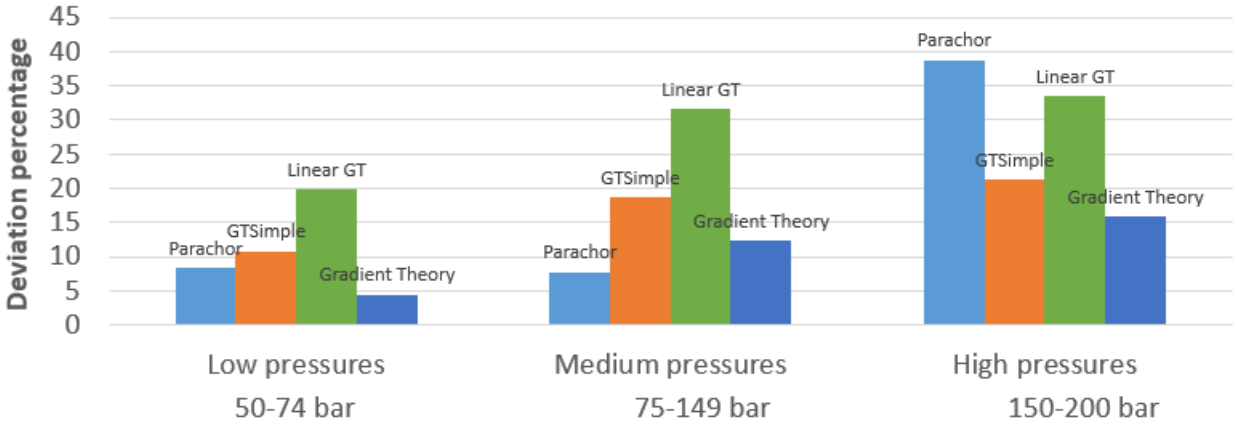

Figure 9.30: Average deviations of calculated and experimental interfacial tensions of this study by pressure groups

The deviations increase with the increase of pressure. The three methods based on Gradient Theory all have their minimum deviation at low pressures. The Parachor Method has its minimum deviation at medium pressures. The smallest deviations at low pressures is provided by the Gradient Theory of 4.5%. All methods have their largest deviations at high pressures, where Gradient Theory again has the smallest. Parachor is significantly better than the other methods

at medium pressures with a deviation of 7.8%. However, the Parachor Method experience noticeably high deviations at high pressures of 38.8%. It is worth noting that the Gradient Theory Simple is consistently providing results similar to the Gradient Theory, but approximately 6% more deviated.

Figure 9.31 displays the total average deviation percentage of the methods for all conditions for both liquid mixtures segregated by the different temperatures.

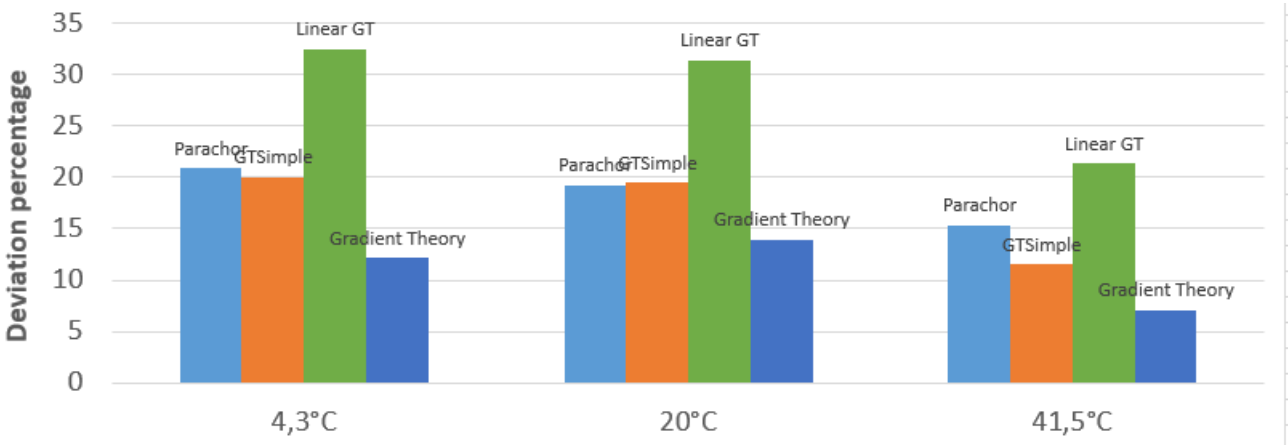

Figure 9.31: Average deviations of calculated and experimental interfacial tensions of this study by temperature

The deviations decrease with the increase of temperature for all methods. The Gradient Theory consistently provides the smallest deviations for all temperatures. Linear Gradient Theory consistently provides the largest deviations for all temperatures. The Parachor Method and the Gradient Theory Simple provide very similar deviations at 4.3 and 20°C. It is worth noting that the Gradient Theory Simple is consistently providing results similar to the Gradient Theory, but approximately 6% more deviated.

The total average deviation percentage of the methods are presented in Figure 9.32.

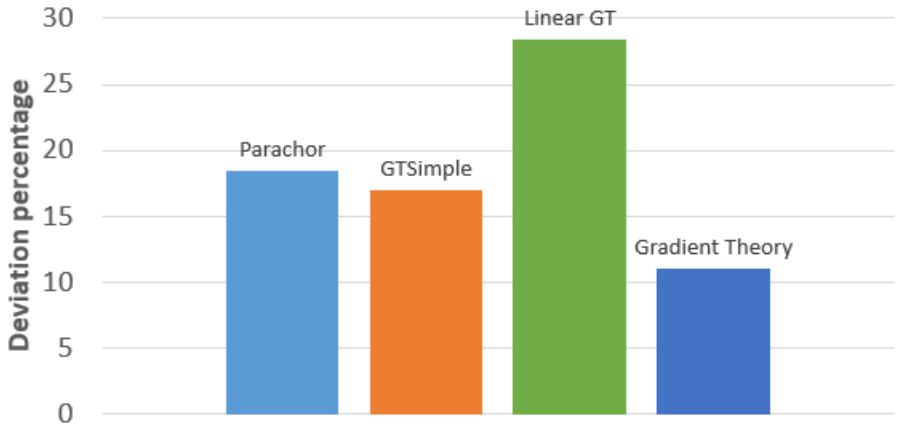

Figure 9.32: Average deviations of calculated and experimental interfacial tensions of this study

The Gradient Theory has the smallest deviations overall of 11.1%. The Gradient Theory Simple (17.0%) and the Parachor Method (18.5%) provide similar deviations. The Linear Gradient Theory provides the largest deviations.

Figures 9.30, 9.31 and 9.32 display that the deviations appear to increase with the increase of pressure, but decrease with the increase of temperature. The Parachor Method provides very small deviations for pressures below 150 bar. The Gradient Theory provide the smallest deviations overall. The Linear Gradient Theory consistently provides the largest deviations for all conditions. The methods based on Gradient Theory consistently simulate values higher than the experimental data. The Parachor Method simulate values lower than the experimental data for pressures higher than 100 bar.

9.3.4 Densities

As mentioned in Section 7.2, measurements were also conducted of the liquid and gas densities. Density is used in interfacial tension calculations and is an important physical property to account for when designing gas-liquid separators.

It is useful for the conclusion of this work to establish whether NeqSim calculates reasonable density values. Comparisons are conducted only for the measured values from this laboratory work, as density comparisons are somewhat outside of the scope of work of this Master's thesis. Simulated values are obtained utilizing the standard SRK-CPA equation of state in NeqSim.

Liquid Density

Figure 9.33 displays the obtained simulated liquid densities in NeqSim compared to the experimental values obtained in this study at 4.3°C and 100 wt% TEG.

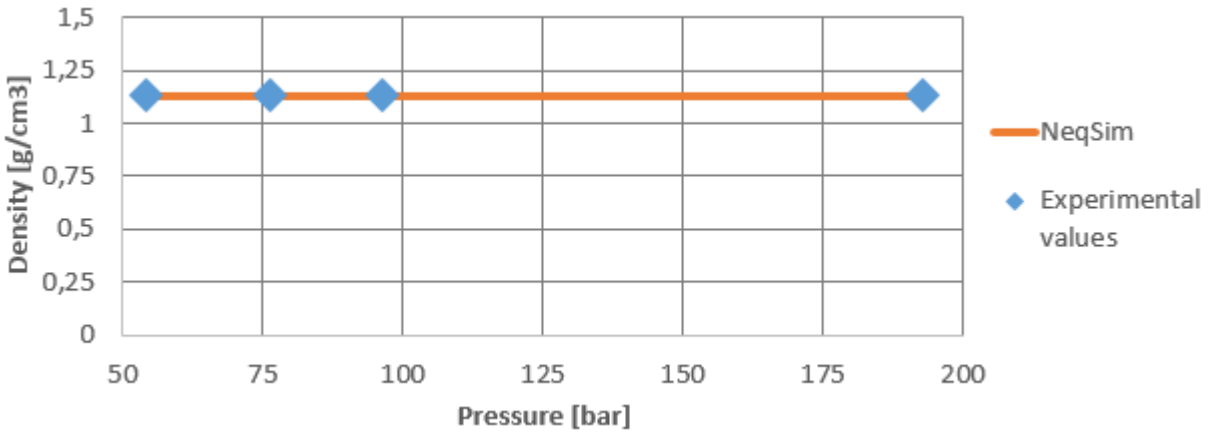

Figure 9.33: Calculated liquid density in NeqSim compared to experimental results of this study at 4.3°C, 100 wt% TEG and pressures 54 - 193 bar.

All simulated values are within 1% deviation of the experimental data. The overall average deviation of the liquid density of 100 wt% TEG for all temperatures is 0.5%. Figure 9.34 displays the obtained simulated liquid densities in NeqSim compared to the experimental values in this study at 41.5°C and 90 wt% TEG.

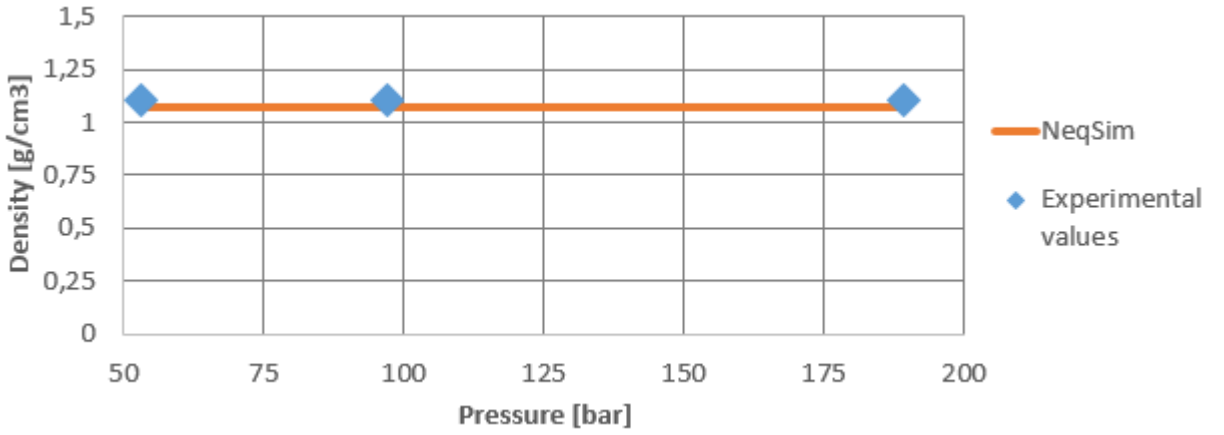

Figure 9.34: Calculated liquid density in NeqSim compared to experimental results of this study at 41.5°C, 90 wt% TEG and pressures 53 - 189 bar.

All simulated values are within 4% deviation of the experimental data. The overall average deviation of the liquid density of 90 wt% TEG for all temperatures is 2.9%. The simulated values are consistently lower than the experimental values, which are the case for all measured condi-

tions in this experimental work for both liquid mixtures. We conclude that NeqSim calculates accurate liquid density values.

Vapor Density

Figure 9.35 displays the obtained simulated liquid densities in NeqSim compared to the experimental values in this study at 4.3°C and 100 wt% TEG.

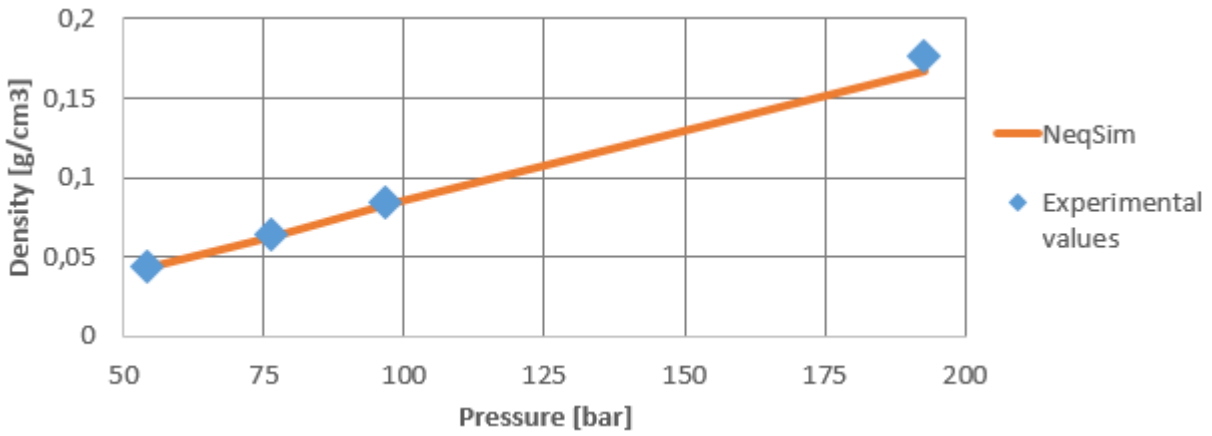

Figure 9.35: Calculated vapor density in NeqSim compared to experimental results of this study at 4.3°C, 100 wt% TEG and pressures 54 - 193 bar.

All simulated values are within 6% deviation of the experimental data. The highest deviation is experienced at the highest pressure. The overall average deviation of the vapor density of 100 wt% TEG for all temperatures is 3.5%. Figure 9.36 displays the obtained simulated vapor densities in NeqSim compared to experimental values obtained in this study at 41.5°C and 90 wt% TEG.

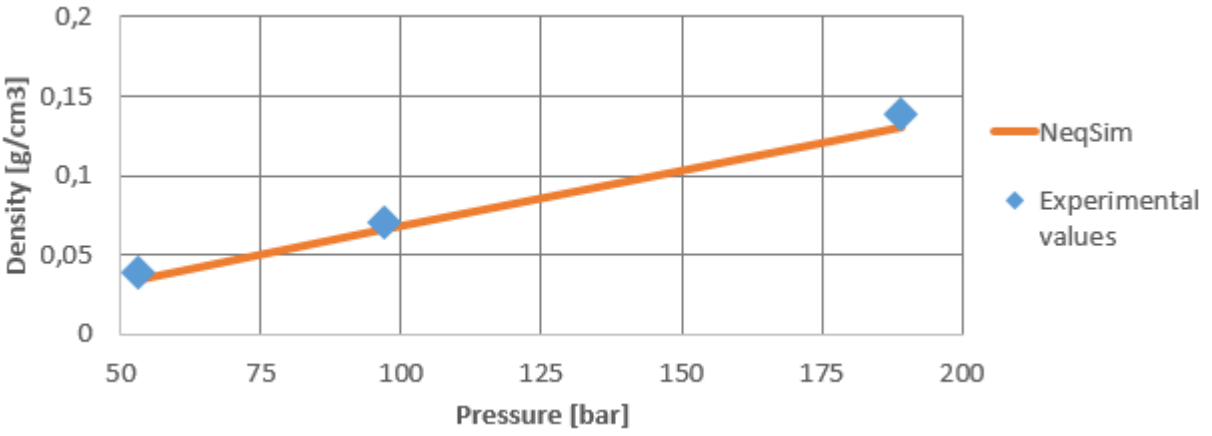

Figure 9.36: Calculated vapor density in NeqSim compared to experimental results of this study at 41.5°C, 90 wt% TEG and pressures 53 - 189 bar.

All simulated values are within 9% deviation of the experimental data. The overall average deviation of the vapor density of 90 wt% TEG for all temperatures is 9.6%. The simulated values are consistently lower than the experimental values, which are the case for all measured conditions in this experimental work for both liquid mixtures. We conclude that NeqSim calculates fairly accurate vapor density values.

9.4 Measured Values of this Study Compared to Ng et al. (2009)

There are several similarities between the experimental work in this study and that of Ng et al. (2009). Ng et al. (2009) conducted high pressure interfacial tension measurements utilizing aqueous TEG comprising 98 wt% TEG and methane. The experiments in this study was conducted at similar conditions, which means it is beneficial to compare the results. The measurements were conducted using the same measurement method, the pendant drop method.

Figure 9.37 plots experimental results from this study and the results from Ng et al. (2009) over pressure.

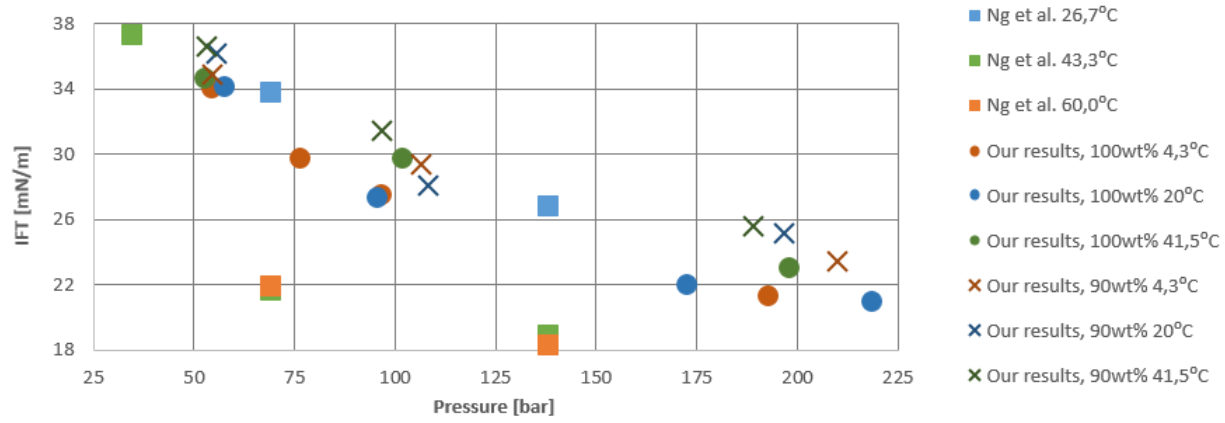

Figure 9.37: Comparison between the experimental results of this study and Ng et al. (2009).

Most of the measurements are located fairly in same area. Four measurements does not comply with the rest. These are the measurements of Ng et al. (2009) at 43.3 and 60°C at 69 and 138 bar. These values are significantly lower than the rest. We have no measurements at a temperature that can be compared to that of 60°C. However it seems unlikely that the temperature increase from 4.3 to 41.5°C results in measurements of roughly the same values, while the temperature increase to 60°C should result in significantly lower values. We do have measurements close to 43.3 and 26.7°C that can be compared.

Figure 9.38 plots experimental results from this study at 20°C and the results from Ng et al. (2009) at 26.7°C over pressure.

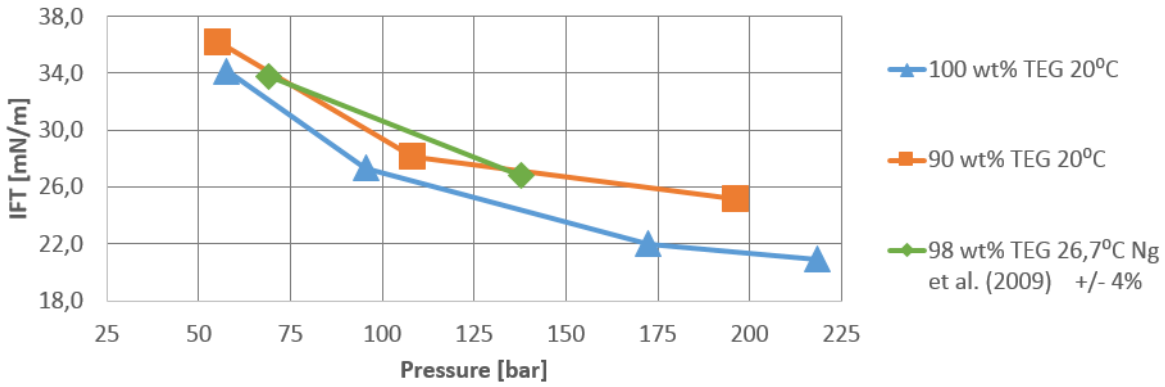

Figure 9.38: Comparison between the experimental results of this study at 20°C and Ng et al. (2009) at 26.7°C.

The experiments are conducted at slightly different temperatures, which can influence the values. However, the results obtained in Ng et al. (2009) and the results from this study are in the same range for all pressures. It seems their numbers comply strongly with the numbers from this study for the liquid mixture of 90 wt% TEG. It would perhaps be expected that their results would be closer to those of 100 wt% TEG, due to their composition of 98 wt% TEG. However, the addition of water to the TEG can be a bigger factor to the interfacial tension values than the amount of water itself. It is also difficult to account for what effect the temperature difference of 6.7°C constitutes.

Figure 9.39 plots experimental results from this study at 41.5°C and the results from Ng et al. (2009) at 43.3°C.

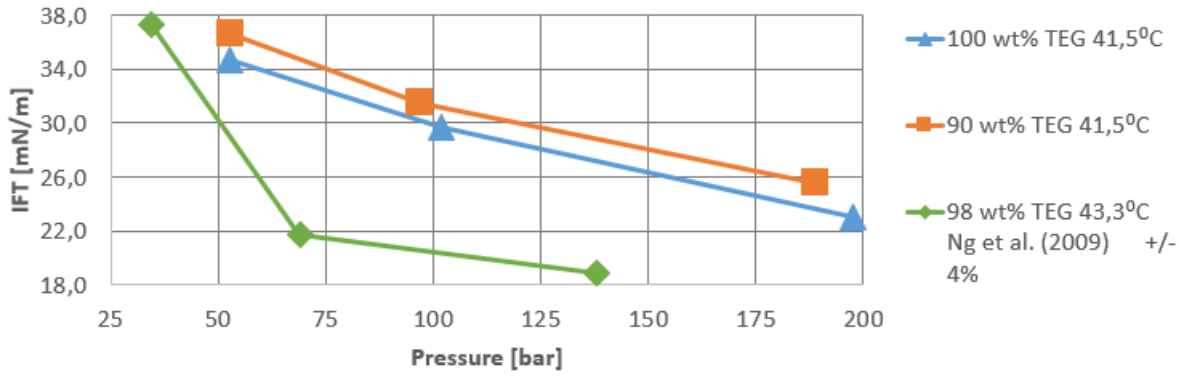

Figure 9.39: Comparison between the experimental results of this study at 41.5°C and Ng et al. (2009) at 43.3°C

The experiments are conducted at slightly different temperatures, which can influence the values. The results obtained in Ng et al. (2009) and the results from this study seem to comply at low pressures, but at higher pressures their values are significantly lower. The measured results

from the experimental work of this study show a linear decrease in interfacial tension with the increase of pressure. The results of Ng et al. (2009) seem to decrease exponentially with the increase of pressure. Naturally, the difference in temperature and composition must be considered as reasons for the deviation, but the difference is bigger than expected.

Overall, the interfacial tension values from the experimental measurements in this study decrease with the increase of pressure. This is in coherence with the results of Ng et al. (2009). However, the magnitude of the decrease appears to be significantly larger for the values from Ng et al. (2009). Another important aspect is the fact that we experienced a small increase in interfacial tension with the increase of temperature, as shown in Figures 8.1 and 8.2. The interfacial tension values from Ng et al. (2009) strongly decrease with the increase of temperature from 26.7 to 40°C, as shown in Figures 6.7 and 6.8.

Reviewing the comparisons with the property generation tools in Section 9.2 and 9.3, it appears the calculated values in NeqSim are more in agreement with the measured results of this study than those of Ng et al. (2009). As shown in Figures 9.17 and C.6 the values from NeqSim project fairly constant interfacial tension values with the increase of temperature. The simulated NeqSim values also project a linear decrease in the interfacial tension values with the increase of pressure, as shown in Figures 9.16, 9.21 and 9.25. These are the same conclusions that the measured values from this study support. The values from Ng et al. (2009) project an exponential decrease in interfacial tension with the increase of both temperature and pressure.

Figure 9.40 displays the overall average deviation percentage of the simulated values in NeqSim compared to the experimental data from this work and Ng et al. (2009).

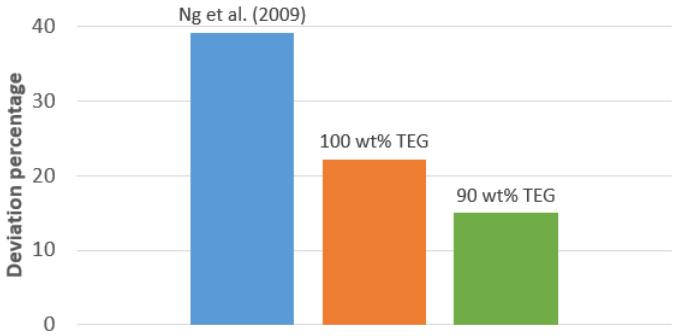

Figure 9.40: Average deviations of calculated results in NeqSim and experimental results of this study and Ng et al. (2009).

The fact that NeqSim predicts values more similar to the experimental data obtained in this study can be an indication of the authenticity of the measured values. It implies that the values from this study are more in coherence with the mathematical models. At 26.7°C, where the numbers from Ng et al. (2009) seem to be in coherence with the numbers from this study, the

average deviation of the calculated values in NeqSim and the experimental data from Ng et al. (2009) is 14%. At 43.3 and 60°C, where their numbers do not comply with the numbers from this study, the average deviations of the simulated values are 43.5% and 60% respectively.

In the literature there is little experimental data of interfacial tension of high pressure TEG and methane. It is therefore hard to conclude which values are correct. Kashefi (2012) established a decrease in interfacial tension of water and methane with the increase of temperature, as displayed in Figure 6.6 and Appendix C.1. This seems to be in agreement with the conclusion from Ng et al. (2009). The temperature increase measured by Kashefi (2012) is however significantly larger than those of this study and Ng et al. (2009), increasing from 37.8°C to 100, 150 and 200°C. Also, Kashefi (2012) measured the decrease in interfacial tension to be an average of 15% per increase of temperature level, and a maximum of 21% between temperatures 150 and 200°C. The values of Ng et al. (2009) decrease by an average of 33% between 26.7 and 43.3°C, which appears unreasonable.

Norgaard and Nygaard (2014) conducted high pressure interfacial tension measurements of the similar glycol MEG (MonoEthylene Glycol), water and methane at 5 and 20°C. The study conducted measurements for three different liquid mixtures, 100 wt% MEG, 80 wt% MEG and 50 wt% MEG in aqueous solution. The interfacial tension measurements proved similar at both temperature levels for all liquid mixtures, as can be seen in Appendix C.5. This is in agreement with the results obtained in this study.

Another factor is that Ng et al. (2009) conducted a total of seven measurements. At 34.5 bar there was conducted only one measurement, at 43.3°C. This means it is hard to thoroughly conclude on the behaviour of the interfacial tension values in regard to changes in pressure and temperature. We conducted 20 measurements, which all display the same behaviour.

To be able to establish the performance of NeqSim and PVTsim in regard to the calculation of interfacial tensions, the obtained measured values from the laboratory work of this Master's thesis will be emphasized for the evaluations.

9.5 Evaluation of Simulation Tools

This chapter has focused on deviations from experimental data. The calculation models are evaluated on the basis of the results of comparisons with experimental data.

9.5.1 Viscosity

A summary of the main deviations found for both property generation tools for liquid viscosity is presented in Table 9.1.

Evaluation	Generation tool	Main deviations
Well suited	NeqSim	Liquid mixtures at high temperatures
Certain flaws	PVTsim	Aqueous TEG at high temperatures Aqueous TEG at high pressures

Table 9.1: Summary of main deviations of liquid viscosity of the property generation tools

For pure TEG at atmospheric pressure PVTsim and NeqSim predict similar and accurate values.

For aqueous TEG containing 1.5 wt% water, PVTsim predicts accurate values at temperatures of 91°C and lower. At temperatures higher than this PVTsim predicts values which are significantly lower than the experimental data. For liquid mixtures containing higher weight fractions of water, PVTsim calculates accurate viscosity values at temperatures up to 80°C.

NeqSim calculates fairly accurate viscosity values for aqueous TEG containing up to 11 wt% water at all temperatures. At higher water weight fractions than this, NeqSim predicts viscosity values which are considerably higher than the experimental data at high temperatures. The deviation of NeqSim is however consistently lower than that of PVTsim for liquid mixtures at high temperatures. At temperatures lower than 109°C NeqSim predicts accurate values for all weight fractions of water.

At high pressures NeqSim predicts values which decrease with the increase of pressure, in coherence with the experimental data. PVTsim predicts liquid viscosity values which increase with the increase of pressure. NeqSim consistently provides smaller deviations than PVTsim at high pressures.

The Åsgard Transport Pipeline

Information provided by Statoil states that the fluid entering Kårstø from the Åsgard transport pipeline is 4°C and 120 bar. The aqueous TEG transported with the fluid comprises 99.9 wt% TEG. Considering the TEG content both NeqSim and PVTsim will provide accurate values at atmospheric pressure. However, the values predicted by NeqSim will be more accurate given the high operating pressure.

The presented literature data for the viscosity of TEG are all measured for temperatures of 20°C and higher. However, Statoil have been conducting measurements of the viscosity of TEG at

temperatures of 0 to 50°C and atmospheric pressure. The results are not published, but we have been granted access to a comparison between the measured values and simulated data. The comparison is presented in Appendix B.4. PVTsim and NeqSim predict similar values for temperatures higher than 30°C, which is in coherence with the comparisons with the literature data in this chapter. At temperatures 0 to 15°C, NeqSim predicts accurate values while PVTsim consistently overestimates the viscosity values. NeqSim will be more accurate at the operating temperature at Kårstø.

9.5.2 Interfacial Tension

A summary of the main deviations found for each calculation method for interfacial tension is presented in Table 9.2.

Evaluation	**Calculation method**	**Main deviations**
Well suited	Gradient Theory	Pure TEG at medium and high pressures
	GTSimple	Pure TEG at medium and high pressures Pure TEG at low temperatures Aqueous TEG with small weight fractions of TEG
Certain flaws	Parachor	High pressures Aqueous TEG at low temperatures
	Linear GT	Pure TEG Aqueous TEG at medium and high pressures Aqueous TEG at low temperatures
Several flaws	Firoozabadi Ramey	TEG
	PVTsim	TEG

Table 9.2: Summary of main interfacial tension deviations of the calculation methods

At atmospheric pressure the methods based on Gradient Theory and the Parachor Method provide similar results. The Firoozabadi Ramey Method and PVTsim overestimates the values significantly with the addition of TEG to the water.

For pressurized pure water, all methods except the Parachor Method provide decent results. The Parachor Method significantly underestimates the values at high pressures.

The simulated values for high pressure aqueous TEG obtained from Firoozabadi Ramey and PVTsim are more than twice as high as the experimental data. These two methods are disregarded as unsuitable.

The measurements conducted in this study display a linear decrease in interfacial tension with the increase of pressure for both liquid mixtures. The slope of the methods based on Gradient Theory is in coherence with this decrease. The slope of the Parachor Method is significantly steeper and the method underestimates the values significantly at pressures higher than 150 bar. However, the Parachor Method predicts the smallest deviations of all methods at pressures lower than this.

The methods based on Gradient Theory all overestimates the interfacial tension compared to the experimental data. They predict smaller deviations from the experimental data for the liquid mixture comprising 90 wt% TEG than for pure TEG. For pure TEG the deviations they provide increase with the increase of pressure. The Parachor Method predicts slightly smaller deviations for pure TEG than for the liquid mixture comprising 90 wt% TEG. Overall, the Gradient Theory provides the smallest deviations. The Gradient Theory Simple provides the second smallest deviations.

The Åsgard Transport Pipeline

The fluid entering Kårstø from the Åsgard transport pipeline is 4°C and 120 bar. The aqueous TEG transported with the fluid comprises 99.9 wt% TEG. Considering the conditions of the entering fluid the Gradient Theory, the Gradient Theory Simple and the Parachor Method will provide fairly accurate values. However, the pressure of the fluid entering the Åsgard transport pipeline is somewhere between 210 and 250 bar. This means the Parachor Method will provide significantly inaccurate values of the entering fluid.

Both the Gradient Theory and the Gradient Theory Simple will provide fairly accurate values. The most accurate interfacial tension values will be calculated by the Gradient Theory.

Chapter 10

Simulations in OLGA

The simulations conducted in OLGA are presented in this chapter. The version of OLGA utilized is 7.3.5. The simulations are conducted using both the standard OLGA module and the OLGA HD module. In section 10.1 the input structure of the simulations are described. Sections 10.2 presents the results of the simulations conducted using the standard OLGA module. Section 10.3 presents the results obtained from the simulations conducted with the OLGA HD module. Section 10.4 evaluates the results of the simulations and compares the two OLGA modules.

10.1 Input Structure

The simulations are conducted as a parameter study in OLGA. It is beneficial to this study to establish how the reviewed key properties affects the simulation of multiphase flow.

To establish the property sensitivity of OLGA, parameter factors are introduced. The factors utilized are 2, 5 and 10. The properties are divided and multiplied by these factors separately, meaning that only one property is altered by a parameter factor for every simulation. The three properties reviewed are liquid viscosity, interfacial tension and mass flow of TEG.

Two different scenarios are considered. The first scenario has TEG present in the rich gas only as carryover from the TEG contactors used for absorption. In the second scenario TEG is also present as an initial bulk volume of 30 m^3. Before the start-up of a gas field the pipeline is usually dried using TEG, which is why this is a realistic scenario. The amount of TEG is usually between 20 and 40 m^3.

The results presented from the simulations are the pressure drop, the accumulated TEG along the pipeline and the entrainment of droplets of TEG in the gas. The pressure drop and accumulated TEG is given as output in OLGA. The entrainment of TEG in the gas is calculated by

$$\text{Entrainment} = \frac{\text{UD"Droplet velocity"} \cdot \text{GAWT"Water droplet volume fraction"}}{\text{USLTWT"Superficial velocity water"}} \tag{10.1}$$

where UD, GAWT and USLTWT are output variables given in OLGA. OLGA does not differentiate between TEG and water. This means that what is presented from OLGA in the following chapter as water is actually TEG with a small percentage of water. The entrainment is the ratio of the mass rate of TEG transported as droplets in the gas to the total mass rate of TEG.

10.1.1 Åsgard Transport

Åsgard transport is the pipeline carrying rich gas from the Åsgard field in the Norwegian Sea to the Kårstø processing plant. Natural gas is also delivered to the pipeline system from Skarv, Norne, Heidrun, Njord and Draugen.

The start point of the simulations is where the gas from Norne enters the Åsgard transport pipeline. When the Norne pipeline was first connected to the Åsgard pipeline it was dried using TEG, as in simulation scenario 2. At this point in the pipeline the temperature of the fluid is fairly low. The end point of the simulations is the outlet of the pipeline, at the processing plant at Kårstø.

10.1.2 NeqSim

Property tables are generated in NeqSim using the Gradient Theory. As shown in Chapter 9 this method predicts the most accurate values compared to the experimental data. The fluid utilized comprise 80 mole% methane, 19 mole% ethane, 0.999 mole% TEG and 0.001 mole% water. This is closely related to what enters Kårstø from the Åsgard transport pipeline.

The pressure range in NeqSim is from 50 to 500 bar. The temperature range is from -60 to 80 °C. The calculations are conducted using 50 grid points for both temperature and pressure, leading to 2500 condition points for each fluid property.

The parameter factor 1 equals the standard property values generated by NeqSim. First, the liquid viscosity values are multiplied by the parameter factors, while the interfacial tension parameter factor remains at 1. The result is seven different property tables. After this, the liquid viscosity parameter factor is set to 1 and the interfacial tension values are multiplied by the parameter factors. The resulting generated property tables are presented in Table 10.1.

Interfacial tension = 1							
Liquid viscosity	0.1	0.2	0.5	1	2	5	10
Liquid viscosity = 1							
Interfacial tension	0.1	0.2	0.5	1	2	5	10

Table 10.1: Property tables generated in NeqSim by parameter factors

10.1.3 PVTsim

One property table is generated in PVTsim with an equivalent fluid composition for comparisons. This is a standard property table, and can be compared to the NeqSim property table with interfacial tension and liquid viscosity parameter factor 1.

The pressure range in PVTsim is from 1 to 301 bar. The temperature range is from -100 to 100 °C. The calculations are conducted using 50 grid points for both temperature and pressure, the same amount as in NeqSim.

10.1.4 OLGA

The simulation file utilized in OLGA was provided by Statoil with the help of Knud Lunde. The conditions of the pipeline and the fluid flow is presented in Table 10.2.

Description	**Unit**	**Value**
Pipeline information		
Number of sections	-	1576
Total length	m	706695
Change in elevation	m	321.07
Pipe diameter	m	1.016
Inner wall conductivity	W/m°C	50
Inner wall density	kg/m^3	7850
Inner wall thermal capacity	J/kg°C	880
Thermodynamic conditions		
Ambient temperature	°C	6
Temperature at pipeline inlet	°C	6
Temperature at pipeline outlet	°C	4
Pressure at pipeline outlet	bar	120
Initial conditions		
Pressure at pipeline inlet	bar	240
Mass flow gas	kg/s	708.64
Mass flow TEG	kg/s	0.0447

Table 10.2: OLGA input structure

Initial conditions have to be given to simulate transient conditions in the pipeline in OLGA.

"Pressure at pipeline inlet" is calculated by using steady state simulations, and acts as a guideline for the transient simulations. The mass flow of gas is calculated from a volume flow of 69 MSm^3/d and remains constant throughout the simulations. The mass flow of TEG is based on the assumption of a carryover of 50 litres of TEG per MSm^3 gas. According to Kordabadi and Dinon (2013), we can expect a maximum carryover of 14 litres of TEG per MSm^3. To ensure that the amount of TEG is not underestimated, the carryover is set to 50 litres of TEG per MSm^3.

Scenario One

In the first scenario TEG is present only as carryover from the TEG contactors used for absorption. In this scenario the mass flow of TEG is varied by using the parameter factors. The TEG mass flow is only varied when utilizing the generated property tables from NeqSim and PVTsim were liquid viscosity and interfacial tension parameter factor is 1. The different mass flows of TEG utilized is presented in Table 10.3 along with the parameter factors and volume flows.

Parameter factors	**0.1**	**0.2**	**0.5**	**1**	**2**	**5**	**10**
Volume flow TEG [litre/MSm^3 gas]	5	10	25	50	100	250	500
Mass flow TEG [kg/s]	0.0045	0.0089	0.0224	0.0447	0.0894	0.2235	0.4472

Table 10.3: Mass flow of TEG parameter factors

Scenario Two

In the second scenario TEG is also present as an initial volume amount of 30 m^3 in the first section of the pipe. In this scenario the TEG mass flow parameter factor is constant at 1 for all simulations. This equals a mass flow of 0.0447 kg/s and a volume flow of 50 litres of TEG per MSm^3 gas.

Time Steps and Simulated Time

Simulations of pressure drop and accumulated TEG along the pipeline are conducted with a time step of 10 hours and a simulation time of 10 days. The pressure drop stabilizes at a simulated time of 5 days. The value of accumulated TEG is not stable at 10 days. To acquire stable values long simulation times in OLGA are needed, and the time step has to be small to avoid instabilities. These are complex calculations, and each simulation would take several hours to complete. To be able to compare all desired simulations, the accumulated TEG volume at a simulated time of 10 days are used.

The entrainment of TEG in scenario 1 are obtained by using the time step of 10 hours and the simulation time of 10 days. In scenario 2 the simulations have to be integrated with small time steps to obtain entrainment of TEG in the gas caused by the initial dump of TEG. The time step

is set to 0.05 hours, and the simulations are conducted until the largest entrainment at any point of the pipeline is less than 1%. The entrainment is considered negligible below this value. The simulated time where this occurs is concluded to be the maximum time of entrainment. The distance with the largest entrainment percentage at this time of simulation is concluded to be the maximum distance of entrainment.

Small time steps and long simulation times leads to an OLGA file which exceeds the maximum file size, and the simulation is aborted. Because of this the maximum simulation time possible with the time step of 0.05 hours is 65 hours. If there is still entrainment of TEG at this time it can not be established at what time the entrainment will disappear. In this case the furthest distance of which the entrainment is higher than 1% is presented for comparisons.

10.2 Simulations with the Standard OLGA Module

10.2.1 Scenario One - Carryover of TEG

A total of 26 simulations are conducted with the standard OLGA module for scenario 1. 19 are conducted using property tables generated by NeqSim, and seven are conducted using the property table generated by PVTsim. Liquid viscosity, interfacial tension and TEG mass flow are altered by the parameter factors.

Pressure Drop

Figure 10.1 displays the simulated pressure along the pipeline in OLGA, along with the geometry of the pipeline. The simulation displayed is for TEG mass flow parameter factor 10, after a simulated time of 10 days. As described above, the interfacial tension and liquid viscosity parameter factor is 1 for this simulation.

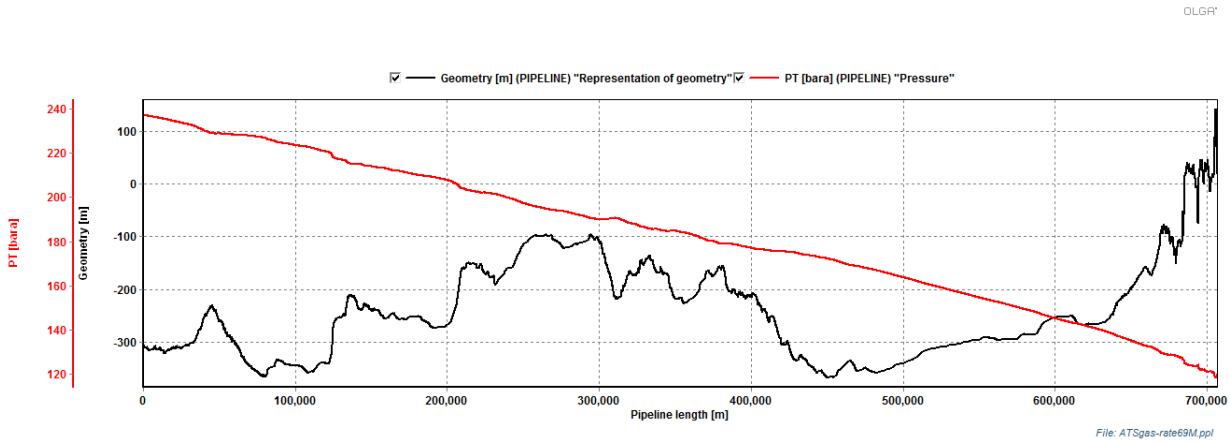

Figure 10.1: Simulated pressure along pipeline with the standard OLGA module and TEG carry-over and TEG mass flow parameter factor 10.

Figure 10.1 displays a decrease in pressure along the pipeline, and an increase in elevation. The stabilized inlet pressure is 236 bar, and the outlet pressure is 120 bar. Figure 10.2 plots the total pressure drop after 10 days for all simulations over the multiplied parameter factors. The exact values are presented in Appendix D.1.

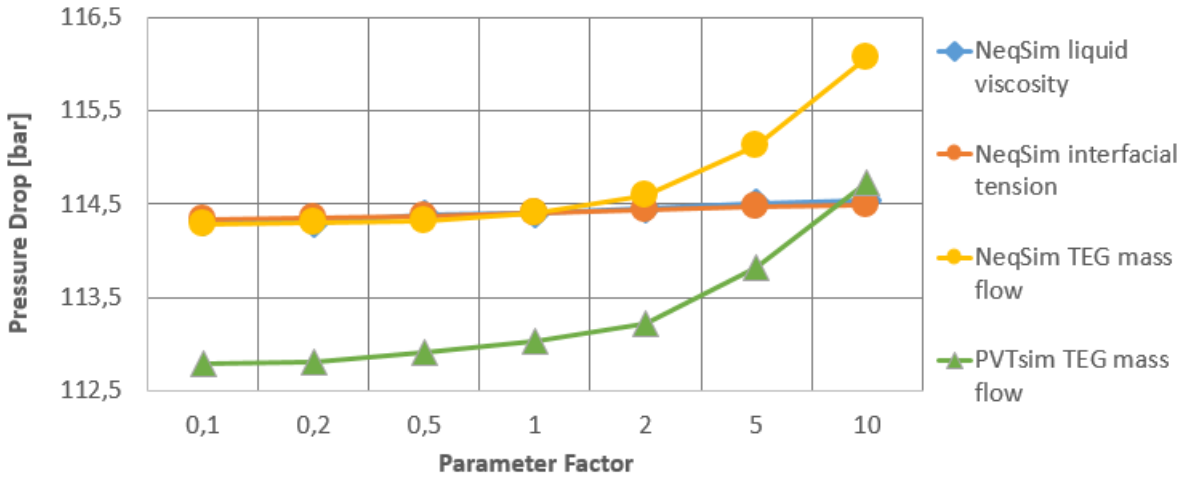

Figure 10.2: Simulated total pressure drop with the standard OLGA module and TEG carryover with parameter factors 0.1 to 10

It appears that the standard OLGA module is very little sensitive to changes in both interfacial tension and liquid viscosity values. OLGA simulates a pressure drop of 114.3 bar for liquid viscosity multiplied by a factor of 0.1. Liquid viscosity multiplied by 10 results in a simulated pressure drop of 114.5. The corresponding numbers for interfacial tension is also 114.3 when multiplied with 0.1 and 114.5 bar when multiplied with 10. The difference of 0.2 bar is negligible.

In regard to TEG mass flow, OLGA displays a larger sensitivity. The pressure drop increases with the increase of TEG mass flow for both PVTsim and NeqSim. NeqSim results in a pressure drop which on average is 1.4 bar higher than that of PVTsim. Both property generators experience an increase in pressure drop of about 2 bar with the increase of TEG mass flow parameter factor from 0.1 to 10. This is low considering that the mass flow is multiplied by a factor of 100.

Accumulated TEG along Pipe

Figure 10.3 displays the simulated accumulated volume of TEG along the pipeline obtained in OLGA, along with the geometry of the pipeline. The simulation displayed is for parameter factor 1 for all properties, after a simulated time of 10 days.

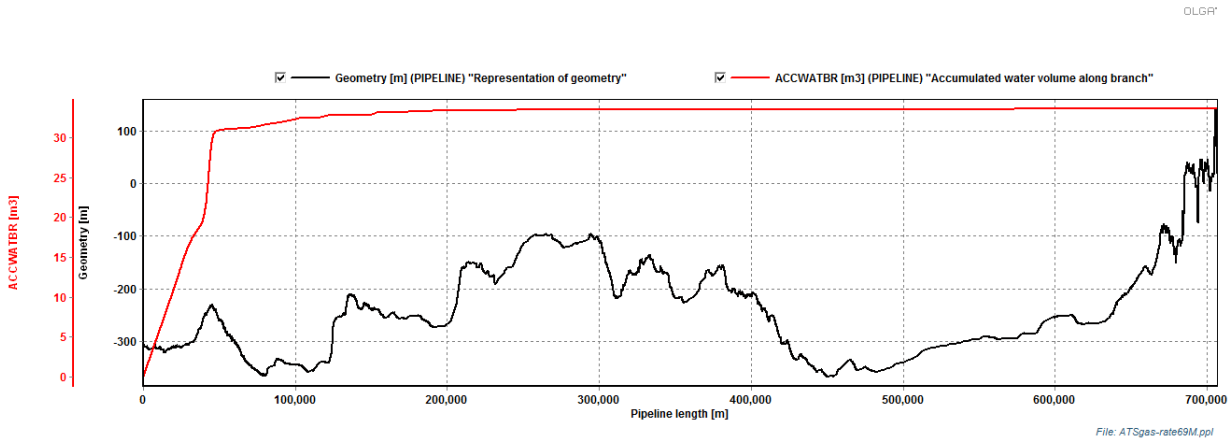

Figure 10.3: Simulated accumulated TEG along pipeline with the standard OLGA module and TEG carryover with parameter factors 1

Figure 10.3 displays a total accumulated TEG volume of 33.6 m^3. Figure 10.4 plots the accumulated TEG volume after 10 days for simulations where liquid viscosity and interfacial tension are multiplied with parameter factors. The exact values are presented in Appendix D.1.

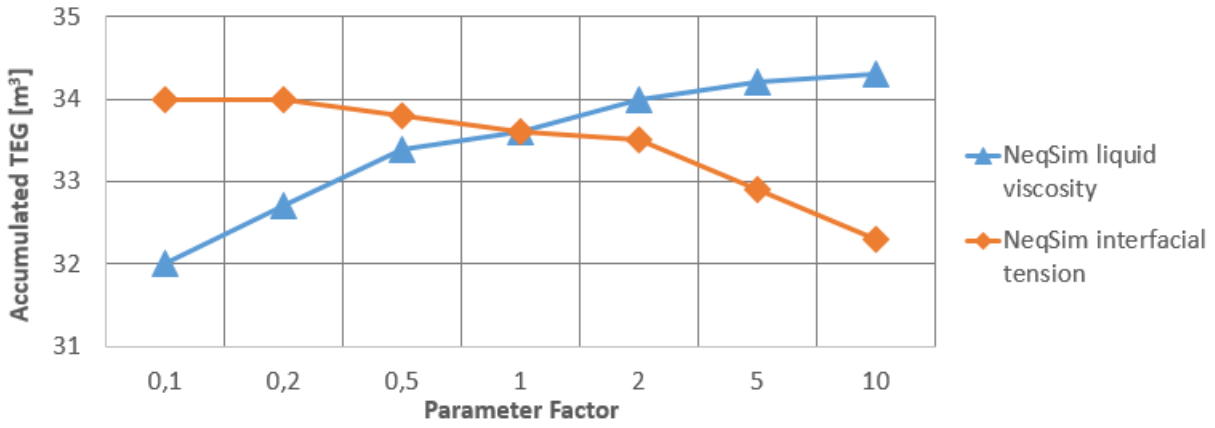

Figure 10.4: Simulated accumulated TEG volume along pipeline with the standard OLGA module and TEG carryover for liquid viscosity and interfacial tension parameter factors 0.1 to 10

OLGA displays small sensitivity to changes in these values. The accumulated TEG volume slightly increases with the increase of liquid viscosity. With the increase of interfacial tension it slightly decreases. Figure 10.5 plots the accumulated TEG volume after 10 days for simulations where the TEG mass flow are multiplied with parameter factors. The exact values are presented in Appendix D.1.

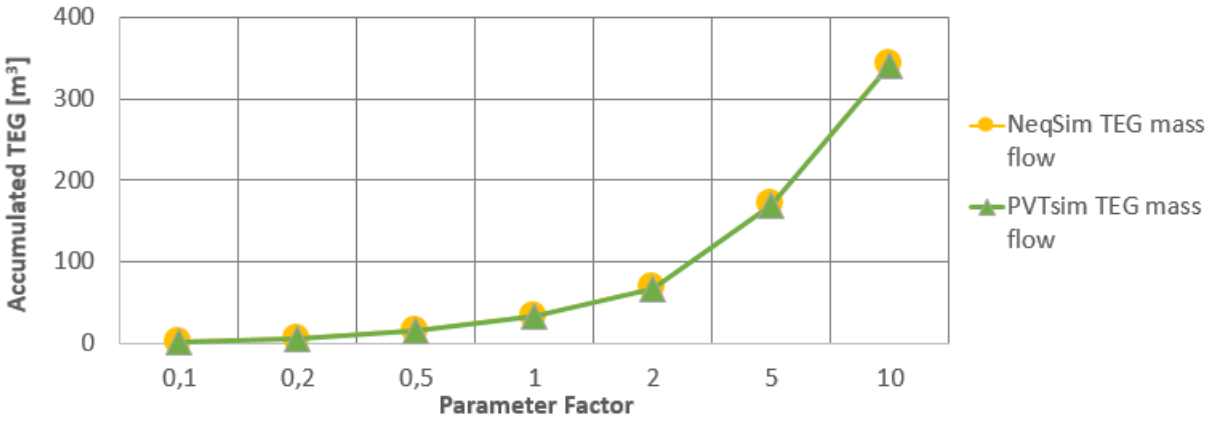

Figure 10.5: Simulated accumulated TEG volume along pipeline with the standard OLGA module and TEG carryover for TEG mass flow parameter factors 0.1 to 10

Logically, the amount of accumulated TEG strongly increases with the increase of TEG mass flow for both property table generation tools. The accumulated TEG volume is on average 1% higher in the simulations conducted using the property table generated by NeqSim than in the simulations using the property table in PVTsim.

Entrainment of TEG

There is no entrainment of TEG at any time in any of the simulations with the standard OLGA module.

10.2.2 Scenario Two - Initial Dump of TEG

As described earlier the TEG mass flow parameter factor is constant at 1 for these simulations. A total of 14 simulations are conducted in OLGA. 13 are conducted using property tables generated by NeqSim, and one is conducted using the property table generated by PVTsim. Liquid viscosity and interfacial tension are altered by the parameter factors.

Pressure Drop

Figure 10.6 plots the pressure drop after 10 days for simulations where liquid viscosity and interfacial tension are multiplied with parameter factors. The exact values are presented in Appendix D.2.

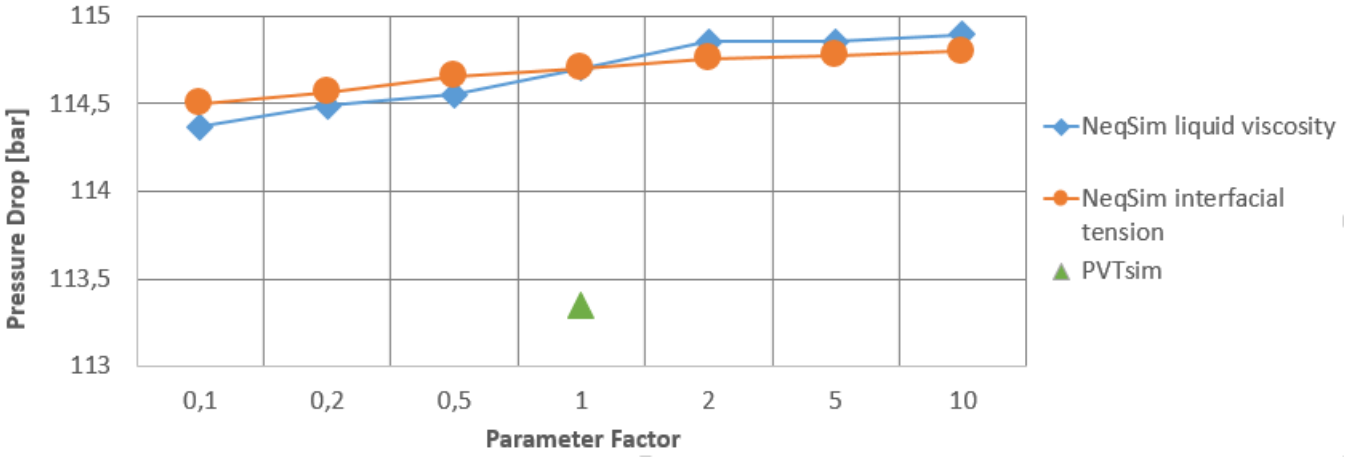

Figure 10.6: Simulated total pressure drop with the standard OLGA module and initial dump of TEG for parameter factors 0.1 to 10

OLGA is not very sensitive to changes in either interfacial tension or liquid viscosity values, however slightly more than in scenario 1. OLGA simulates a pressure drop of 114.4 bar for liquid viscosity multiplied by a factor of 0.1. Liquid viscosity multiplied by 10 results in a simulated pressure drop of 114.9. The increase is 0.5 bar. The corresponding numbers for interfacial tension is 114.5 when multiplied with 0.1 and 114.8 bar when multiplied with 10. An increase of 0.3 bar. The property table from PVTsim simulates a pressure drop of 113.3 bar. This is 1.4 bar lower than the standard table in NeqSim.

Accumulated TEG along Pipe

Figure 10.7 plots the accumulated TEG volume after 10 days for all simulations over the multiplied parameter factors. The exact values are presented in Appendix D.2.

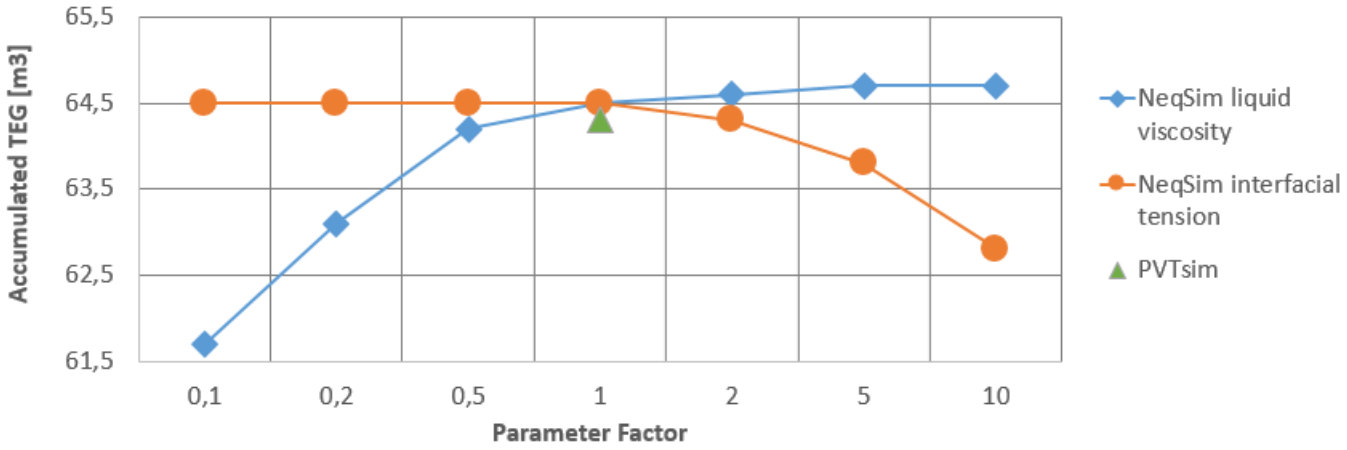

Figure 10.7: Simulated accumulated TEG volume along pipeline with the standard OLGA module and initial dump of 30 m^3 TEG for parameter factors 0.1 to 10

OLGA displays small sensitivity to the parameter factors. The accumulated TEG volume slightly increases with the increase of liquid viscosity. With the increase of interfacial tension it slightly decreases. The simulation using the property table from PVTsim results in 64.3 m^3 accumulated TEG, compared to 64.5 m^3 when using the standard NeqSim property table.

Entrainment of TEG

The simulations have to be integrated with small time steps to obtain entrainment of TEG in the gas caused by the initial dump of TEG. Figure 10.8 displays the entrainment percentage of TEG in the gas over the pipeline distance after a simulated time of 6 minutes and liquid viscosity multiplied by a parameter factor of 0.2.

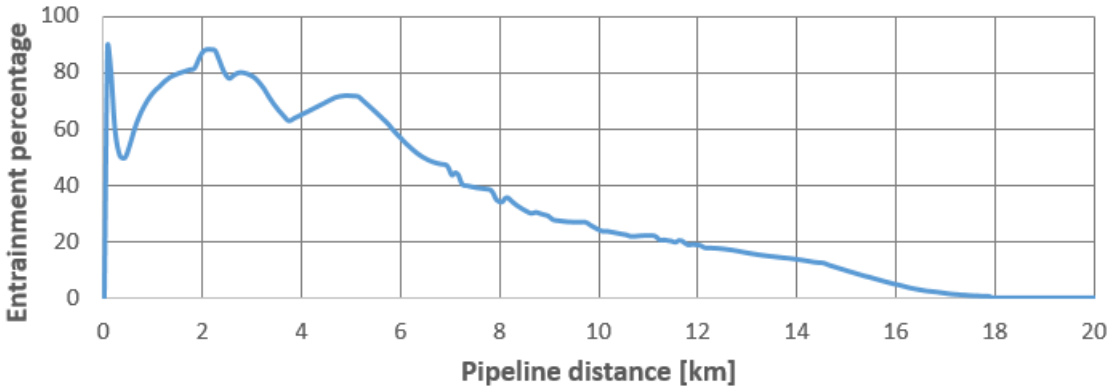

Figure 10.8: Simulated entrainment percentage of TEG in gas with the standard OLGA module after 6 minutes and liquid viscosity parameter factor 0.2

At this point of time in the simulation there is entrainment from the inlet and 18 kilometres into the pipe. The initially large entrainment percentage is caused by the dump of 30 m^3 TEG. Figure 10.9 displays the entrainment percentage of TEG in the gas over the pipeline distance for the same situation after a simulated time of 22.5 hours.

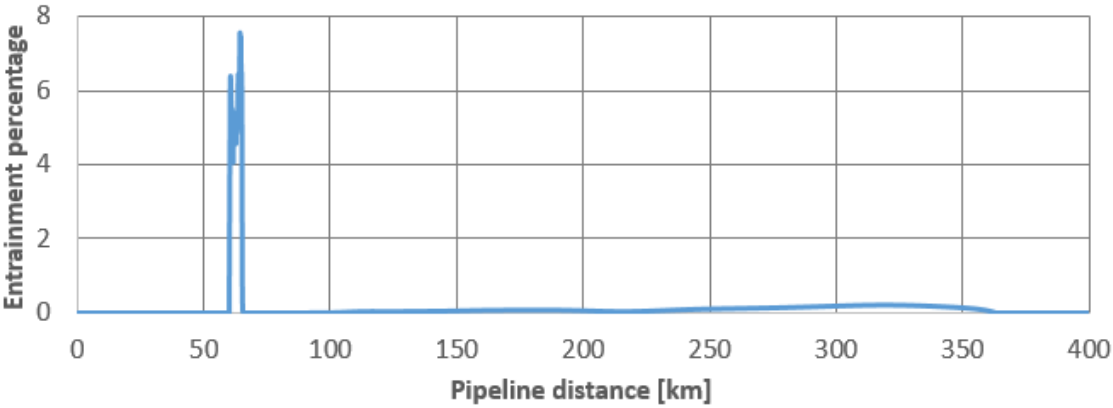

Figure 10.9: Simulated entrainment percentage of TEG in gas with the standard OLGA module after 22.5 hours and liquid viscosity parameter factor 0.2

The entrainment percentage is much smaller after 22.5 hours. Figure 10.9 displays how the initial dump of TEG has been been spread out and the majority of it transported a distance of 65 kilometres into the pipe. There are also small amounts of entrainment 350 kilometres into the pipe. The obtained maximum time and distance of entrainment as described earlier in the chapter are presented for all simulations in Table 10.4.

Factor	Liquid Viscosity	Interfacial Tension	PVTsim
0.1	65 h, 189 km	45 h, 86 km	
0.2	40 h, 114 km	30 h, 57 km	
0.5	15 h, 40 km	15 h, 35 km	
1	5.6 h, 15 km	5.6 h, 15 km	1.5 h, 6.3 km
2	1 h, 8.7 km	4 h, 15 km	
5	1 h, 9.1 km	0.3 h, 1.8 km	
10	No entrainment	0.3 h, 1.8 km	

Table 10.4: Maximum time and distance of entrainment of TEG in gas, standard OLGA

The only simulation where the maximum time of entrainment can not be established is for liquid viscosity with parameter factor 0.1. In this case the amount of entrainment are not decreasing noticeably around 65 hours, and it is conceivable that the entrainment will eventually reach the outlet of the pipeline. The maximum time and distance of entrainment of TEG is generally decreasing with the increase of liquid viscosity and interfacial tension. It appears that both properties highly affect the calculations. The simulated entrainment in OLGA display a slightly higher sensibility to liquid viscosity than to interfacial tension. The property table generated by PVTsim results in less entrainment than the standard property table generated by NeqSim. The simulated entrainment for all situations display the same behaviour. There is an initially large amount of entrainment, caused by the 30 m^3 of TEG. As the simulation time increases the TEG is spread out along the pipe. What remains is a single spike of entrainment which travels through the pipe and decreases with time, similar to that in Figure 10.9. The simulated entrainment appear to be independent of the geometry of the pipeline.

10.3 Simulations with the OLGA HD Module

All simulations conducted with the standard OLGA module results in stratified flow regimes. The OLGA HD module is specifically designed to be beneficial for these conditions, as described in Section 5.1.1. To compare the results the simulations are repeated using the OLGA HD module.

10.3.1 Scenario One - Carryover of TEG

A total of 26 simulations are conducted with the OLGA HD module. 19 are conducted using property tables generated by NeqSim, and seven are conducted using the property table generated in PVTsim. Liquid viscosity, interfacial tension and TEG mass flow are altered by the parameter factors.

Pressure drop

Figure 10.10 plots the total pressure drop along the pipe after 10 days for simulations where liquid viscosity and interfacial tension are multiplied with the parameter factors. The exact values are presented in Appendix D.3.

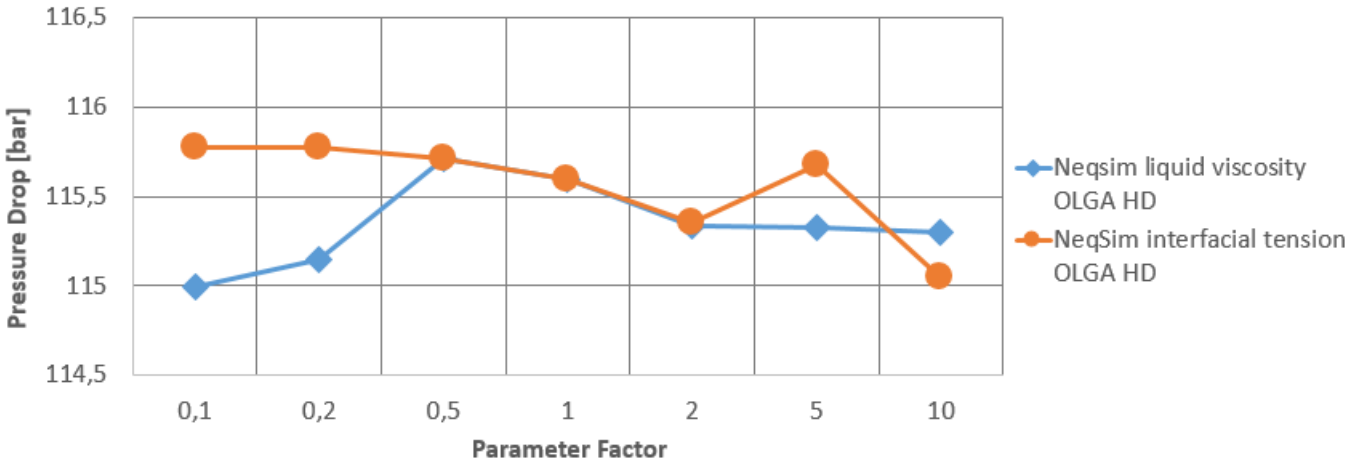

Figure 10.10: Simulated total pressure drop with the OLGA HD module and TEG carryover for liquid viscosity and interfacial tension parameter factors 0.1 to 10

OLGA HD display some sensitivity to changes in these properties. OLGA HD simulates a pressure drop of 115.8 bar for interfacial tension multiplied by a factor of 0.1. Interfacial tension multiplied by 10 results in a simulated pressure drop of 115.0. The decrease is 0.8 bar. The corresponding numbers for liquid viscosity is 115.0 bar when multiplied with 0.1 and 115.3 bar when multiplied with 10. Liquid viscosity experience the highest pressure drop when multiplied by the parameter factor 0.5.

Figure 10.11 plots the total pressure drop along the pipe after 10 days for simulations where TEG mass flow are multiplied by the parameter factors. The exact values are presented in Appendix D.3.

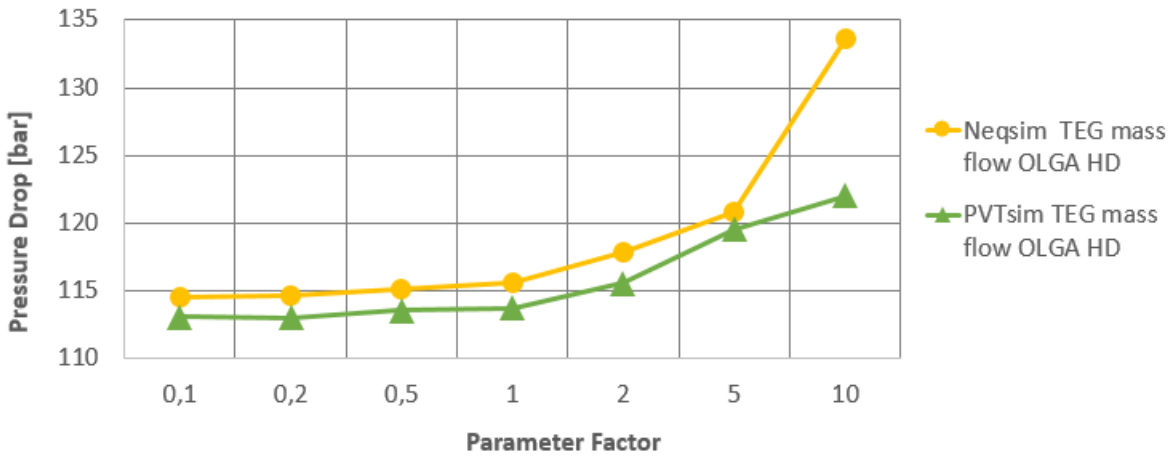

Figure 10.11: Simulated total pressure drop with the OLGA HD module and TEG carryover for mass flow parameter factors 0.1 to 10

The simulations in OLGA HD displays an increase of total pressure drop with the increase of TEG mass flow for both NeqSim and PVTsim. NeqSim experience an increase in pressure drop of about 19 bar with the increase of TEG mass flow parameter factor from 0.1 to 10. The corresponding number for PVTsim is 9 bar. NeqSim provides a pressure drop which on average is 1.6 bar higher than that of PVTsim for parameter factors 0.1 to 5. When multiplied with a parameter factor of 10 NeqSim simulates a pressure drop 11 bar higher than that of PVTsim.

Accumulated TEG along Pipe

Figure 10.12 plots the accumulated TEG volume after 10 days for simulations where liquid viscosity and interfacial tension are multiplied with parameter factors. The exact values are presented in Appendix D.3.

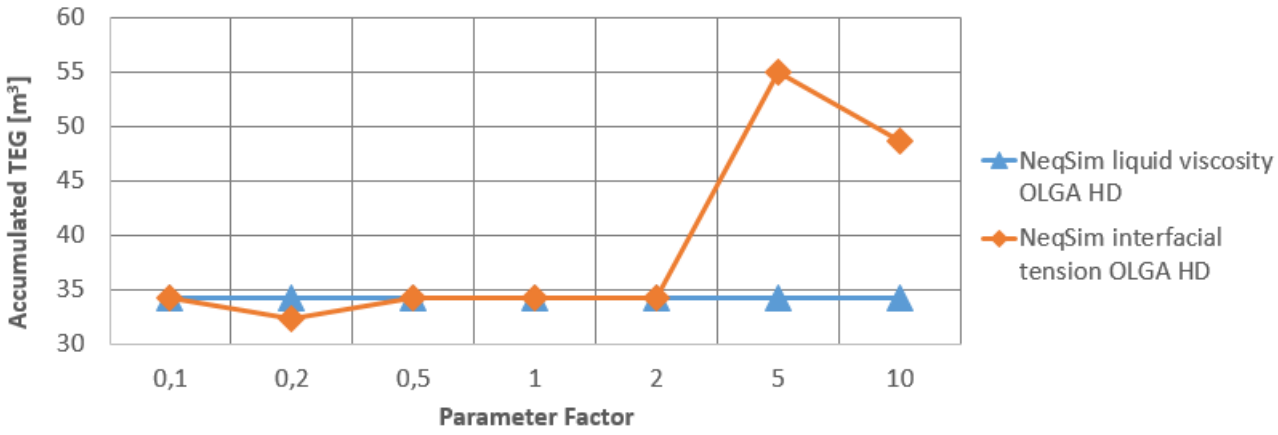

Figure 10.12: Simulated accumulated TEG volume along pipeline with the OLGA HD module and TEG carryover for liquid viscosity and interfacial tension parameter factors 0.1 to 10

OLGA HD displays no sensitivity to changes in liquid viscosity. The amount of accumulated TEG along the pipeline is 34.3 m^3 for all parameter factors. Interfacial tension multiplied with parameter factors 0.1 to 2 also simulates around 34 m^3 of TEG. When interfacial tension is multiplied with parameter factors 5 and 10 there is a distinct increase in accumulated TEG.

Figure 10.13 plots the accumulated TEG volume after 10 days for simulations where TEG mass flow are multiplied with the parameter factors. The exact values are presented in Appendix D.3.

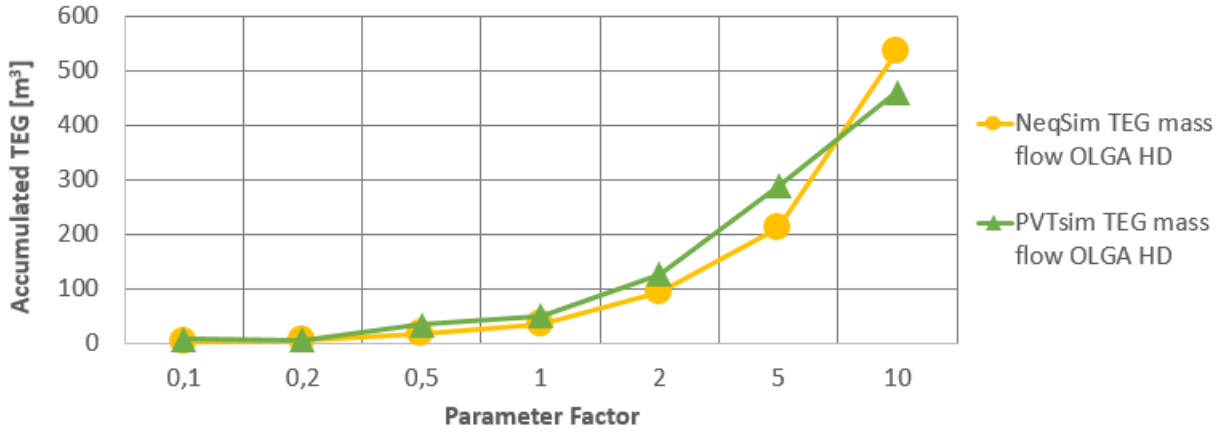

Figure 10.13: Simulated accumulated TEG volume along pipeline with the OLGA HD module and TEG carryover for mass flow parameter factors 0.1 to 10

Figure 10.13 displays an increase in accumulated TEG along the pipeline with the increase of TEG mass flow for both generation tools. This is expected as a higher TEG mass flow should lead to more accumulated TEG in the pipe. PVTsim consistently results in higher values than NeqSim, except at the parameter factor 10.

Entrainment of TEG

There are entrainment of TEG for some parameter factors with the OLGA HD module. Because there are no dump of TEG in this scenario, the entrainment that occurs do not disappear with time or distance. It is also increasing over time.

Entrainment were obtained in simulations with liquid viscosity multiplied by parameter factors 0.1 and 0.2. There was no entrainment for any interfacial tension parameter factors. Apparently entrainment are more sensitive to changes in liquid viscosity than changes in interfacial tension. There was also obtained entrainment for TEG mass fraction parameter factors 2, 5 and 10 for both PVTsim and NeqSim.

10.3.2 Scenario Two - Initial Dump of TEG

As with the simulations conducted with the standard OLGA module, the TEG mass flow parameter factor is 1 for these simulations. A total of 14 simulations are conducted with the OLGA HD module. 13 are conducted using property tables generated by NeqSim, and one is conducted using the property table generated by PVTsim. Liquid viscosity and interfacial tension is altered by the parameter factors.

Pressure Drop

Figure 10.14 plots the pressure drop after 10 days over the parameter factors. The exact values are presented in Appendix D.4.

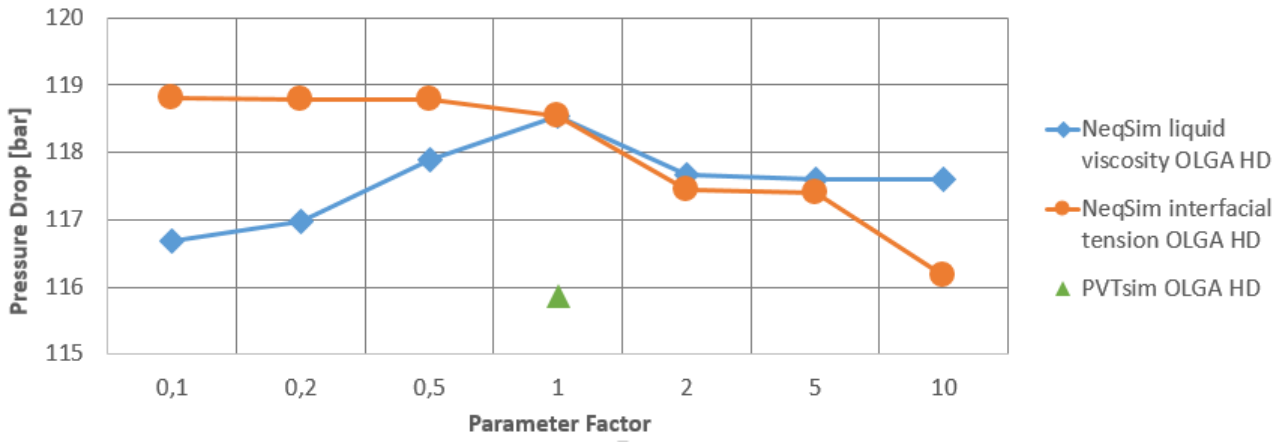

Figure 10.14: Simulated pressure drop with OLGA HD module with initial dump of 30 m^3 TEG and parameter factors 0.1 to 10

OLGA HD displays a slightly higher sensitivity to the parameter factors than in scenario 1. The largest pressure drop simulated by altering liquid viscosity is at parameter factor 1 of 118.5 bar. The increase of interfacial tension results in a decrease of pressure drop. OLGA HD simulates a pressure drop of of 118.8 bar at parameter factor 0.1. At parameter factor 10 the simulated pressure drop is 116.2 bar. The decrease is 2.6 bar. The property table from PVTsim simulates a pressure drop of 115.9 bar, 2.7 bar lower than the standard table in NeqSim.

Accumulated TEG along Pipe

Figure 10.15 plots the accumulated TEG volume after 10 days over the parameter factors. The exact numbers are presented in Appendix D.4.

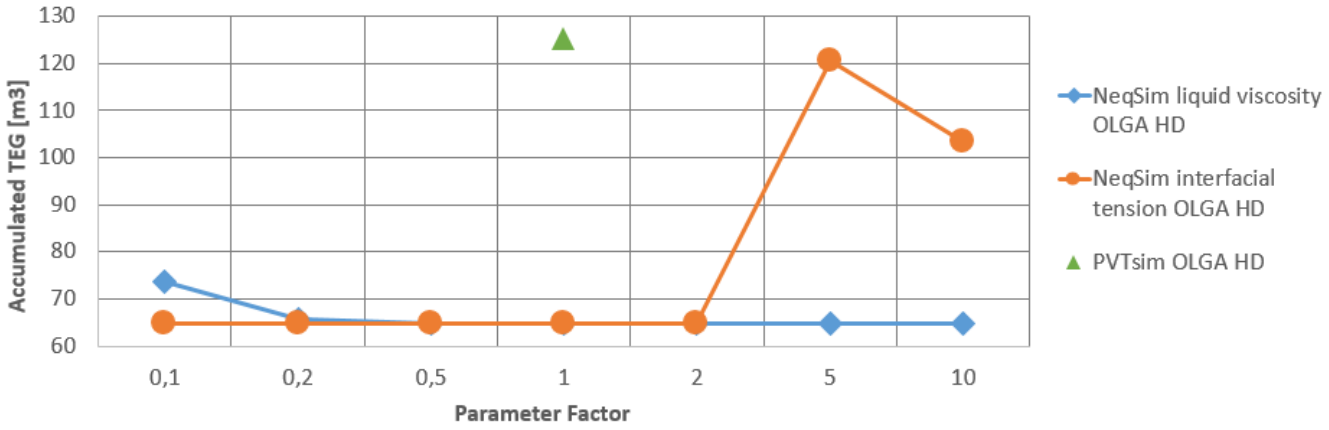

Figure 10.15: Simulated accumulated TEG with OLGA HD module and initial dump of 30 m^3 TEG for parameter factors 0.1 to 10

OLGA HD displays small sensitivity to changes in liquid viscosity. Interfacial tension multiplied with parameter factors 0.1 to 2 also simulates similar accumulated TEG volumes. When interfacial tension is multiplied with parameter factors 2 and 5 there is a distinct increase in accumulated TEG.

Entrainment

Figure 10.16 displays the entrainment percentage of TEG over the pipeline distance with parameter factors 1 and a simulated time of 65 hours, along with the geometry of the pipeline.

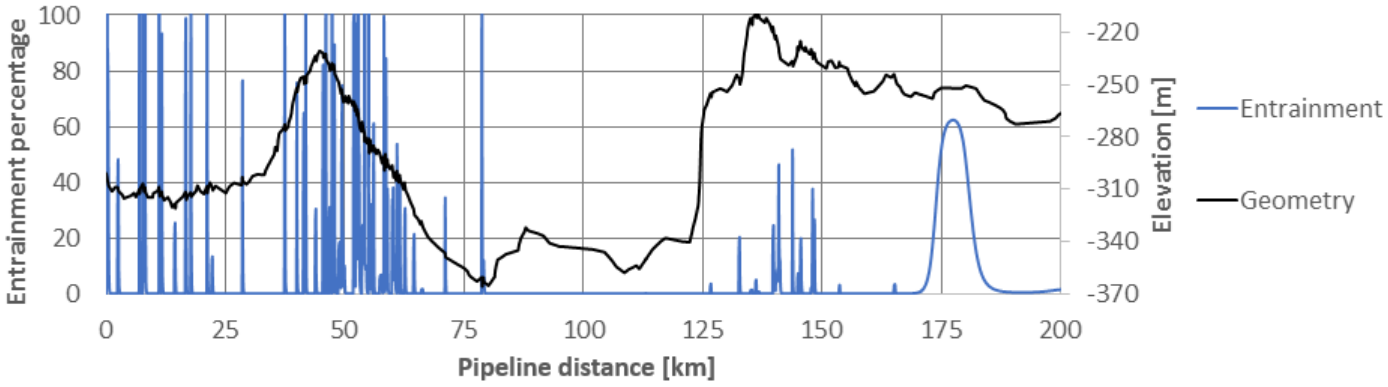

Figure 10.16: Simulated percentage entrainment of TEG in the gas after 65 hours with the OLGA HD module and parameter factors 1

Figure 10.16 displays an entrainment percentage which remains high and spreads out along the pipeline over time. The entrainment appear highly dependent on the geometry of the pipeline.

Figure 10.17 displays the entrainment percentage over the pipeline distance with liquid viscosity parameter factor 10 and a simulated time of 65 hours, along with the geometry of the pipeline.

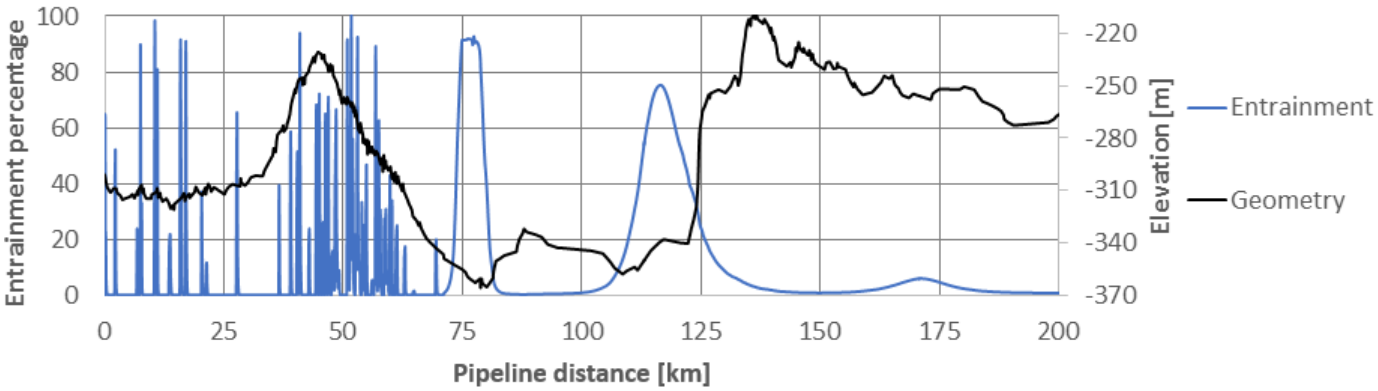

Figure 10.17: Simulated percentage entrainment of TEG in the gas after 65 hours with the OLGA HD module and liquid viscosity parameter factor 10

Figure 10.17 displays a similar pattern of high and geometry dependent entrainment of TEG. The simulations for all parameter factors results in lots of entrainment in the pipe at 65 hours. This means that the maximum time of entrainment can not be established. The entrainment plots for the simulations display individual differences, as can be seen by comparing Figures 10.16 and 10.17, but these are hard to quantify. The distance of entrainment is the most straightforward parameter to compare the simulations. The obtained distance of entrainment for all simulations at 65 hours in OLGA HD are presented in Table 10.5.

Factor	Liquid Viscosity	Interfacial Tension	PVTsim
0.1	186 km	200 km	
0.2	180 km	189 km	
0.5	207 km	166 km	
1	186 km	186 km	124 km
2	147 km	174 km	
5	186 km	136 km	
10	190 km	155 km	

Table 10.5: Distance of entrainment of TEG in gas at 65 hours of simulated time, OLGA HD

Both properties highly affect the entrainment distance. The disparity in distance caused by alterations in property values are as high as 71 kilometres. Most of the simulations end up with entrainment about 190 kilometres into the pipe. The longest is simulated with liquid viscosity parameter factor 0.5. High interfacial tension values results in shorter entrainment distances. The entrainment is conceivable to eventually reach the outlet of the pipeline for all simulations. The simulation with PVTsim results in the shortest entrainment distance of all simulations.

The simulated entrainment for all simulations display similar behaviours overall. There is an initially large amount of entrainment, caused by the 30 m^3 dump of TEG. The entrainment percentage remains high and spreads out along the pipe over time. The simulations also appear highly dependent on the geometry of the pipeline, as is illustrated in Figures 10.16 and 10.17.

10.4 Evaluation of OLGA Simulations

10.4.1 The Standard OLGA Module

Table 10.6 presents the sensitivity of the standard OLGA module to the parameter factors based on the results from both scenarios.

Parameter	**Pressure drop**	**Accumulated TEG**	**Entrainment**
NeqSim liquid viscosity	Very low	Low	Very high
NeqSim interfacial tension	Very low	Low	High
NeqSim TEG mass flow	Low	Very high	-
PVTsim TEG mass flow	Low	Very high	-

Table 10.6: Sensitivity of the standard OLGA module to the parameter factors, both scenarios

The simulations display a negligible sensitivity to alterations in liquid viscosity and interfacial tension in regard to pressure drop. The effect on accumulated TEG is also small. The entrainment of TEG with the initial dump of TEG in scenario 2 are highly affected by the parameter factors. The maximum entrainment time and distance are noticeably higher for low values of liquid viscosity and interfacial tension. The entrainment of TEG appear to be slightly more dependent on liquid viscosity than interfacial tension. The entrainment appears to be independent of the geometry of the pipeline.

OLGA displays a higher sensitivity to the increase of TEG mass flow in regard to pressure drop and accumulated TEG. The pressure drop increases by about 2 bar when increasing the TEG mass flow by a factor of 100 for both NeqSim and PVTsim. The accumulation of TEG increases by a factor of around 120 for both property generators with the increase of TEG mass flow, which seems logical.

NeqSim consistently results in pressure drops about 1.4 bar higher than those of PVTsim for both scenarios with alterations in TEG mass flow. In scenario 2 there is a slightly higher sensitivity than in scenario 1 to changes in interfacial tension and liquid viscosity values for pressure drop and accumulated TEG. This is probably caused by the increased amount of TEG in scenario 2.

10.4.2 The OLGA HD Module

The OLGA HD module displays a higher sensitivity to the parameter factors than the standard OLGA module for all properties. Table 10.7 presents the sensitivity of the OLGA HD module to the parameter factors based on the results from both scenarios.

Parameter	Pressure drop	Accumulated TEG	Entrainment
NeqSim liquid viscosity	Low	Very low	Very high
NeqSim interfacial tension	Low	Medium	High
NeqSim TEG mass flow	High	Very high	Very high
PVTsim TEG mass flow	Medium	High	Very high

Table 10.7: Sensitivity of the OLGA HD module to the parameter factors, both scenarios

The simulations display some sensitivity to alterations in liquid viscosity and interfacial tension in regard to pressure drop. In general the pressure drop decreases with the increase of interfacial tension. Increasing or decreasing the liquid viscosity from the parameter factor 1 leads to a decrease in pressure drop. The effect on accumulated TEG is negligible in regard to liquid viscosity. However, when multiplying the interfacial tension by parameter factors 5 and 10, there is a profound increase of accumulated TEG along the pipeline.

The entrainment of TEG in scenario 1 reveals a sensitivity to liquid viscosity. Entrainment occurs when liquid viscosity is multiplied by parameter factors 0.1 and 0.2. There is no entrainment for any alterations in interfacial tension parameter factors. In scenario 2 there are lots of entrainment for all simulations at 65 hours. The entrainment distance are highly affected by the parameter values. There are also individual differences in the behaviour of the entrainment along the pipe, but these are difficult to quantify. There is however no doubt that both parameter factors strongly influence the entrainment of the simulations. The entrainment also appear to be highly dependent on the geometry of the pipeline.

OLGA displays a higher sensitivity to the increase of TEG mass flow in regard to pressure drop and accumulated TEG. The pressure drop increases by 19 bar when increasing the TEG mass flow by a factor of 100 with the NeqSim table. Especially when increasing the TEG mass flow from parameter factor 5 to 10, the increase in pressure drop of 13 is noticeable. It appears that OLGA HD is especially sensitive to the TEG mass flow when the mass flow is sufficiently high. The accumulated TEG increases by a factor of 163 when the TEG mass flow increases with a factor of 100. The pressure drop with PVTsim increases by 9 bar, and the accumulated TEG by a factor of 63.

NeqSim consistently results in pressure drops more than 1.5 bar higher than those of PVTsim for both scenarios. In scenario 2 there is a slightly higher sensitivity than in scenario 1 to changes

in interfacial tension and liquid viscosity values for pressure drop and accumulated TEG. This is probably caused by the increased amount of TEG in scenario 2.

10.4.3 Comparing OLGA Modules and Scenarios

The sensitivity of standard OLGA and OLGA HD to the parameter factors have been established. It is beneficial to establish differences between the modules in regard to both scenarios. The comparison will mainly focus on the generated property tables with all parameter factors set to 1.

Pressure Drop

Table 10.8 presents the pressure drops for both scenarios and property generation tools with all parameter factors set to 1.

Generation Tool	**Scenario**	**OLGA [bar]**	**OLGA HD [bar]**
NeqSim	Carryover of TEG	114.4	115.6
	Initial dump of TEG	114.7	118.6
	Increase between scenarios	0.3	3.0
PVTsim	Carryover of TEG	113.0	113.7
	Initial dump of TEG	113.3	115.9
	Increase between scenarios	0.3	2.2

Table 10.8: Simulated pressure drop after 10 days in OLGA and OLGA HD with parameter factor 1

The OLGA HD module generally simulates higher pressure drops than the standard OLGA module. The increase in pressure drop between scenario 1 and 2 is also noticeably higher in the OLGA HD module for both property generators. The table generated by NeqSim consistently results in higher pressure drops than the table from PVTsim.

Accumulated TEG

Table 10.9 presents the accumulated TEG for both scenarios and property generation tools with all parameter factors set to 1.

Generation Tool	Scenario	OLGA [m^3]	OLGA HD [m^3]
NeqSim	Carryover of TEG	33.6	34.3
	Initial dump of TEG	64.5	64.9
	Increase between scenarios	30.9	30.6
PVTsim	Carryover of TEG	33.3	51.3
	Initial dump of TEG	64.3	125.1
	Increase between scenarios	31.0	73.8

Table 10.9: Simulated accumulated TEG after 10 days in OLGA and OLGA HD with parameter factor 1

With the table from NeqSim, both the standard OLGA module and the OLGA HD module simulates similar volumes of accumulated TEG. The increase of accumulated TEG from scenario 1 to scenario 2 is around 30 m^3 for both OLGA modules, which seems logical due to the dump of 30 m^3 TEG in the pipe. The standard OLGA module simulates similar values for the NeqSim and PVTsim tables. However, the OLGA HD module simulates noticeable higher values for the PVTsim table. The increase of 73.8 m^3 between scenario 1 and 2 appears large.

Entrainment of TEG

Table 10.10 presents the time and distance of entrainment for scenario 2 for both property generation tools with all parameter factors set to 1.

Generation Tool	OLGA	OLGA HD
NeqSim	5.6 h, 15 km	65 h, 186 km
PVTsim	1.5 h, 6.3 km	65 h, 124 km

Table 10.10: Simulated maximum time and distance of entrainment in OLGA and OLGA HD with parameter factor 1

The OLGA HD module simulates more entrainment than the standard OLGA module for both property generators. The standard OLGA module simulates more entrainment with the property table from NeqSim than the table from PVTsim. The amount simulated in OLGA HD is similar for PVTsim and NeqSim, but the distance with PVTsim is significantly shorter than that of NeqSim.

In general the OLGA HD module consistently simulates more entrainment of TEG than the standard OLGA module. In scenario 1 there is not entrainment in any of the simulations with the standard OLGA module. With the OLGA HD module there is entrainment with liquid viscosity multiplied with parameter factors 0.1 and 0.2. There is also entrainment with the TEG mass flow parameter factor set to 2, 5 and 10 for both property generators.

In scenario 2 there is entrainment for all simulations with the OLGA HD module at 65 hours. With the standard OLGA module all simulations except one experiences a maximum entrainment time of less than 65 hours. The entrainment simulated with OLGA HD spreads out along the pipe, and is dependent on the geometry. The simulated entrainment with the standard OLGA module consist of a single spike which appears independent of geometry. This is easily observed by comparing Figures 10.9, 10.16 and 10.17. The entrainment obtained in OLGA HD appears more realistic than that of standard OLGA.

Chapter 11

Discussion

The results are discussed in detail in Chapters 8, 9 and 10. This chapter discusses assumptions, simplifications and certain deviations found in the study.

11.1 Laboratory Work

An uncertainty analysis is presented in Section 8.3. However, there are certain inaccuracies in the measurement process which cannot be quantified. These inaccuracies should still be considered.

The experimental equipment described in Section 7.1 have some limitations. During the measurements the temperature test chamber had to be turned off. The chamber vibrates while turned on, which makes the creation of stable droplets impossible. The measurements would typically take 20 minutes. Over the course of this time the temperature of the fluid would change by a maximum of 0.1°C. The temperature increased for the measurements at 4.3 and 20°C, and decreased for the measurements for 41.5°C.

The process of reaching equilibrium between liquid and gas was not a problem. The fluid would circulate for 24 hours before measurements were taken. Acquiring a stable droplet shape however, was problematic. The droplet would shrink over time, especially at high pressures. The volume and area of each droplet decreased during measurements with no exceptions. The decrease was noticeably larger at high pressures. The droplets at around 50 bar experienced a decrease of both volume and area by an average of less than 1%. At around 200 bar the average droplet decrease was 2%. The decrease was higher at 41.5°C than at 4.3°C. However, the shape parameters used for the calculations, R_0 and β, remained constant for all measurements.

The pressure decreased during the measurement process. The pressure decrease was between 0.1 and 0.6 bar for all measured conditions, and independent of measurement pressure. The

liquid and gas densities also changed during the measurement process. This change was small. The liquid density changed by between 0.0001 and 0.0031 g/cm^3. The gas density changed by between 0.0001 and 0.0005 g/cm^3.

The interfacial tension values obtained from the measurements are fairly consistent. However, there are two measurements which appear to be incoherent with the rest. In Figure 8.1, the measured values at 41.5°C are higher than those of the two other temperature levels at 100 and 200 bar. However, the measurement at 41.5°C and 50 bar is similar to the other temperature levels, which seems peculiar. In Figure 8.2 the values at 20 and 41.5°C are similar, and higher than those at 4.3°C. The exception is the values at around 100 bar. At this point the value at 20°C is the lowest value of all temperatures.

These two measurements appear incoherent from the rest. The deviation from the expected values is still small. For 100 wt% TEG the interfacial tension values for 41.5°C is around 2 mN/m higher than those for 4.3 and 20°C at 100 and 200 bar. This means that the expected value of the measurement at 41.5°C and 50 bar is 36 mN/m, while the measured value is 34.7 mN/m. The deviation is 1.3 mN/m or 3.7%. For 90 wt% TEG the interfacial tension values of 4.3 and 41.5°C leads to an expected value of 30.5 mN/m at 20°C and 100 bar. The measured value is 28.1 mN/m. The deviation is 2.4 mN/m or 8.5%. These two situations should be remeasured, to determine if the values are correct.

Given the lack of high pressure interfacial tension measurements of TEG and methane before this study, there were uncertainties regarding the values which would be obtained. According to Statoil the processing equipment at Kårstø can accommodate liquid - vapor interfacial tensions as low as 10 mN/m. At values lower than this, bigger scrubbers would need to be developed, as the separation process is slower. Based on the measured interfacial tensions this is not necessary.

11.2 Comparison of Experimental and Simulated Data

The comparisons in Chapter 9 are presented along with the reported uncertainties of the literature data. The reported fluid compositions were used to generate properties in PVTsim and NeqSim. The exact fluid composition utilized in our laboratory work was measured at Statoil with the help of Marie Vikre Danielsen.

The high complexity of liquid molecular structures and interactions makes it difficult to generate accurate viscosities for liquid mixtures. Both PVTsim and NeqSim are based on empirical equations and parameters that applies the Grunberg and Nissan (1949) mixing rule. That these empirically based calculation methods struggle when applied to liquid mixtures, high temper-

atures and high pressures are not surprising. Improvements in calculated values can be accomplished by further tuning of these equations and parameters. Though the generation tools are based on the same principles, the calculations are conducted using different equations and compound parameters in NeqSim and PVTsim. This is the reason for the differences of the simulated values of the generation tools.

The Firoozabadi Ramey Method is an empirical method especially developed to calculate the interfacial tension of pure water and hydrocarbon mixtures. That the method performs poorly with the addition of TEG to the water is unsurprising. On a side note, the methods in both PVTsim and NeqSim predicts noticeable accurate interfacial tension values for pure water and methane at high pressures.

The Parachor Method heavily depends on the empirical parachor parameter. It is therefore logical that the method predicts fairly accurate interfacial tension values for most conditions, but struggles when applied to certain situations. The method predicts accurate interfacial tension values at low and medium pressures, but struggles at high pressures. The method performs better for pure TEG than for 90 wt% TEG. Improvements in generated values can be accomplished by tuning the parachor parameter for the compounds simulated.

The Gradient Theory is a highly complex and advanced mathematical model. All three methods based on this theory predict fairly accurate interfacial tension values overall, particularly the one named "Gradient Theory". The methods consistently overestimate the values, but predict a similar slope of decrease of values with the increase of pressure as the experimental measurements. The methods performs better for the mixture of 90 wt% TEG and water than for pure TEG.

An important aspect when choosing calculation method is the time consumption of the method. The empirical methods generate properties on a significantly faster rate than the Gradient Theory methods. If the fluid composition is complex, the Gradient Theory methods are highly time consuming. At some point there will be a trade-off between the need for accurate properties and time consumption. Logically it is necessary to consider the fluid composition and conditions. The Parachor Method predicts accurate interfacial tension values at pressures below 150 bar. The Firoozabadi Ramey Method predict accurate values for fluid compositions comprising pure water and hydrocarbons. In situations unlike these the Gradient Theory methods will be needed for accurate values.

The only existing dataset comparable to the obtained measured values from this study deviated significantly. The reasons for this have been discussed earlier in the report, as a decision had to be made of which values to emphasize in the comparisons with NeqSim and PVTsim.

11.3 Simulations in OLGA

The simulation file utilized in OLGA was provided by Statoil. This means that all conditions are set by information provided by Statoil. The exception is the mass flow of TEG, which is discussed earlier in the report. The ambient temperature is known to alter over a year by about 1°C. The simulations have been run with altered ambient temperatures and the effects are negligible.

The time steps utilized in OLGA are 10 hours for the simulations of pressure drop and accumulated TEG. Small time steps and long simulation times leads to an OLGA file size which exceeds the maximum, and the simulation is aborted. The time step of 10 hours makes it possible to simulate 10 days. The results have been compared to smaller time steps and shorter simulations to ensure the results are equal. To accurately simulate the entrainment in scenario 2, caused by the initial dump of TEG, smaller time steps are needed. The time step utilized is 0.05 hours. The simulations are conducted until the amount of entrained TEG is negligible or the maximum simulation time of 65 hours is reached.

The calculation process in OLGA is complex and sensitive to the time step. The property tables from NeqSim and PVTsim have to cope with the extremes in values that occurs. This is the reason for the large pressure and temperature ranges of the property tables utilized.

The fluid transported in the Åsgard pipeline is more complex than the fluid utilized in this study. The real fluid comprise 28 different compounds. However, methane, ethane, TEG and water constitute 90 mole% and 78 wt% of the fluid. To establish the simulated effects of liquid viscosity, interfacial tensions and mass flow of TEG the simplified fluid is sufficient.

The simulations with the standard OLGA module display a smaller sensitivity to alterations in liquid viscosity and interfacial tensions than expected. In regard to pressure drop and accumulated TEG it seems the need for precise property values is not that high. The entrainment of TEG is very sensitive to alterations in liquid viscosity and interfacial tensions. Entrainment is the relation of interfacial shear force to the interfacial tension. Theoretically the increase of interfacial tension leads to a decrease of entrainment, which is in coherence with the simulated results.

The sensitivity to the liquid viscosity and interfacial tension parameter factors are slightly higher in scenario 2 than in scenario 1. This is probably caused by the increased amount of TEG caused by the initial dump in scenario 2. It is conceivable that there will be a stronger need for accurate properties if the simulated fluid comprise a higher percentage of TEG. Overall, the parameter factors applied in the simulations leads to the conclusion that all calculation models in both NeqSim and PVTsim predict sufficiently accurate liquid viscosities and interfacial tensions for simulations with the standard OLGA module of the Åsgard transport pipeline.

The standard OLGA module displays a higher sensitivity to the increase of TEG mass flow. Considering the multiplication factor of 100 the pressure drop sensitivity is still smaller than expected. The increase of accumulated TEG closely resembles the increase in TEG mass flow.

The simulations with the OLGA HD module display a larger sensitivity to the alterations in liquid viscosity and interfacial tensions than the standard OLGA module, but still small. The exception is accumulated TEG when the interfacial tension values are sufficiently increased. In regard to pressure drop and accumulated TEG it seems the need for precise property values is low. The entrainment of TEG is very sensitive to alterations in liquid viscosity and interfacial tensions. The entrainment is more sensitive to alterations in liquid viscosity than interfacial tension. It is conceivable that there will be entrainment of TEG at the pipeline outlet for all simulations in scenario 2 in OLGA HD.

The sensitivity to the liquid viscosity and interfacial tension parameter factors are higher in scenario 2 than in scenario 1. As with the standard OLGA module, it is conceivable that there will be a stronger need for accurate properties if the simulated fluid comprise a higher percentage of TEG. However, the parameter factors applied in the simulations still leads to the conclusion that all calculation models in both NeqSim and PVTsim predict sufficiently accurate liquid viscosities and interfacial tensions for simulations with OLGA HD of the Åsgard transport pipeline.

OLGA HD displays a high sensitivity to the increase of TEG mass flow, especially with the NeqSim table. The increase in pressure drop is particularly large at high mass flows of TEG. The increase of accumulated TEG is larger than the increase of mass flow, but within reasonable values.

The introduced initial dump of TEG in scenario 2 leads to a negligible increase in pressure drop of 0.3 bar with the standard OLGA module for both property generators. The OLGA HD module simulates a higher pressure drop of 3.0 bar with NeqSim and 2.2 bar with PVTsim tables. Overall, the OLGA HD module simulates higher pressure drops than the standard OLGA module. The results for accumulated TEG seem sensible for both OLGA modules with an increase of around 30 m^3. The exception is the increase in the OLGA HD module with the PVTsim table, which seems unreasonably high. The entrainment simulated in OLGA HD appear more realistic than that simulated with the standard OLGA module. The OLGA HD entrainment shows a stronger dependability on the pipeline geometry.

It is a known problem in Statoil that OLGA tends to underestimate the effect the amount of liquids in the pipeline inflict on the pressure drop. There has been an incident where the pressure drop of the Åsgard transport pipeline increased by 7 bar, which caused a decrease in hydraulic capacity. It was concluded that the increased pressure drop was likely to be caused by an in-

crease of liquids in the pipeline. However, Statoil was unable to recreate an equivalent simulated increase in pressure drop in OLGA. Simulations in OLGA were conducted with an initial dump of 20 m^3 MEG and 2 m^3 TEG. The simulations resulted in an increase in pressure drop of 0.3 bar with the introduction of the initial dump. This value coincides with the obtained result in this Master's thesis with the standard OLGA module.

It is known that liquid presence in pipelines results in more resistance to the gas flow, which in turn increases the pressure drop. One reason for this is that the liquid film on the pipe wall may increase the roughness. In OLGA, there are several simplifications and assumptions that may make the transport of liquid too efficient, resulting in a smaller liquid effect on pressure drop.

- The liquid phase is assumed to flow efficiently in the bottom of the pipe. Deviations from this ideal behaviour makes the transport less efficient and as a result increase the liquid holdup. In a pipeline of 707 km this assumption can add up to a considerable difference.
- The effect of 10 000 welds of 1-2 mm in height on the liquid film flow and gas flow is omitted. These welds cause increased flow resistance in the real pipeline. The simplification also causes inaccuracies in liquid holdup.
- Uncertainties regarding the accuracy of the pipeline profile has led to a minimum pipe section length of 100 meters in the simulation file in OLGA. There are probably areas of the real pipeline where the elevation is steeper than it is in the OLGA profile. Steeper elevation causes increased flow resistance, and differences in liquid holdup.

The increase of pressure drop between scenario 1 and 2 in OLGA HD is more in coherence with the experienced increased pressure drop of 7 bar in the Åsgard transport pipeline. The OLGA HD module is specifically developed to provide more consistent and accurate predictions of pressure drop and holdup for systems with stratified flow, which is the flow regime present in the Åsgard transport pipeline. In these flow regimes the interfacial friction forces and the friction forces between the wall and the fluid are significant. The OLGA HD module is a friction model, and the friction forces are calculated more complexly than in the standard OLGA module. The entrainment of TEG in OLGA HD appear more reasonable and dependent on the pipeline geometry, which could be caused by more accurate holdup simulations. The entrainment is noticeably higher in OLGA HD than in standard OLGA. Given that entrainment is the relation of interfacial shear force to the interfacial tension, it seems the friction model in OLGA HD results in higher interfacial shear forces. This can in turn explain the increased pressure drops simulated in OLGA HD.

The standard table from NeqSim consistently simulates higher pressure drops than the table from PVTsim for both OLGA modules. The increase of accumulated TEG between scenario 1 and 2 with PVTsim in OLGA HD seems unreasonably high. The entrainment of TEG is higher with the NeqSim table. It has been established that NeqSim calculates more accurate interfacial

tension and liquid viscosity values than PVTsim. However, the differences in the OLGA simulations can not be explained by these two properties alone. The obtained pressure drop in NeqSim between scenario 1 and 2 are more in coherence with the experienced increased pressure drop of 7 bar. It appears that the tables from NeqSim provide more accurate simulations, but it is impossible to thoroughly conclude on this.

Several variables have been compared in this study. It appears that liquid viscosity and interfacial tension have a negligible influence on the simulations of multiphase flow in the current version of OLGA. However, in a simulated case where the fluid comprise larger amounts of TEG the properties could prove influential. In regard to oil and gas processing, larger amounts of TEG in the pipeline is unlikely to be experienced. With the OLGA HD module the influence of the properties are higher than with the standard OLGA module. This is most emphasized in regard to pressure drop. There are significant deviations in values from the calculation methods in NeqSim and PVTsim of the two properties. However, the deviations are too small to distinctly affect simulations in OLGA version 7.3.5.

Chapter 12

Conclusion

The purpose of this Master's thesis was to develop and evaluate NeqSim as a property generator for multiphase flow simulations. Two different property generation tools have been included in this thesis: NeqSim and PVTsim. In NeqSim, several theoretical models were included for the calculations of interfacial tensions. The accuracy of the calculation methods have been evaluated by comparison to experimental data from laboratory work and from the literature.

Experimental work has been conducted to determine the interfacial tensions of high pressure aqueous TEG and methane. The work comprised measuring interfacial tension and density. The measurements were conducted at Statoil Research and Developing Center at Rotvoll, utilizing the pendant drop method. The results have been satisfactory. The uncertainty of the interfacial tension measurements were calculated on the basis of recommendations of ISO. The overall average uncertainty of the measurements was calculated to be 1.8%. The measured results show a decrease of interfacial tension with the increase of pressure. The interfacial tension increases with the addition of water to the mixture.

The experimental results obtained deviated significantly from a similar study. It was decided to emphasize the experimental results from this Master's thesis for the comparisons with the software. The reasons for this was that the measured values of this study are more in coherence with the simulated data, and therefore the mathematical models. Also, there was conducted more measurements in this study, which all obtained consistent values.

Relevant experimental data were collected and compared with the values generated by NeqSim and PVTsim. The results of this, together with the comparisons with the laboratory work, was used to evaluate the generation tools and the different models utilized. The emphasis has been on deviations between the calculated results from the fluid packages and the experimental data.

Both NeqSim and PVTsim generated accurate liquid viscosity values for pure TEG and aque-

ous TEG at atmospheric pressure. The results deviated for aqueous TEG at high temperatures. At high pressures NeqSim performed better than PVTsim. Overall, NeqSim displayed more resilience and better performance in regard to computing liquid viscosity.

The Firoozabadi Ramey Method is utilized by PVTsim for interfacial tension calculations and is also included in NeqSim. The values predicted by this method were fairly accurate for pure water and hydrocarbons for all pressures. The values calculated for aqueous TEG were highly deviated at all conditions. The methods were disregarded as unsuitable for calculations with fluids comprising TEG.

NeqSim includes other methods to calculate interfacial tensions. At atmospheric pressure the methods based on Gradient Theory and the Parachor Method predicted similar and fairly accurate results. At high pressures the Parachor Method significantly underestimated the interfacial tension values. The Gradient Theory methods predicted fairly accurate values for all pressures. Overall, the most advanced version of the Gradient Theory provided the most accurate values.

A parameter study was conducted in OLGA to establish how alterations in liquid viscosity and interfacial tension affects the simulation of multiphase flow. The simulations were conducted using field data provided by Statoil of the Åsgard transport pipeline. This allowed us to simulate an existing pipeline with realistic conditions. The simulations were conducted using both the standard OLGA module and the OLGA HD module, which is specifically developed for stratified flow regimes. Two different scenarios were simulated. In the first scenario there was a mass flow of TEG which was altered by the parameter factors. In the second scenario there was an initial dump of 30 m^3 TEG in the pipeline and a constant TEG mass flow.

Alterations in liquid viscosity and interfacial tension values did not have the impact on the simulations as was expected prior to this study. Increasing the liquid mass flow did impact the simulations. With the standard OLGA module the impact was not proportional to the parameter factors applied. With the OLGA HD module the impact was significant. The property tables generated by NeqSim and PVTsim resulted in differences in the simulations in OLGA. The differences can not be explained by the differences in interfacial tension and liquid viscosity values alone. It appears that the table from NeqSim results in more accurate simulations, but this was not thoroughly established.

The results from the two OLGA modules were compared and discussed. The OLGA HD module provided more accurate simulations of the multiphase flow. With the current OLGA version 7.3.5 the need for precise liquid viscosity values and interfacial tensions are moderate. Both PVTsim and NeqSim calculates sufficiently accurate property values.

12.1 Further work

The focus of this Master's thesis was to develop and evaluate NeqSim as a property generator for multiphase flow simulation. The development of NeqSim is a continuous process. This section suggest improvements for the further development of NeqSim as a property generator.

12.1.1 Liquid Viscosity Calculations in NeqSim

This study has shown that NeqSim overestimates the liquid viscosity of aqueous TEG with high water fractions at high temperatures. This problem can be solved either by improving the compound parameters in the Statoil database, or by implementing the other liquid viscosity calculation models described in Section 4.2. As described in 5.2.2 the development of other models in NeqSim is started, though not finalized.

12.1.2 Interfacial Tension in NeqSim

This study has shown that the Parachor Method in NeqSim underestimates the interfacial tension values of aqueous TEG and methane at high pressures. Improvements in this regard can be accomplished by tuning the parachor parameter in the Statoil database.

It is shown that the Gradient Theory models predict fairly accurate interfacial tensions for aqueous TEG and methane. However, the most accurate model overestimate the values by an average of 11%. The full Gradient Theory model is being developed in NeqSim. Finalizing and implementing this model can result in more accurate values.

12.1.3 Other Properties in NeqSim

This study has conducted a parameter study in OLGA for the properties liquid viscosity and interfacial tensions of aqueous TEG, methane and ethane. OLGA version 7.3.5 displayed a moderate need for accurate values of these properties. The liquid and gas densities are established to be accurately calculated in NeqSim in Section 9.3.4. Other properties NeqSim calculates are gas mass fraction, gas viscosity, heat capacity, enthalpy, thermal conductivity and entropy.

Similar studies should be conducted to establish the accuracy of NeqSim in regard to these properties. Additional parameter studies should be conducted in OLGA to determine the sensitivity of OLGA on the properties. The differences in this study between the OLGA simulations conducted with property tables generated by NeqSim and PVTsim can not be explained by differences in liquid viscosity and interfacial tension alone. Other properties affect the simulations.

12.1.4 Wax tables

The deposition of wax on pipeline walls is a common problem in the oil and gas industry. Wax formation happens at low temperatures, as hydrocarbons containing wax molecules deposit these on the pipe wall. According to Bratland (2010), these deposits tend to build up, and may cause many of the same problems as hydrate formation.

If simulating wax depositions in OLGA, data for wax properties must be provided in a separate wax table file. PVTsim can generate these files, and the structure is similar to that of the fluid property tables. NeqSim has the potential to generate wax tables. The content of wax molecules in the hydrocarbons could be acquired from the thermodynamic library in NeqSim. Some wax flash functions for the eventual wax depositions in the simulations are already implemented in the NeqSim scripts (Bjortuft, 2014).

Bibliography

(2004). *Pendent Drop Interfacial Tension Cell - Instruction Manual*. Temco, Inc.

(2008). Evaluation of measurement data - guide to the expression of uncertainty in measurement.

Anyadiegwu, C., Kerunwa, A., and Oviawele, P. (2014). Natural gas dehydration using triethylene glycol (teg). *Petroleum & Coal*, 56(4):407–417. Department of Petroleum Engineering, Federal University of Technology, Owerri, Nigeria.

Begum, S. K., Clark, R. J., Ahmed, M. S., Begum, S., and Saleh, M. A. (2012). Volumetric, viscosimetric and surface properties of aqueous ssolution of triethylene glycol, tetraethylene glycol, and tetraethylene glycol dimethyl ether. *Journal of Molecular Liquids*, 177:11–18.

Bjortuft, K. R. (2014). Implementation and evaluation of neqsim as property generator for multiphase flow simulation. Master's thesis, Norwegian University of Science and Technology.

Bratland, O. (2010). *Pipe Flow 2: Multi-phase Flow Assurance*. www.drbratland.com.

Calsep (2016). *PVTsim Technical Overview*. Calsep.

Cengel, Y. A. and Cimbala, J. M. (2014). *Fluid Mechanics - Fundamentals and Applications*. McGraw-Hill Global Education Holdings, 3. edition.

Chapman, S. and Cowling, T. G. (1970). *The Mathematical Theory of Non-uniform Gases: An Account of The Kinetic Theory of Viscosity, Thermal Conduction and Diffusion in Gases*. Cambrigde University Press, 3 edition.

Chung, T.-H., Ajlan, M., Lee, L. L., and Starling, K. E. (1988). Generalized multiparameter correlations for nonpolar and polar fluid transport properties. *Industrial & Engineering Chemistry Research*, 27(4):671–679.

Company, T. D. C. (2007). Triethylene glycol.

D.Biberg, Staff, G., Hoyer, N., and Holm, H. (2015). Accounting for flow model uncertainties in gas-condensate field design using the olga high definition stratified flow model. *BHR Group 2015 Multiphase 17*.

Firoozabadi, A. and Ramey, H. J. (1988). Surface tension of water-hydrocarbon systems at reservoir conditions. *Journal of Canadian Petroleum Technology*, 27(3):41–48.

Grunberg, L. and Nissan, A. H. (1949). Mixture law for viscosity. *Nature*, 164:799–802.

Guo, B. and Ghalambo, A. (2005). *Natural Gas Engineering Handbook*. Gulf Publishing Company.

Guo, Z., Zhang, J., Zhang, T., Li, C., Zhang, Y., and Bai, J. (2011). Liquid viscosities, excess properties, and viscous flow thermodynamics of triethylene glycol + water mixtures at t= (298.15 , 303.15, 303.15, 313.15, and 318.15) k. *Journal of Molecular Liquids*, 165:27–31.

Haaland, S. (1983). Simple and explicit formulas for the friction factor in turbulent pipe flow. *Journal of Fluids Engineering*, 105(1):89–90.

Huang, S. H. and Radosz, M. (1990). Equation of state for small, large, polydisperse, and associating molecules. *Industrial & Engineering Chemistry Research*, 29(11):2284–2294.

Ishii, M. (1975). *Thermo-Fluid Dynamic Theory of Two-Phase Flow*. Eyrolles.

Kashefi, K. (2012). *Measurement and Modelling of Interfacial Tension and Viscosity of Reservoir Fluids*. PhD thesis, Heriot-Watt University.

Kidnay, A. J., Parrish, W. R., and McCartney, D. G. (2011). *Fundamentals of Natural Gas Processing*. CRC Press, 2nd edition.

Kontogeorgis, G. M., Voutsas, E. C., Yakoumis, I. V., and Tassios, D. P. (1996). An equation of state for associating fluids. *Industrial & Engineering Chemistry Research*, 35(11):4310–4318.

Kordabadi, H. and Dinon, M. (2013). Manage teg liquid and corrosion in sales gas pipelines. *World Oil*, 234(10):29–34.

Laidler, K. J. (1984). The development of the arrhenius equation. *Journal of Chemical Education*, 61(6):494.

Lohrenz, J., Bray, B. G., and Clark, C. R. (1964). Calculating viscosities of reservoir fluids from their compositions. *Journal of Petroleum Technology*, 16(10):1171–1176.

Michelsen, M. L. and Mollerup, J. (1986). Partial derivatives of thermodynamic properties. *AIChE Journal*, 32(8):1389–1392.

Mork, P. C. (2004). *Overflate og kolloidkjemi - Grunnleggende prinsipper og teorier*. NTNU - Institutt for kjemisk prosessteknologi, Trondheim, 8. edition.

Negi, A. S. and Anand, S. C. (1985). *A textbook of physical chemistry*. New Age International.

Ng, H.-J., Jia, N., Cheng, Y., Schmidt, K. A. G., and Schroeder, H. (2009). Vapour-liquid equilibrium, interfacial tension and transport properties of aqueous solutions of ethylene glycol or triethylene glycol in the presence of methane, carbon dioxide and hydrogen sulfide. *Gas Processors Association*.

Nilsen, H. N. (2001). *Experimental Characterization of Interfacial Behaviours of Hydrocarbon Mixtures in High Pressure Systems*. PhD thesis, NTNU.

Nilsen, H. N. (2008). Calculation of interfacial tension of methane + n-butane mixture with gradient theory near critical conditions. *NTNU - Department of Energy and Process Engineering*.

Norgaard, H. and Nygaard, L. (2014). Measurement and calculation of surface tension of oil, gas and glycol. Master's thesis, NTNU.

Paar, A. (2004). Density measuring cells for high pressures and high temperatures -.

Paroscientific, I. (2005). Absolute pressure transducers- series 4000kr.

Pedersen, K. S. and Fredenslund, A. (1987). An improved corresponding states model for the prediction of oil and gas viscosities and thermal conductivities. *Chemical Engineering Science*, 42(1):182–186.

Pedersen, K. S., Fredenslund, A., Christensen, P. L., and Thomassen, P. (1984). Viscosity of crude oils. *Chemical Engineering Science*, 39(6):1011–1016.

Polling, B. E., Prausnitz, J. M., and O'Connel, J. P. (2001). *The Properties of Gases and Liquids*. McGRAW-HILL, 5. edition.

Quinones-Cisneros, S. E. and Deiters, U. K. (2006). Generalization of the friction theory for viscosity modelling. *Journal of Physical Chemistry*, 110(25):12820–12834.

Quinones-Cisneros, S. E., Zeberg-Mikkelsen, C. K., and Stenby, E. H. (2000). The friction theory (f-theory)-theory) for viscosity modelling. *Fluid Phase Equilibria*, 169(2):249–276.

Quinones-Cisneros, S. E., Zeberg-Mikkelsen, C. K., and Stenby, E. H. (2001). One parameter friction theory models for viscosity. *Fluid Phase Equilibria*, 178(1-2):1–16.

Rojey, A. (1997). *Natural Gas - Production Processing Transport*. Editions Technip, 1st edition.

Sagdeev, D., Fomina, M. G., Mukhamedzyanov, G. K., and Abdulagatov, I. M. (2011). Experimental study of the density and viscosity of polyethylene glycols and their mixtures at temperatures from 293k to 473k and at atmospheric pressure. *The Journal of Chemical Thermodynamics*, 43:1824–1843.

Schlumberger (2013). *The OLGA 7 User Manual*. 7.3.5 edition.

Solbraa, E. (2002). *Equilibrium and Non-Equilibrium Thermodynamics of Natural Gas Processing*. PhD thesis, Norwegian University of Science and Technology.

Sun, T. and Teja, A. S. (2003). Density, viscosity, and thermal conductivty of aqueous ethylene, diethylene and triethylene glycol mixtures between 290 k and 450 k. *Journal of Chemical & Engineering Data*, 48:198–202.

Touloukian, Y. S., Saxena, S. C., and Hestermans, P. (1975). *Viscosity*. Springer.

Tsai, C.-Y., Soriano, A. N., and Li, M.-H. (2009). Vapor pressures, densities, and viscosities of the aqueous solutions containing (triethylene glycol or propylene glycol) and (licl or libr). *Journal of Chemical Thermodynamics*, 41:623–631.

Viswanath, D. S., Ghosh, T., Prasad, D. H. L., Dutt, N. V. K., and Rani, K. Y. (2007). *Viscosity of Liquids: Theory, Estimation, Experiment and Data*. Springer.

Wallis, G. B. (1969). *One-Dimensional Two Phase Flow*. McGraw-Hill.

Webster, J. G. (1999). *The Measurement, Instrumentation and Sensors*. CRC Press.

Weinaug, C. F. and Katz, D. L. (1943). Surface tensions of methane-propane mixtures. *Industrial & Engineering Chemistry*, 35(2):239–246.

Young, T., Fevang, O., Christoffersen, K., and Ivarrud, E. (2007). Lbc viscosity modelling of gas condensate to heavy oil. *Society of Petroleum Engineers*.

Zuo, Y.-X. and Stenby, E. H. (1996). A linear gradient theory model for calculating interfacial tensions of mixtures. *Journal of Colloid and Interface Science*, 182(0443):126–132.

Appendix A

The OLGA HD Module

Considering two phase flow and simplifying slightly by neglecting the possibility of partial flash back flow, allows the expression for the gas and liquid wall friction to be written as

$$\frac{\tau}{\rho U^2} = F(Re, k_s, h, \tau_i, K) \tag{A.1}$$

The function F represents an integral of the velocity distribution over the flow area. The wall friction, Equation A.1, depends on the Reynolds number, Re, and wall roughness k_s, as in single-phase flow. In addition, there is a dependency on the interface friction τ_i, layer height h and the turbulence parameter K. The turbulence parameter is given by

$$K = \frac{\nu_i^T}{\kappa u_i^* h} \tag{A.2}$$

representing the eddy viscosity, ν_i^T, at the interface, scaled by the interfacial friction velocity $u_i^* = \sqrt{|\tau_i|/\rho}$ and layer height h. $\kappa \approx 0.41$ is the von Kármán constant. The interfacial friction is given by

$$sgn(\tau_i)\sqrt{|\tau_i|} = \frac{\Phi(Re_g, k_s, h_g, K_g)U_g - \Phi(Re_l, k_s, h_l, K_l)U_l}{\Psi(K_g)/\sqrt{\rho_g} + \Psi(K_l)/\sqrt{\rho_l}} \tag{A.3}$$

where $h_g = D - h_l$. The functions Φ andΨ represent integrals of the velocity distribution over the interface. The interface friction, Equation A.3, depends on the bulk velocities, phase densities, Reynolds number and interfacial turbulence levels of both layers in addition to the wall roughness and holdup (D.Biberg et al., 2015).

Altogether this yields a consistent set of expressions for wall and interface frictions and velocity shape factors comprising a three dimension flow description at one dimension evaluation speed (Schlumberger, 2013).

Appendix B

Additional Viscosity Information

B.1 Viscosity of Aqueous TEG, Begum et al. (2012)

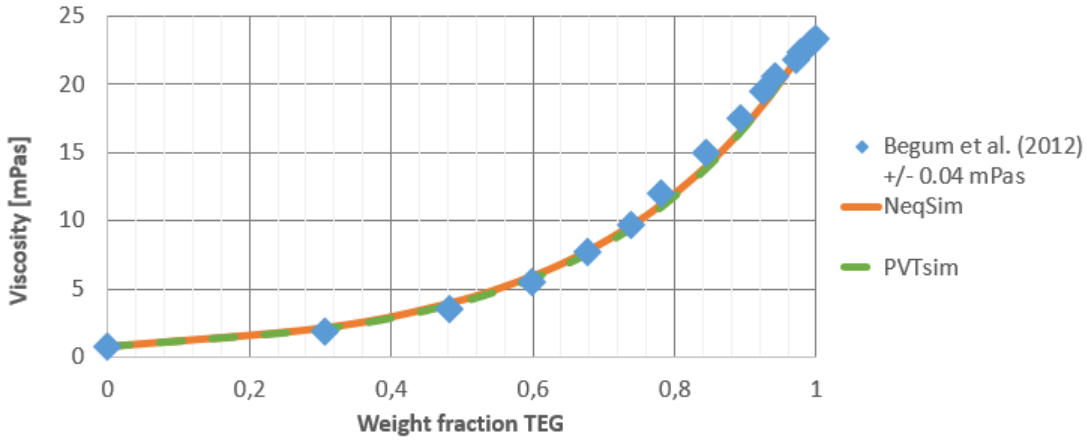

Figure B.1: Calculated liquid viscosities of weight fractions 0 to 1 of TEG in aqueous solution compared to experimental data at atmospheric pressure and 35°C, Begum et al. (2012).

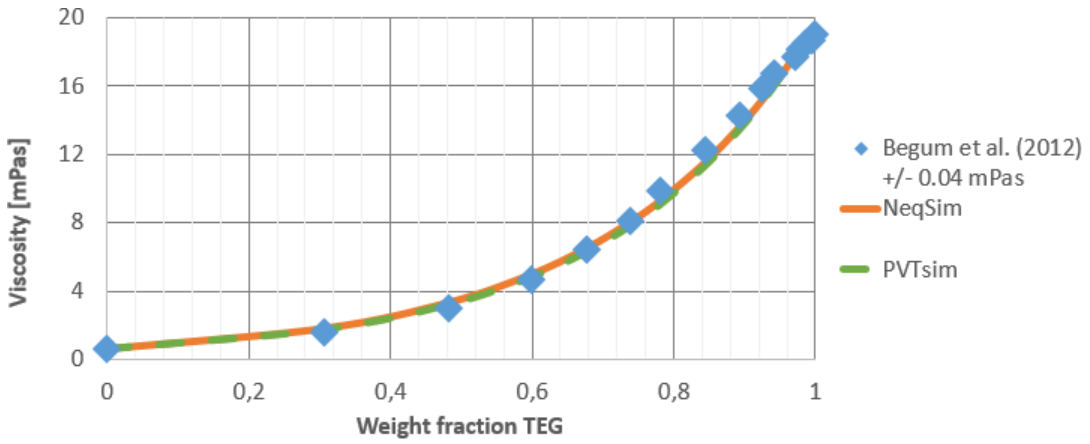

Figure B.2: Calculated liquid viscosities of weight fractions 0 to 1 of TEG in aqueous solution compared to experimental data at atmospheric pressure and 40°C, Begum et al. (2012).

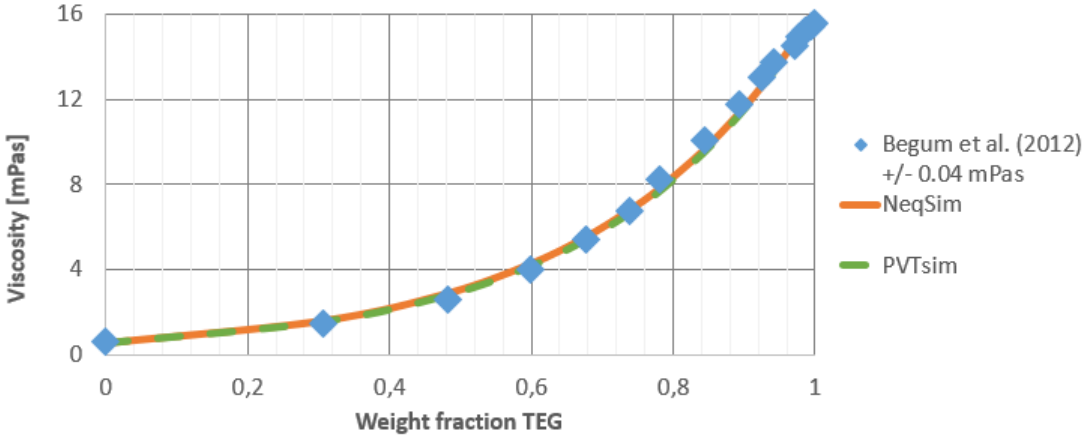

Figure B.3: Calculated liquid viscosities of weight fractions 0 to 1 of TEG in aqueous solution compared to experimental data at atmospheric pressure and 45°C, Begum et al. (2012).

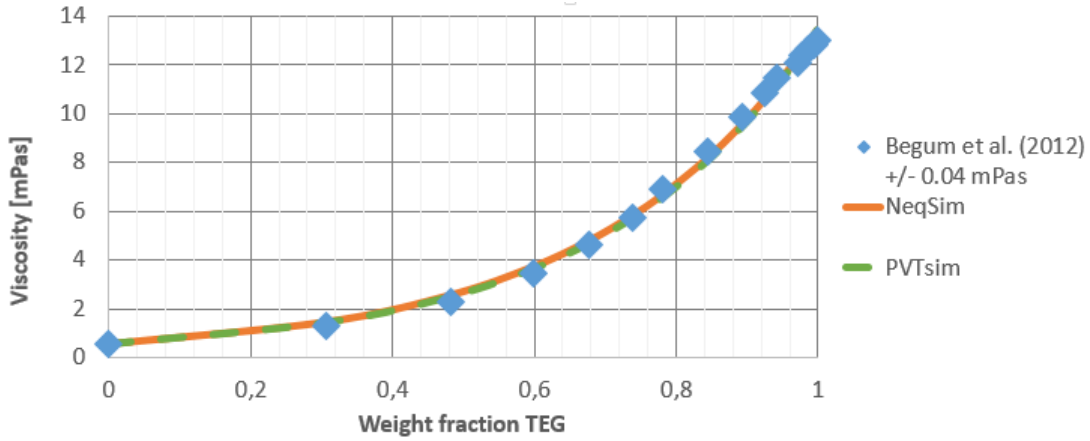

Figure B.4: Calculated liquid viscosities of weight fractions 0 to 1 of TEG in aqueous solution compared to experimental data at atmospheric pressure and 50°C, Begum et al. (2012).

B.2 Viscosity of Aqueous TEG, Sun and Teja (2003)

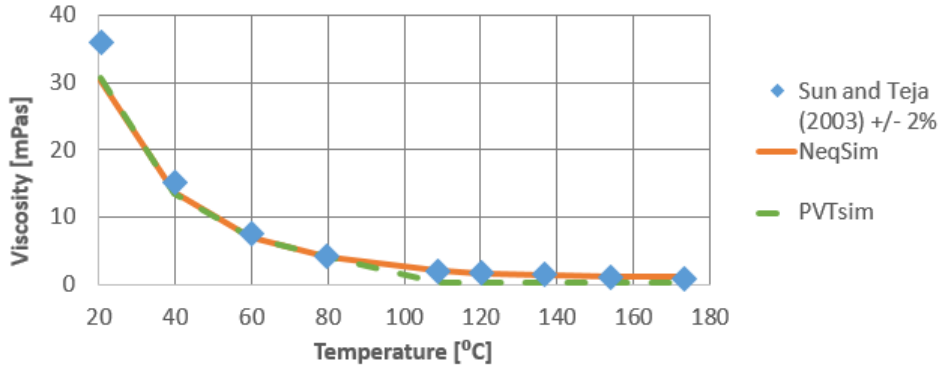

Figure B.5: Calculated liquid viscosities of 0.89 weight fraction of TEG in aqueous solution compared to experimental data at atmospheric pressure and temperatures 21 - 174°C, Sun and Teja (2003).

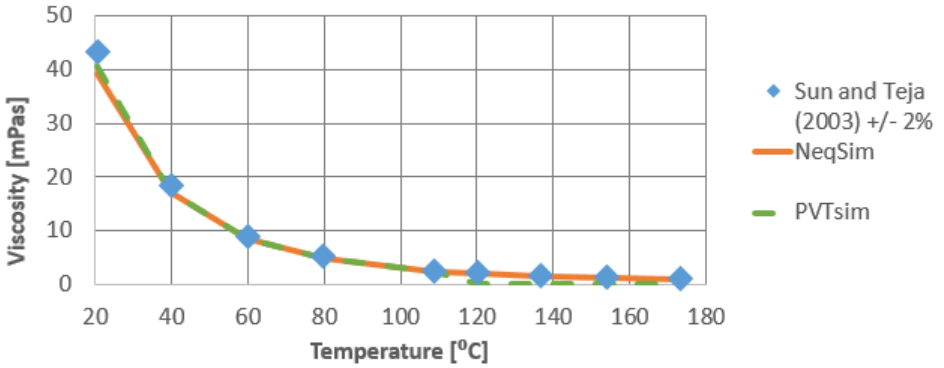

Figure B.6: Calculated liquid viscosities of 0.96 weight fraction of TEG in aqueous solution compared to experimental data at atmospheric pressure and temperatures 21 - 175°C, Sun and Teja (2003).

B.3 Viscosity of High Pressure Aqueous TEG and Methane, Ng et al. (2009)

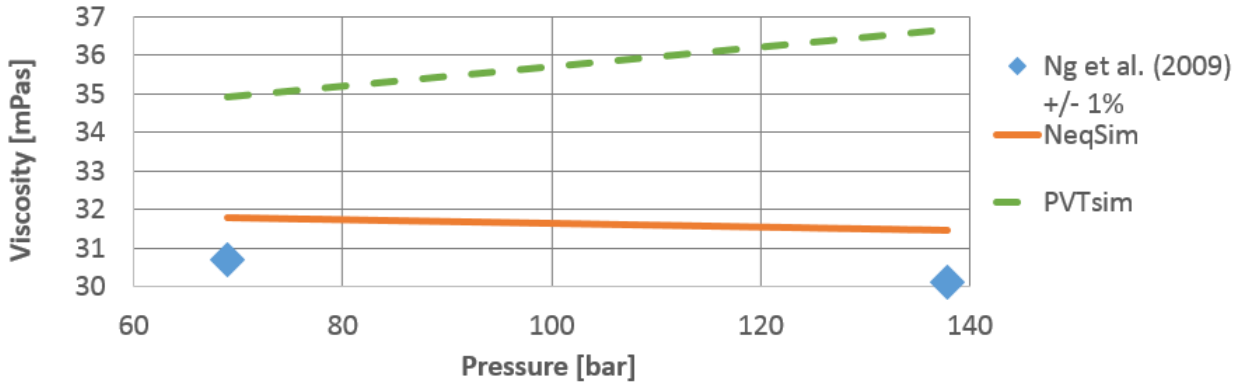

Figure B.7: Calculated liquid viscosities of aqueous TEG compared to experimental data at 26.7°C and pressures 69 - 138 bar, Ng et al. (2009).

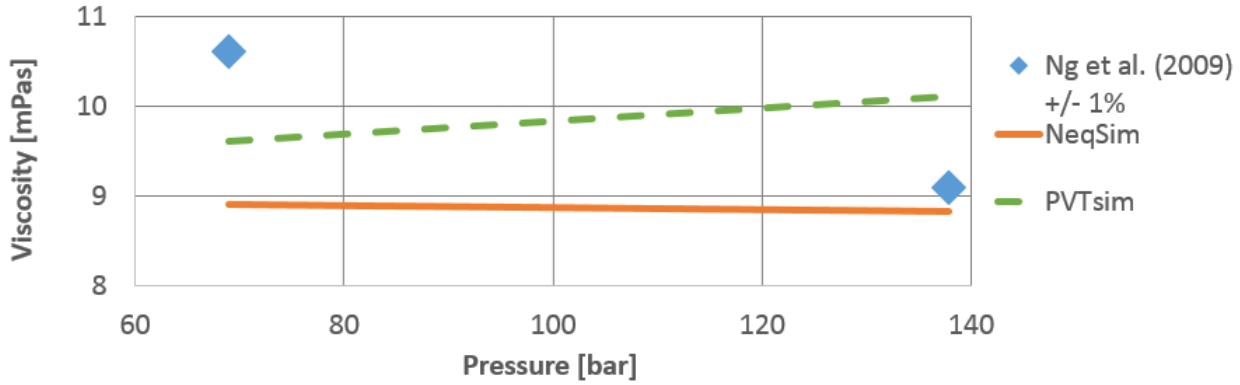

Figure B.8: Calculated liquid viscosities of aqueous TEG compared to experimental data at 60°C and pressures 69 - 138 bar, Ng et al. (2009).

B.4 Viscosity Data from Statoil

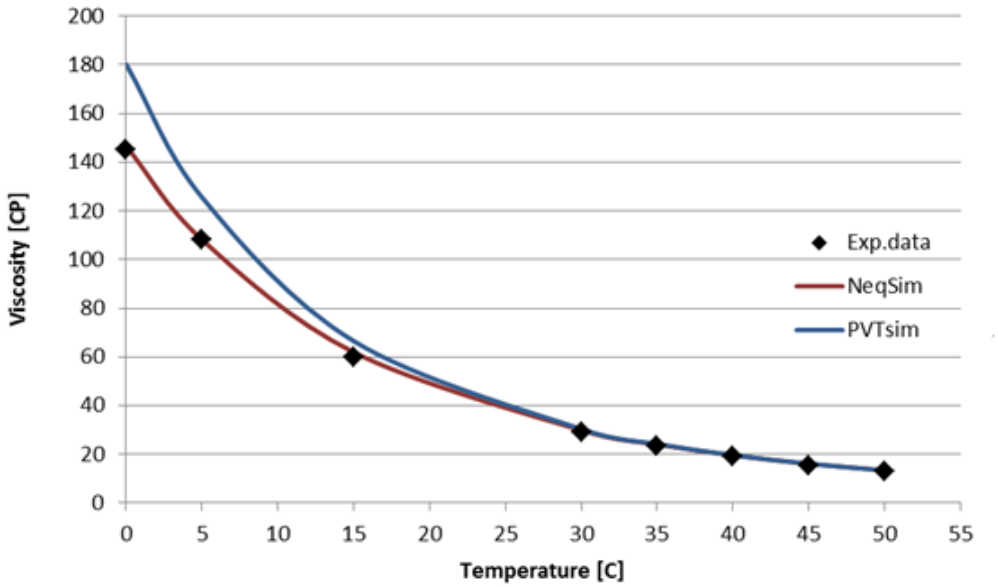

Figure B.9: Calculated liquid viscosities of TEG compared to experimental data at atmospheric pressure and temperatures 0 - 50 °C.

Appendix C

Additional Interfacial Tension Information

C.1 Interfacial Tension of High Pressure Water and Methane, Kashefi (2012)

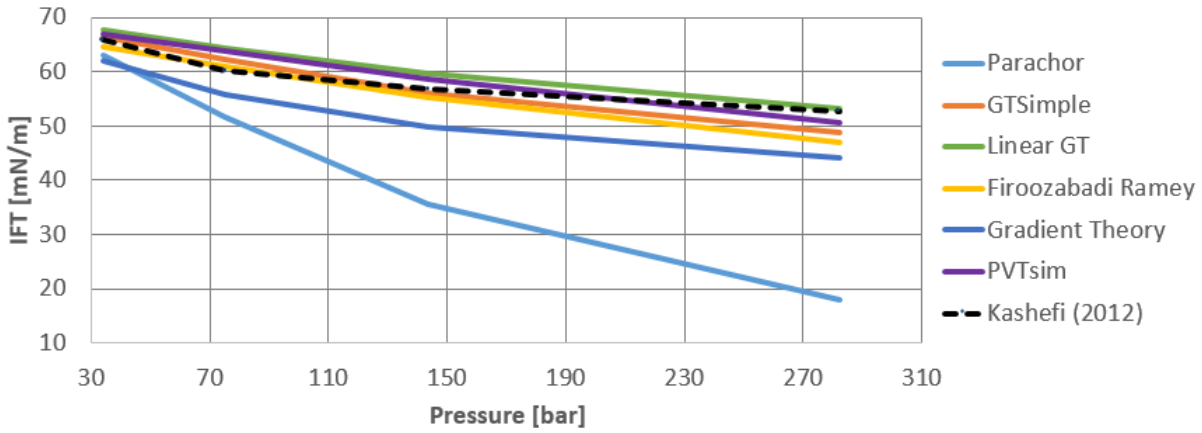

Figure C.1: Calculated interfacial tensions of methane and aqueous TEG compared to experimental data at 37°C and pressures 34 - 282 bar, Kashefi (2012).

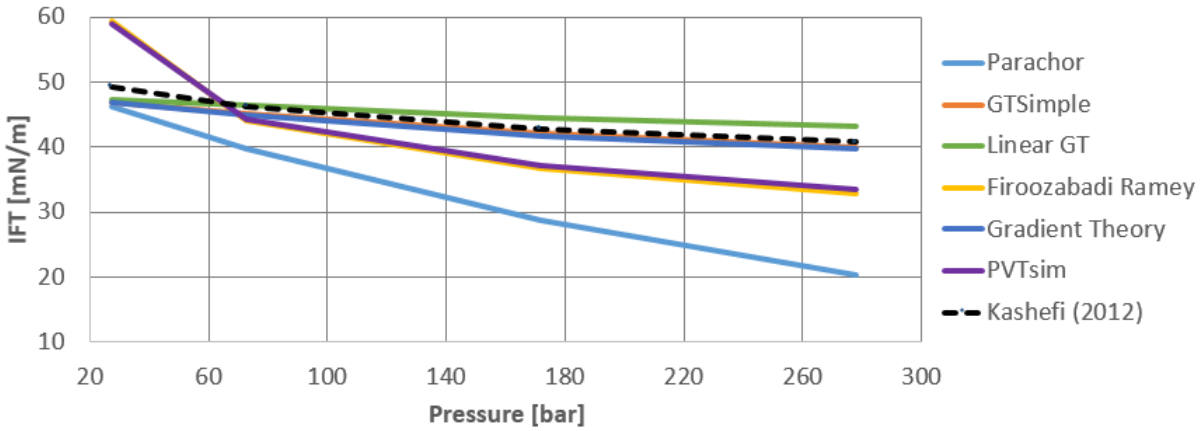

Figure C.2: Calculated interfacial tensions of methane and aqueous TEG compared to experimental data at 150°C and pressures 27 - 278 bar, Kashefi (2012).

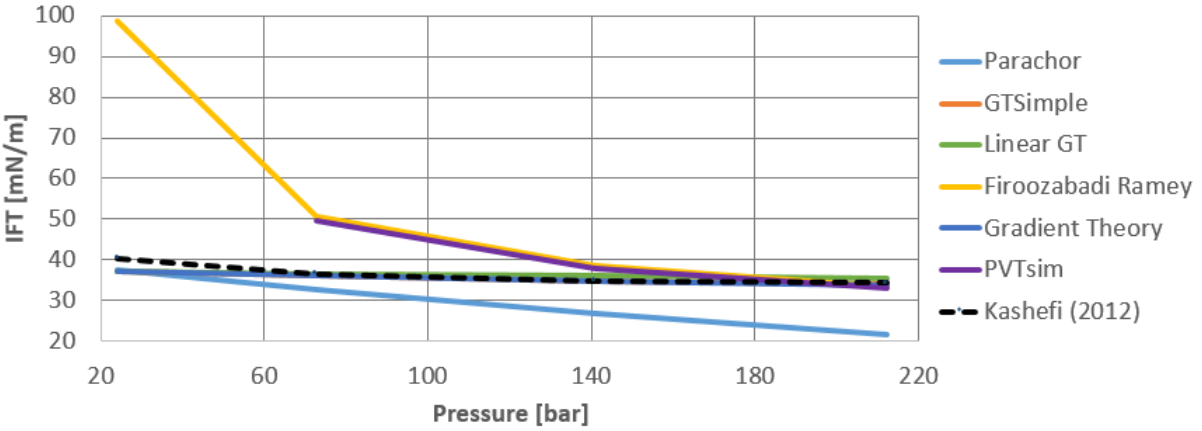

Figure C.3: Calculated interfacial tensions of methane and aqueous TEG compared to experimental data at 200°C and pressures 24 - 212 bar, Kashefi (2012).

C.2 Interfacial Tension of High Pressure Aqueous TEG and Methane, Ng et al. (2009)

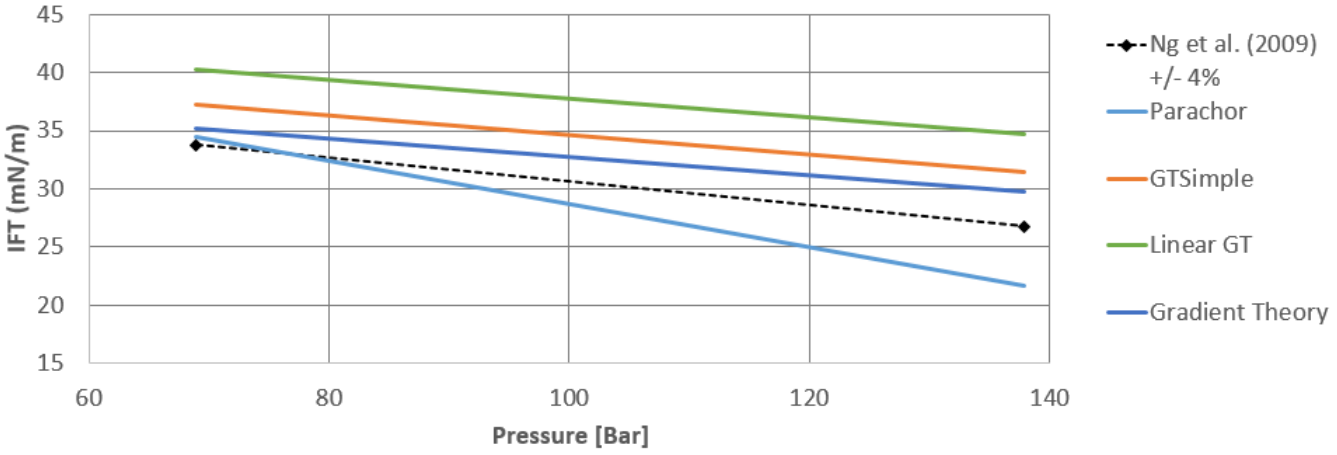

Figure C.4: Calculated interfacial tensions of methane and aqueous TEG compared to experimental data at 26.7°C and pressures 69 - 138 bar, Ng et al. (2009)

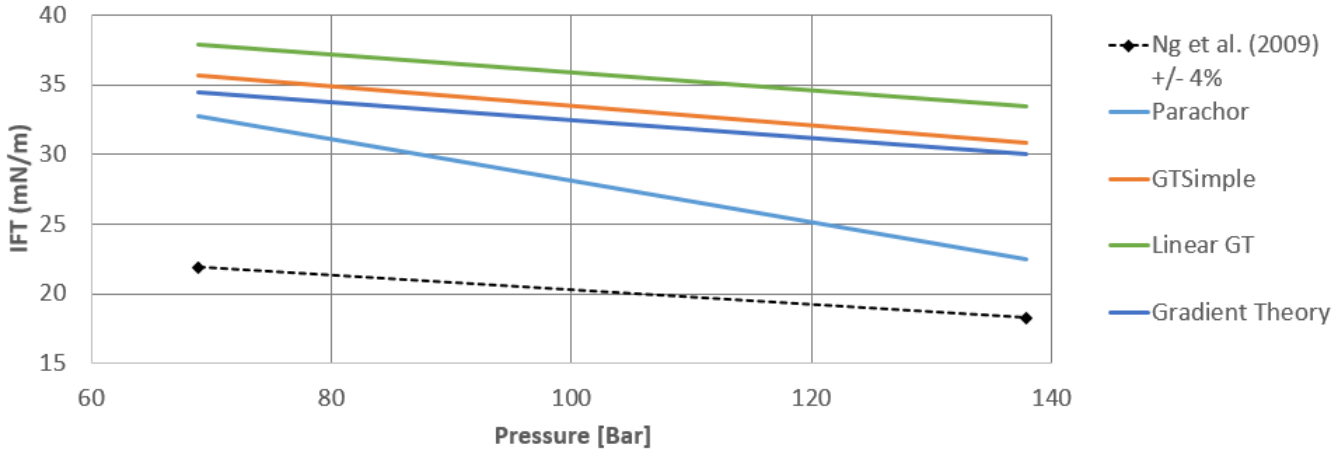

Figure C.5: Calculated interfacial tensions of methane and aqueous TEG compared to experimental data at 60°C and pressures 69 - 138 bar, Ng et al. (2009)

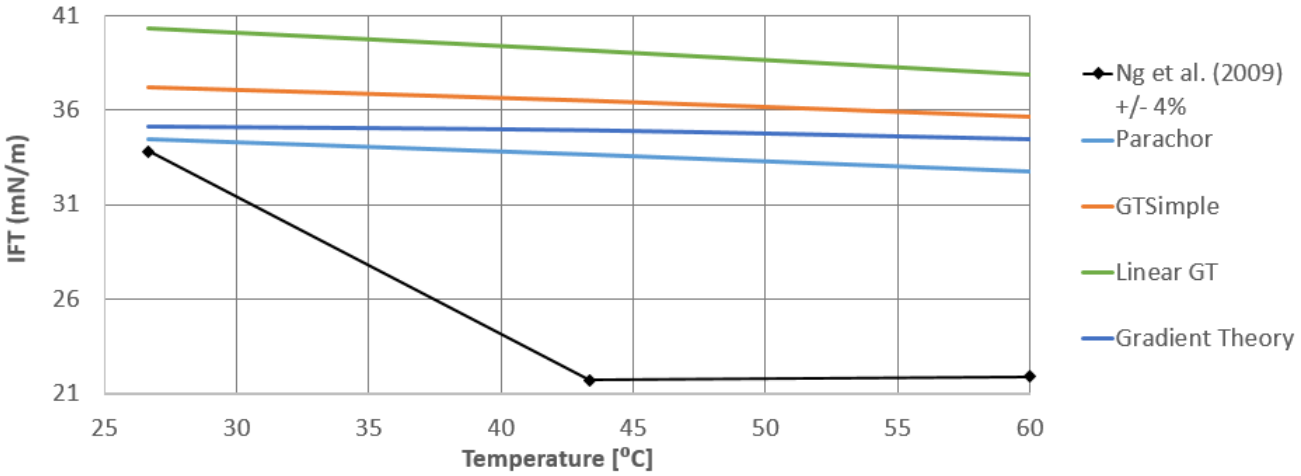

Figure C.6: Calculated interfacial tensions of methane and aqueous TEG compared to experimental data at 69 bar and temperatures 26.7 - 60°, Ng et al. (2009)

C.3 Measured Values of this Study Compared to NeqSim, 100 wt% TEG

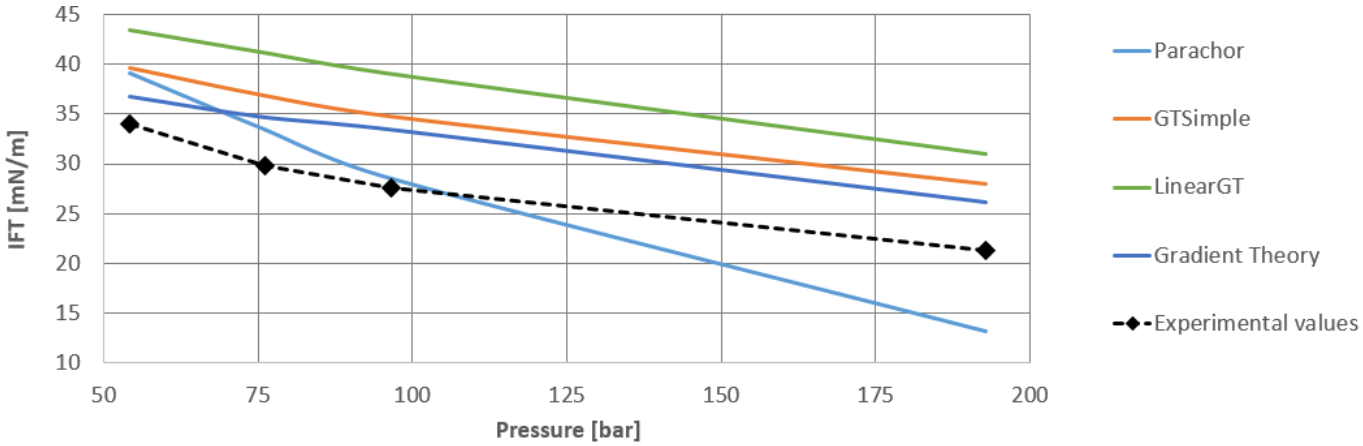

Figure C.7: Calculated interfacial tensions of methane and TEG compared to the experimental results of this study at 4.3°C and pressures 54 - 193 bar.

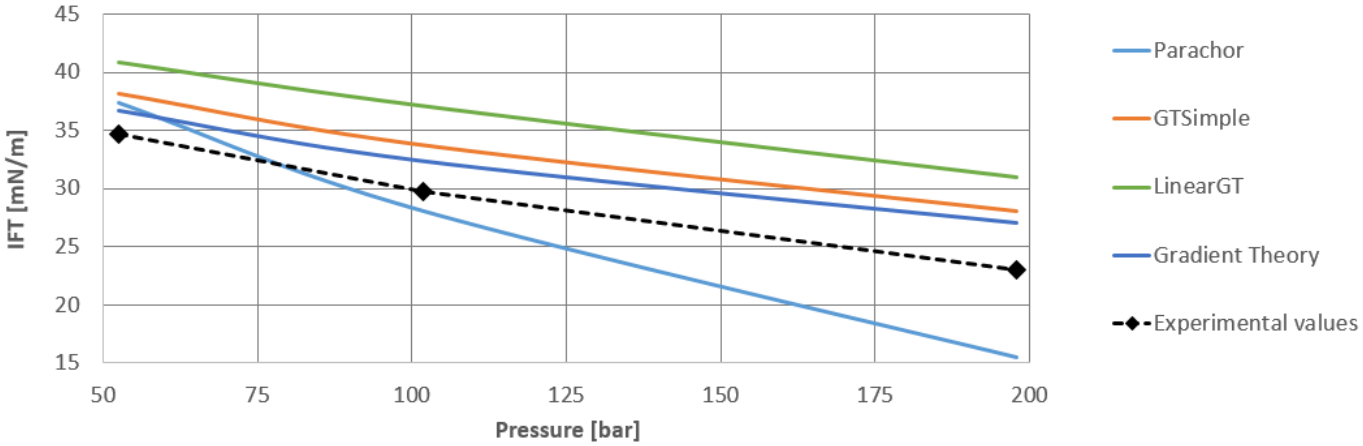

Figure C.8: Calculated interfacial tensions of methane and TEG compared to the experimental results of this study at 41.5°C and pressures 53 - 198 bar.

C.4 Measured Values of this Study Compared to NeqSim, 90 wt% TEG

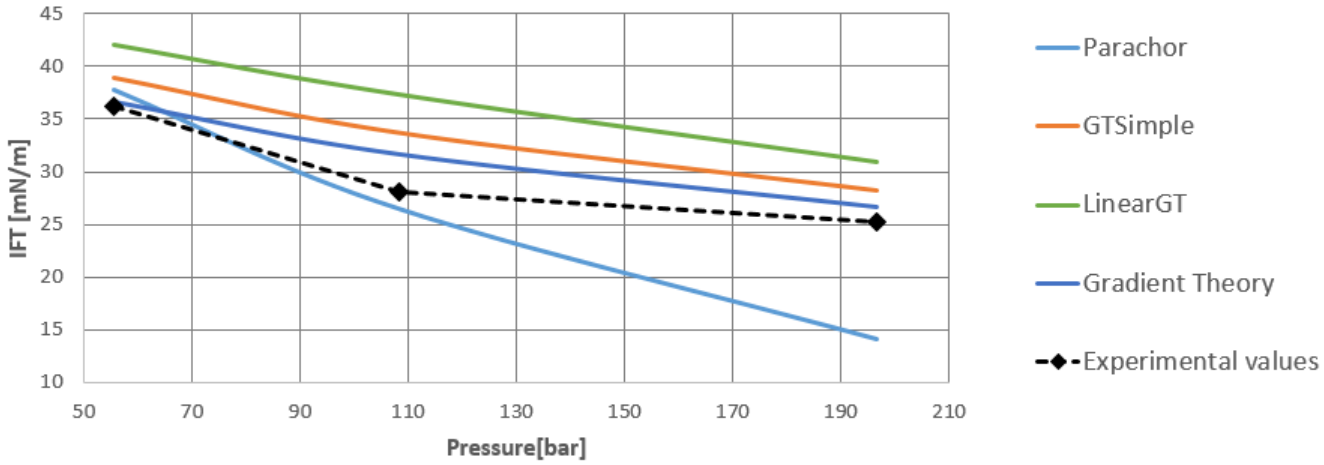

Figure C.9: Calculated interfacial tensions of methane and aqueous TEG compared to the experimental results of this study at 20°C and pressures 55 - 197 bar

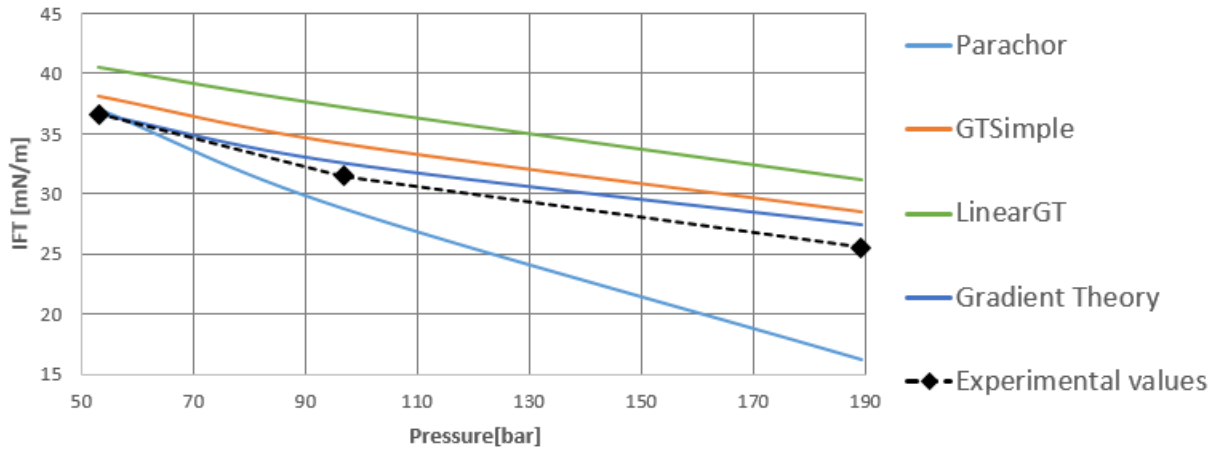

Figure C.10: Calculated interfacial tensions of methane and aqueous TEG compared to the experimental results of this study at 41.5°C and pressures 53 - 189 bar

C.5 Interfacial Tension of High Pressure Aqueous MEG and Methane, Norgaard and Nygaard (2014)

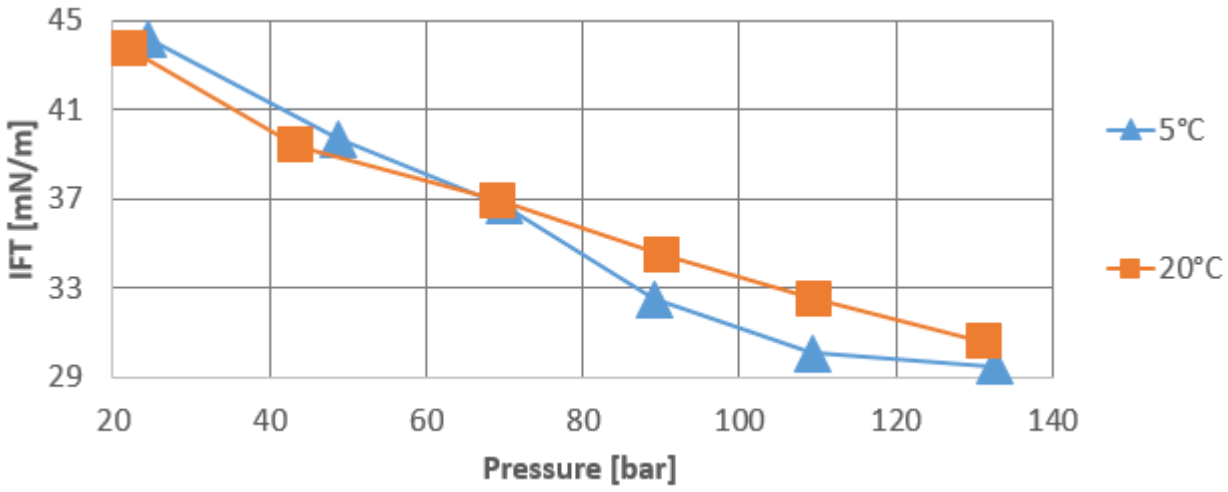

Figure C.11: Experimental data of the interfacial tension of methane and MEG in equilibrium at pressures 22 - 133 bar, 100 wt% MEG, Norgaard and Nygaard (2014).

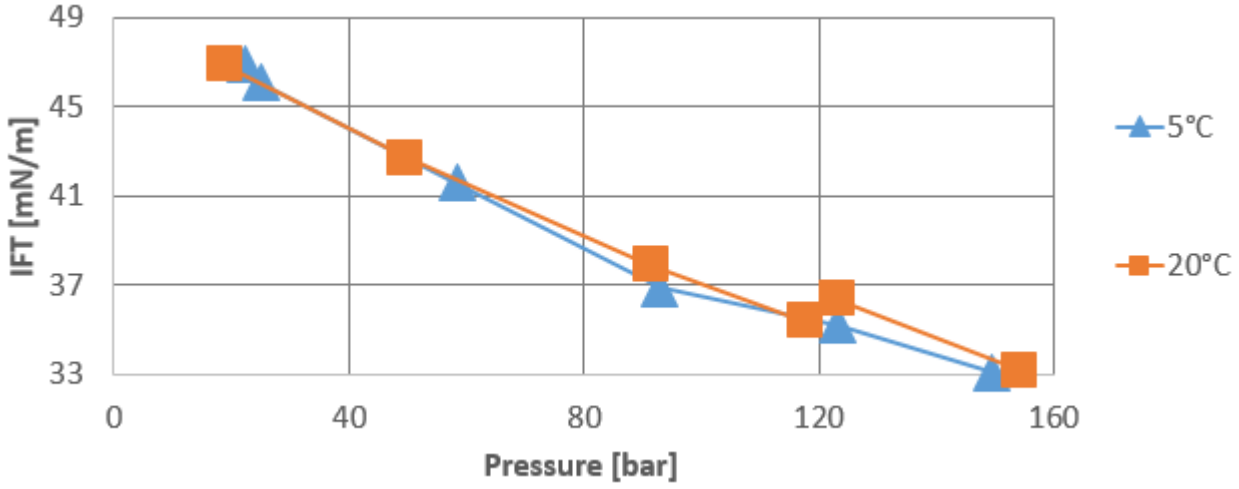

Figure C.12: Experimental data of the interfacial tension of methane and aqueous MEG in equilibrium at pressures 19 - 154 bar, 80 wt% MEG, Norgaard and Nygaard (2014).

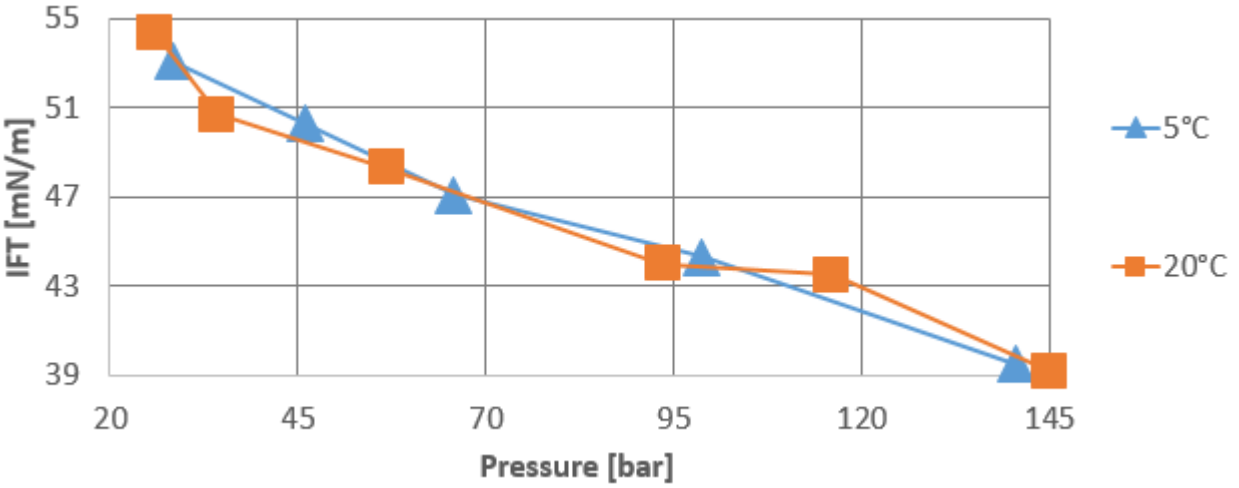

Figure C.13: Experimental data of the interfacial tension of methane and aqueous MEG in equilibrium at pressures 26 - 145 bar, 50 wt% MEG, Norgaard and Nygaard (2014).

Appendix D

Parameter Study Results

D.1 Simulated values with carryover TEG, OLGA

Pressure Drop [bar]	NeqSim						
Factor	0.1	0.2	0.5	1	2	5	10
Liquid Viscosity	114.313	114.303	114.393	114.409	114.453	114.499	114.533
Interfacial Tension	114.342	114.355	114.374	114.409	114.438	114.474	114.492
Liter TEG/MSm^3 gas	5	10	25	50	100	250	500
Mass flow TEG [kg/s]	0.0047	0.0089	0.02235	0.0447	0.0894	0.2235	0.4472
	114.288	114.3	114.323	114.409	114.591	115.132	116.072

Table D.1: Simulated pressure drop from parameter studies with NeqSim property tables. Scenario 1.

Accumulated TEG along branch [m^3]	NeqSim						
Factor	0.1	0.2	0.5	1	2	5	10
Liquid Viscosity	32	32.7	33.4	33.6	34	34.2	34.3
Interfacial Tension	34	34	33.8	33.6	33.5	32.9	32.3
Liter TEG/MSm^3 gas	5	10	25	50	100	250	500
Mass flow TEG [kg/s]	0.0047	0.0089	0.02235	0.0447	0.0894	0.2235	0.4472
	2.9	6.2	16.5	33.6	68.2	171.2	343.4

Table D.2: Simulated accumulated TEG from parameter studies with NeqSim property tables. Scenario 1.

Pressure Drop [Bar]	PVTsim						
Liter TEG/MSm^3 gas	5	10	25	50	100	250	500
Mass flow TEG [kg/s]	0.0047	0.0089	0.02235	0.0447	0.0894	0.2235	0.4472
	112.792	112.807	112.915	113.021	113.216	113.813	114.743

Table D.3: Simulated pressure drop from parameter studies with PVTsim property tables. Scenario 1.

Accumulated water along branch [m^3]	PVTsim						
Liter TEG/MSm^3 gas	5	10	25	50	100	250	500
Mass flow TEG [kg/s]	0.0047	0.0089	0.02235	0.0447	0.0894	0.2235	0.4472
	2.7	6.2	16.3	33.3	67.3	169.4	340

Table D.4: Simulated accumulated TEG from parameter studies with PVTsim property tables. Scenario 1.

D.2 Simulated values with TEG dump, OLGA

Pressure Drop [bar]	NeqSim						
Factor	0.1	0.2	0.5	1	2	5	10
Liquid Viscosity	114.37	114.486	114.553	114.703	114.854	114.855	114.897
Interfacial Tension	114.5	114.565	114.659	114.703	114.76	114.777	114.801

Table D.5: Simulated pressure drop from parameter studies with NeqSim property tables. Scenario 2.

Accumulated TEG along branch [m^3]	NeqSim						
Factor	0.1	0.2	0.5	1	2	5	10
Liquid Viscosity	61.7	63.1	64.2	64.5	64.6	64.7	74.7
Interfacial Tension	64.5	64.5	64.5	64.5	64.3	63.8	62.8

Table D.6: Simulated accumulated TEG from parameter studies with NeqSim property tables. Scenario 2.

PVTsim	
Pressure drop [bar]	113.348
Accumulated water along branch [m^3]	64.3

Table D.7: Results from parameter studies with PVTsim property tables. Scenario 2.

D.3 Simulated values with carryover TEG, OLGA HD

Pressure Drop [bar]	NeqSim						
Factor	0.1	0.2	0.5	1	2	5	10
Liquid Viscosity	114.995	115.15	115.713	115.593	115.334	115.324	115.296
Interfacial Tension	115.771	115.771	115.713	115.593	115.353	115.674	115.048
Liter TEG/MSm^3 gas	5	10	25	50	100	250	500
Mass flow TEG [kg/s]	0.0047	0.0089	0.02235	0.0447	0.0894	0.2235	0.4472
	114.515	114.611	115.075	115.593	117.861	120.798	133.635

Table D.8: Simulated pressure drop from parameter studies with NeqSim property tables. Scenario 1 with the OLGA HD module

Accumulated TEG along branch [m^3]	NeqSim						
Factor	0.1	0.2	0.5	1	2	5	10
Liquid Viscosity	34.3	34.3	34.3	34.3	34.3	34.3	34.3
Interfacial Tension	34.3	32.3	34.3	34.3	34.3	54.9	48.9
Liter TEG/MSm^3 gas	5	10	25	50	100	250	500
Mass flow TEG [kg/s]	0.0047	0.0089	0.02235	0.0447	0.0894	0.2235	0.4472
	3.3	6.7	17.08	34.3	94.2	212.1	536.5

Table D.9: Simulated accumulated TEG from parameter studies with NeqSim property tables. Scenario 1 with the OLGA HD module.

Pressure Drop [Bar]	PVTsim						
Liter TEG/MSm^3 gas	5	10	25	50	100	250	500
Mass flow TEG [kg/s]	0.0047	0.0089	0.02235	0.0447	0.0894	0.2235	0.4472
	113.061	113.035	113.563	113.7435	115.558	119.558	122.001

Table D.10: Simulated pressure drop from parameter studies with PVTsim property tables. Scenario 1 with the OLGA HD module

Accumulated water along branch [m^3]	PVTsim						
Liter TEG/MSm^3 gas	5	10	25	50	100	250	500
Mass flow TEG [kg/s]	0.0047	0.0089	0.02235	0.0447	0.0894	0.2235	0.4472
	7.35	7.009	35.018	51.255	127.142	289.236	460.937

Table D.11: Simulated accumulated TEG from parameter studies with PVTsim property tables. Scenario 1 with the OLGA HD module.

D.4 Simulated values with TEG, OLGA HD

Pressure Drop [bar]	NeqSim						
Factor	0.1	0.2	0.5	1	2	5	10
Liquid Viscosity	116.693	116.981	117.885	118.538	117.666	117.608	117.599
Interfacial Tension	118.8	118.797	118.786	118.538	117.447	117.408	116.178

Table D.12: Simulated pressure drop from parameter studies with NeqSim property tables. Scenario 2 with the OLGA HD module.

Accumulated TEG along branch [m^3]	NeqSim						
Factor	0.1	0.2	0.5	1	2	5	10
Liquid Viscosity	73.69	65.68	64.85	64.86	64.7	64.87	64.88
Interfacial Tension	64.86	64.86	64.86	64.86	64.66	120.537	103.276

Table D.13: Simulated accumulated TEG from parameter studies with NeqSim property tables. Scenario 2.

PVTsim	
Pressure drop [bar]	115.878
Accumulated water along branch [m^3]	125.1

Table D.14: Results from parameter studies with PVTsim property tables. Scenario 2 with the OLGA HD module